UNIVERSIDAD POLITÉCNICA DE MADRID
Escuela Técnica Superior de Ingenieros Industriales

Modular Simulation Methodology for the Economical and Environmental Optimization of District Heating/Cooling Systems to Achieve Net Zero

DOCTORAL THESIS

Submitted for the degree of Doctor by:

Juan José Roncal Casano
Master in Energy Engineering, Chemical Engineer

Madrid, 2024

UNIVERSIDAD POLITÉCNICA DE MADRID
Escuela Técnica Superior de Ingenieros Industriales

Doctoral Degree in Sustainable, Nuclear and Renewable Energy

Modular Simulation Methodology for the Economical and Environmental Optimization of District Heating/Cooling Systems to Achieve Net Zero

DOCTORAL THESIS

Submitted for the degree of Doctor by:

Juan José Roncal Casano
Master in Energy Engineering, Chemical Engineer

Under the supervision of:
Dr. Javier Rodríguez Martín(Supervisor)
Dr. Alberto Abánades Velasco(Cosupervisor)

Madrid, 2024

Title: Modular Simulation Methodology for the Economical and Environmental Optimization of District Heating/Cooling Systems to Achieve Net Zero

Author: Juan José Roncal Casano

Doctoral Programme: Sustainable, Nuclear and Renewable Energy

Thesis Supervision:

Dr. Javier Rodríguez Martín, Associate Professor, Universidad Politécnia de Madrid(Supervisor)

Dr. Alberto Abánades Velasco, Full Professor, Universidad Politécnia de Madrid(Cosupervisor)

External Reviewers:

Thesis Defense Committee:

Thesis Defense Date:

This thesis was performed under the framework of the WeDistrict project, which has received funding from the European Union's Horizon 2020 research and innovation programme under grant agreement N°857801.

To everyone, those near and those far.

ABSTRACT

Under the need to reduce CO_2 emissions, district heating has been identified as a viable alternative to implement renewable technologies to supply the climatization demand.

Although software is available for simulating district heating networks, it is challenging for inexperienced users to use. Additionally, these tools lack flexibility in generating new combinations of technologies for district heating and cooling networks.

This thesis presents the development of a methodology for simulating district heating and cooling networks. This methodology, called Modular Simulation Methodology (or MSM) aims to make this technology available to anyone in the position to make such a decision about future installations for heating, ventilation, and air conditioning (HVAC) on a big scale, as to migrate to a reduced more environmentally friendly option. This methodology was originally focused on the technologies developed within the Wedistrict project, but it is scalable and designed to expand its library of technologies.

The methodology consists in reducing and simplifying the amount of information to be added by the user at an early stage, by correlating all possible information. It involves making standard nomenclature for the different variables to identify complex systems in a more orderly manner. And simplifying the results displayed at the end of the process to be able to compare with other available technologies.

The MSM also allows for the production of parametric results for a series of cases, being able to use it to obtain optimum design values for equipment in district networks. By storing these parametric analyses, databases have been generated.

One result of the methodology is simulating Demonstration Sites before their construction. These sites, three different locations chosen to test various technologies developed within the Wedistrict project. Once the methodology was proven, it was replicated in a series of Demonstration Followers, which were new sites which desired to install district heating networks, or existing networks which want to test, by simulation, other technological combinations to reduce their environmental impact.

The production of parametric results was also presented in different academic papers, to find optimum sizes for proposed systems or evaluate different technological combinations.

At the end of the work, a web-based tool was developed using results databases generated using the MSM. This tool is accessible to all and has been developed as part of the H2020 Wedistrict project. Future works could expand the locations in which this tool can obtain results as the combination of technologies available.

This methodology is particularly flexible for future networks because it allows the combination of technologies from different energy sources, making it especially strong as energy sources vary by location.

RESUMEN

Ante la necesidad de reducir las emisiones de CO_2, la climatización distrital se ha identificado como una alternativa viable para implantar tecnologías renovables que abastezcan la demanda de climatización.

Existe software para la simulación de redes de climatización, pero son difíciles de manejar para los usuarios inexpertos. Además, estas herramientas carecen de la flexibilidad necesaria para generar nuevas combinaciones de tecnologías para las redes distritales de calor y frio.

Esta tesis ilustra la generación de una metodología para la simulación de redes distritales de calefacción y refrigeración. Esta metodología, denominada Metodología de Simulación Modular (o MSM) pretende poner esta tecnología a disposición de cualquiera que esté en posición de tomar una decisión sobre futuras instalaciones de calefacción, ventilación y aire acondicionado (HVAC) a gran escala, como migrar a una opción reducida más respetuosa con el medio ambiente. Esta metodología se centró originalmente en las tecnologías desarrolladas dentro del proyecto Wedistrict, pero es escalable y está diseñada para ampliar su biblioteca de tecnologías.

La metodología consiste en reducir y simplificar la cantidad de información que debe añadir el usuario en una fase temprana, correlacionando toda la información posible. Hacer una nomenclatura estándar de las distintas variables para poder identificar sistemas complejos de forma más ordenada. Y en simplificar los resultados mostrados al final del proceso para poder compararlos con otras tecnologías disponibles.

La MSM también permite obtener resultados paramétricos para una serie de casos, pudiéndose utilizar para obtener valores óptimos de diseño de equipos en redes de distrito. Mediante el almacenamiento de estos análisis paramétricos se han generado bases de datos.

Uno de los resultados de la metodología es la simulación de Demo Sites antes de su construcción. Se trata de tres emplazamientos diferentes elegidos para probar diversas tecnologías desarrolladas en el marco del proyecto Wedistrict. Una vez probada la metodología, se replicó en una serie de Demonstration Followers, que eran nuevos emplazamientos que deseaban instalar redes de climatización distrital, o redes existentes que querían probar, mediante simulación, otras combinaciones tecnológicas para reducir su impacto ambiental.

La producción de resultados paramétricos también se plasmó en diferentes artículos académicos, para encontrar tamaños óptimos para los sistemas propuestos, o evaluar diferentes combinaciones tecnológicas.

Al final del trabajo, se desarrolló una herramienta web utilizando estas bases de datos. Es accesible al público y es el resultado del proyecto H2020 Wedistrict. Trabajos futuros podrían ampliar las localizaciones en las que esta herramienta puede obtener resultados, asi como la combinación de tecnologías disponibles.

Esta metodología es especialmente flexible para las redes del futuro porque permite combinar tecnologías de distintas fuentes de energía, lo que la hace especialmente sólida ya que las fuentes de energía varían según la localización.

Acknowledgments

Last years may have been strange for most of us. Considering the transition from the pandemic to the new normality I think all of us experienced a wide range of feelings.

I strongly thank Javier for being there all along the PhD and for the optimistic view and guidance offered during this whole period, without whom this work would not have been possible. Also, Alberto, the one supervising this thesis without losing faith in the outcome.

Colleagues from the Wedistrict project which have gone above and beyond to complete a task that, at first, seemed inconceivable. Paolo, Joaquim, Ignasi, Christi, and many others. Thanks for making this task achievable and enjoyable at the same time.

Friends from the university who coped with days in which spirits were not at the highest pitch, Magdalena, Rubén, Andrés, Antonio, Jesús, Carlos. Friends made at the stay in Torino, which made a dent outside of the little time I stayed with you, you made Polito feel like home from day one. Friends from home, Alejo, Sofía and Santi, which I left some years ago in Argentina but never left my heart. Eugenia, for having been an inspiration on resilience and work ethics. Friends in general to whom I swore I was finishing in the following weeks to find myself having to continue to expand.

My family for having been supportive of my life outside my place of birth, and always feeling close no matter the distance.

And last Juliana, who has helped even proofreading the thesis, has been there all the time and showed me a positive approach to things that I sometimes miss. I think the best is yet to come, so let's create that shared view.

This thesis was performed under the framework of the WeDistrict project, which has received funding from the European Union's Horizon 2020 research and innovation programme under grant agreement N°857801.

Contents

Abstract i
Abstract . . . i
Resumen . . . i

Acknowledgments iii

List of Figures ix

List of Tables xiii

1 Introduction 1
1.1 Actual energetic context . . . 1
1.2 District Heating Systems . . . 5
1.2.1 Description . . . 5
1.2.2 Advantages and Disadvantages . . . 7
1.2.3 District Heating generations . . . 8
1.2.4 District Cooling generations . . . 10
1.2.5 Actual situation . . . 12
1.3 Research Methodology . . . 17
1.4 Thesis Structure . . . 17
1.5 Related publications . . . 18
1.5.1 Peer-reviewed journals . . . 18
1.5.2 Conference Proceedings . . . 18

2 State of the Art 20
2.1 District Heating Simulation . . . 20
2.1.1 Software Available for Generation Side . . . 21
2.1.2 End-users . . . 25
2.2 Objectives . . . 27

3 MSM Technologies 29
3.1 Heating generation . . . 29
3.1.1 Solar Technologies . . . 29
3.1.2 Boilers . . . 39
3.2 Cooling generation . . . 44
3.2.1 Compression-driven . . . 44

3.2.2 Absorption . . . 49
3.3 Storage technology . . . 54
3.3.1 Methods for thermal energy storage . . . 55
3.3.2 Time classification for storage . . . 57
3.3.3 Simulation . . . 59

4 Modular Simulation Methodology **61**
4.1 Simulation . . . 61
4.1.1 Software . . . 61
4.1.2 Modular Simulation Methodology . . . 61
4.1.3 Key Performance Indicators (KPIs) . . . 70

5 Technologies **82**
5.1 General Types . . . 82
5.1.1 Pipes (TRNSYS Type 709) . . . 82
5.1.2 Pumps (TRNSYS Type 110) . . . 84
5.1.3 Heat exchanger (TRNSYS Type 5b) . . . 88
5.1.4 Control with hysteresis (TRNSYS Type 2) . . . 88
5.2 Meteo . . . 89
5.2.1 Meteorological files generation . . . 90
5.3 Solar Thermal . . . 91
5.3.1 Hypotheses . . . 92
5.3.2 Heat and Mass Balance . . . 92
5.3.3 Parametrization . . . 93
5.3.4 Control . . . 93
5.3.5 Results . . . 94
5.4 Conventional Absorption Chiller . . . 95
5.4.1 Hypotheses . . . 95
5.4.2 Heat and Mass Balance . . . 96
5.4.3 Parametrization . . . 96
5.4.4 Control . . . 97
5.4.5 Results . . . 98
5.5 Compression Chiller . . . 98
5.5.1 Hypotheses . . . 99
5.5.2 Heat and Mass Balance . . . 100
5.5.3 Parametrization . . . 100
5.5.4 Control . . . 101
5.5.5 Results . . . 101
5.6 Heat Pumps . . . 101
5.6.1 Hypotheses . . . 103
5.6.2 Heat and Mass Balance . . . 103
5.6.3 Parametrization . . . 104
5.6.4 Control . . . 104
5.6.5 Results . . . 105
5.7 Boiler . . . 105

5.7.1 Hypotheses . . . 105
5.7.2 Heat and Mass Balance . . . 106
5.7.3 Parametrization . . . 107
5.7.4 Control . . . 108
5.7.5 Results . . . 108
5.8 Storage . . . 109
5.8.1 Hyphotheses . . . 109
5.8.2 Heat and Mass Balance . . . 110
5.8.3 Parametrization . . . 111
5.8.4 Control . . . 111
5.8.5 Results . . . 111
5.9 Molten Salts Storage . . . 111
5.9.1 Hyphotheses . . . 112
5.9.2 Heat and Mass Balance . . . 114
5.9.3 Parametrization . . . 115
5.9.4 Control . . . 116
5.9.5 Results . . . 116
5.10 Demand . . . 116
5.10.1 Hypotheses . . . 118
5.10.2 Heat and Mass Balance . . . 118
5.10.3 Parametrization . . . 118
5.10.4 Control . . . 119
5.10.5 Results . . . 119
5.10.6 Demand files generation . . . 119
5.10.7 Tool . . . 121

6 Results **124**
6.1 Demonstration Sites . . . 124
6.1.1 Luleå . . . 125
6.1.2 Bucharest . . . 125
6.1.3 Alcalá de Henares . . . 126
6.2 Demonstration Followers . . . 131
6.2.1 SeiMilano . . . 132
6.2.2 Montegancedo . . . 133
6.2.3 Playa del Inglés . . . 135
6.2.4 Tecnoalcalá . . . 135
6.2.5 Independencia and Recoleta . . . 135
6.2.6 Parc de l'Alba . . . 137
6.2.7 University of Cyprus . . . 139
6.2.8 Żyrardów . . . 141
6.2.9 Valladolid . . . 143
6.2.10 Focşani . . . 143
6.2.11 Mrągowo . . . 150
6.3 Parametric Studies . . . 154
6.3.1 Solar Field Sizing for District Heating and Cooling . . . 154

6.3.2 Parametric Studies Future Works . . . 156
6.4 Tool . . . 156
6.4.1 Tool Future Works . . . 159

7 Validation **160**
7.1 Bucharest Demo site . . . 160
7.1.1 Technologies used . . . 160
7.1.2 TRNSYS . . . 160
7.1.3 Results Obatined . . . 164

8 Conclusion and Future Works **168**
8.1 Thesis Conclusion . . . 168
8.2 Future Works . . . 171

References **173**

List of Figures

1.1 End-user energy consumption distribution in EU and Spain by use [2] 2
1.2 Energy consumption distribution in EU and Spain by fuel [2] 3
1.3 Market share of DH vs renewable heat [3] 4
1.4 End-user energy consumption distribution in Poland by use [2] 4
1.5 District heating components 6
1.6 Evolution in the generations of District Heating [9]. 6
1.7 Evolution in the generations of District Cooling [18]. 13
1.8 District Heating Atlas [22]. 14

2.1 EnergyPRO example screen. 22
2.2 EnergyPlus screen. 22
2.3 Polysun example file screen. 23
2.4 Energyplan home screen. 24
2.5 Different categories of demand simulation based on scale [49]. 26
2.6 Energy-hub screen from the nPro tool [55]. 27

3.1 Possible concentrating collector configurations: (a) Tubular absorbers with diffuse back reflector; (b) tubular absorbers with specular cusp reflectors; (c) plane receiver with plane reflectors; (d) parabolic concentrator; (e) Fresnel reflector; (f) array of heliostat with central receiver. From [57] modified. . . 31
3.2 Fresnel Lens Collector diagram. From [56]. 32
3.3 WeSSun collector diagram. 33
3.4 Schematic representation of a typical three-pass fire-tube boiler from [64] modified. 40
3.5 Pulverized coal-fired power-generation water-tube boiler. from [65] modified. 41
3.6 Condensing and non-condensing boilers efficiencies vs inlet temperature [69] modified. 45
3.7 Idealized carnot vapor compression heat pump/chiller with T-s state diagram [67] modified. 46
3.8 Simplified compression heat pump/chiller cycle with T-s state diagram [67] modified. 47
3.9 Compression cycle from [68] modified. (a) Cooling Cycle. (b) Heating Cycle. 48
3.10 Variation in the COP of a heat pump in heating mode (a) and in cooling mode (b) for various evaporator–temperature combinations, assuming a Carnot efficiency (ratio of actual to ideal COP) of 0.64 [70]. 49

3.11 Absorption cycle from [71] modified. (a) Cooling Cycle. (b) Heating Cycle. Note that in (b) there is no cooling water flow in the condenser nor the absorber. 50
3.12 Absorption cycle in Dühring diagram for LiBr [72]. 51
3.13 Variation of COP with generator temperature ($T_{eva} = 7.2°C$, $T_{cond} = T_{abs}$) [73]. 52
3.14 Effect of absorber temperature on COP ($T_{gen} = 87.8°C$, $T_{cond} = 37.8°C$, $T_{eva} = 7.2°C$) [73]. 53
3.15 Effect of evaporator temperature on COP ($T_{cond} = T_{abs} = 37.8°C$ $T_{gen} = 87.8°C$) [73]. 53
3.16 Heating and cooling demand distribution in northern and southern climates, on an annual and daily basis [76] 54
3.17 Storage Phases 55
3.18 Heat storage as sensible and latent TES [77] 57
3.19 TRL levels according to NASA aligned with CRI values 58

4.1 Simulation workflow at Wedistrict project using MSM. 62
4.2 TRNSYS Type. 63
4.3 MSM macro Scheme. 64
4.4 Macros connected to generate a DH network 65
4.5 Macros connected to generate a DHC network. 65
4.6 Macros coding developed 66
4.7 Variable code for the mass flow going in the first pump of the boiler 67
4.8 jEPlus user interface. 70
4.9 Wedistrict Energy variables shown using Figure 4.5 71
4.10 KPI calculation in MSM. 80

5.1 TRNSYS pipe scheme 83
5.2 TRNSYS variable speed pump 85
5.3 TRNSYS heat exchanger scheme 88
5.4 Control function 89
5.5 TRNSYS meteorological macro 90
5.6 Screen capture of PVGIS online interface [96] 91
5.7 Macro M1200 scheme and energy and mass balance 92
5.8 Macro M1200 in TRNSYS simulation studio 93
5.9 Macro M4200 in TRNSYS simulation studio 96
5.10 Macro M4200 scheme and energy and mass balance 97
5.11 Macro M4300 in TRNSYS simulation studio 99
5.12 Macro M4300 scheme and energy and mass balance 100
5.13 Macro M4600 in TRNSYS simulation studio 102
5.14 Macro M4610 in TRNSYS simulation studio 102
5.15 Macro M4600 scheme and energy and mass balance 104
5.16 Macro M3100 in TRNSYS simulation studio 106
5.17 Macro M3100 scheme and energy and mass balance 107
5.18 First version of M2100 TRNSYS macro 109
5.19 Last version of M2100 TRNSYS macro 110
5.20 Macro M2100 scheme and energy and mass balance. 111

5.21 M2200 TRNSYS macro . . . 112
5.22 Charging operation comparison between TRNSYS model and MATLAB model. 114
5.23 Discharge operation comparison between TRNSYS model and MATLAB model. 115
5.24 Macro M2200 scheme and energy and mass balance. . . . 115
5.25 Macro M8100 in TRNSYS simulation studio . . . 117
5.26 Macro M8100 scheme and energy and mass balance . . . 118
5.27 HDD and CDD calculations examples. . . . 120
5.28 TRNSYS DD generation file . . . 120
5.29 Daily distribution for space heating and DHW. . . . 121

6.1 Wedistrict Technologies . . . 125
6.2 Proposed solution for Luleå. . . . 126
6.3 Proposed network POLITEHNICA Bucharest. . . . 127
6.4 Demand profile in Alcalá de Henares. . . . 128
6.5 First proposed network for Alcalá de Henares. . . . 129
6.6 Final proposed network for Alcalá de Henares. . . . 130
6.7 Heating demand results in Alcalá. . . . 131
6.8 Cooling demand results in Alcalá. . . . 132
6.9 SeiMilano network. . . . 133
6.10 Montegancedo demo-follower site. . . . 134
6.11 Tecnoalcalá demo-follower site. In red, where the original demo-site building was located, and in green, where the construction of the plant was proposed. In blue, the park's datacenter. . . . 136
6.12 University of Cyprus demo-follower site. . . . 140
6.13 Żyrardów location. . . . 141
6.14 Żyrardów S4 solution sketch. . . . 142
6.15 Valladolid demo-follower site. . . . 144
6.16 Focşani S1 diagram. . . . 145
6.17 Focşani S2 diagram. . . . 145
6.18 Focşani S3 diagram. . . . 146
6.19 Focşani S1 KPIs considering different advance absorption chiller's capacity. . . . 147
6.20 Focşani S1 emissions vs LCOE only for the heating network. . . . 147
6.21 Focşani S1 emissions vs LCOE only for the cooling network. . . . 148
6.22 Focşani S2 emissions vs LCOE. . . . 149
6.23 Focşani S3 emissions vs LCOE. . . . 149
6.24 Mrągwogo S1 diagram. . . . 150
6.25 Mrągwogo S2 diagram. . . . 151
6.26 Mrągwogo S3 diagram. . . . 151
6.27 Parametric solutions from S1. . . . 152
6.28 Parametric solutions from S2. . . . 153
6.29 Parametric solutions from S3. . . . 153
6.30 System scheme analyzed in article. . . . 154
6.31 Results from system analyzed. . . . 155
6.32 Tool conceptualization. . . . 156
6.33 Tool combinations for district heating. . . . 157

6.34 Tool combinations for district heating and cooling. 158

7.1 UNSTPB demonstrator Thermal Scheme from Wedistrict project modified. . 161
7.2 Geothermal Heat Exchanger validation model. 162
7.3 Flow data to consumers, UNSTPB first batch. Divided by operation periods. 163
7.4 W-W HP pump validation model. 163
7.5 W-W HP validation model with integrated BHX. 163
7.6 Results on the first day of the analyzed period. (a) shows results on temperatures and flows. While (b), shows the temperature percentual difference between calculated and received in experimental data. 165
7.7 W-W HP validation model without BHX. 166
7.8 Temperature results of the system 166
7.9 Heat delivered results of the system 167

List of Tables

1.1 Overview of some example national design temperatures for heating networks [10] . . . 7
1.2 Total installed heat capacity per technology type (MWth) [24]. . . . 15
1.3 Existing DHN examples by generation [25]. . . . 16

2.1 Software used for DHC simulation and their limitations. . . . 24
2.2 Prediction error for different methods [28] . . . 25

3.1 Thermal and physical properties of commonly used HTFs [59] . . . 34
3.2 Solar Collectors. Note: Concentration ratio is defined as the aperture area divided by the receiver/absorber area of the collector [58] . . . 39
3.3 Proximate analysis of some biomass feedstocks (wt%) [66] . . . 42
3.4 Thermal capacities at 20°C of some common TES materials [79] . . . 56

4.1 TRNSYS types used for different macros. . . . 64
4.2 Letters used for variables . . . 67
4.3 Macro Codes for different technologies. First two numbers of macro code . . . 68
4.4 Weighting factors (based on gross or net calorific value) from [90, Table B.16.] 79

5.1 Pressure drop for different pumps in different macros. . . . 87
5.2 Types used in M0100. . . . 90
5.3 Types used in M1200 . . . 94
5.4 Types used in M4200. . . . 97
5.5 Types used in M4300. . . . 98
5.6 Types used in M4600. . . . 103
5.7 Types used in M3100. . . . 107
5.8 Types used in M2100 . . . 109
5.9 Types used in M2200 . . . 113
5.10 Operation Modes M2200 . . . 116
5.11 Types used in M8100. . . . 117
5.12 Eurostat. Disaggregated final energy consumption in households in percentage year 2021 . . . 122
5.13 Locations selected for Wedistrict Tool. . . . 123
5.14 Cooling ratios obtained. . . . 123

6.1 Resulting KPIs for proposed system in Alcalá de Henares. . . . 131

6.2 Solutions proposed for SeiMilano Demo-follower. . . . 133
6.3 Solutions proposed for Montegancedo Demo-follower. . . . 134
6.4 Solution proposed for Playa del Inglés Demo-follower. . . . 135
6.5 Solutions proposed for Tecnoalcalá Demo-follower. . . . 136
6.6 Survey on the possible main consumers. . . . 137
6.7 Demand Calculation 138
6.8 KPIs and capacity of system 138
6.9 Parc de l'alba 139
6.10 Solutions proposed for UCY after preliminary assessment. . . . 140
6.11 Solutions proposed for Żyrardow after preliminary assessment. . . . 142
6.12 Żyrardów S4 parameters 142
6.13 Żyrardów S4 parameters 143
6.14 Solutions proposed for Focşani demo-follower. . . . 144
6.15 Focşani parameters variation. Consider for S3 that HP Heating Capacity= 0.75∗Cooling Capacity. . . . 146
6.16 Focşani Solutions optimized capacities and KPIs. . . . 148
6.17 Focşani Solutions optimized capacities and KPIs for S3. . . . 148
6.18 Solutions proposed for Mrągowo demo-follower. . . . 150
6.19 Mrąwogo parameters variation 152
6.20 Mragowo Solutions optimized capacities and KPIs. . . . 154
6.21 Cases analyzed for study. . . . 155

7.1 Index acceptance values according to [107]. . . . 165
7.2 Statistic values for POLITEHNICA 167

Nomenclature

Acronyms

Symbol	Description
BES	Building Energy Simulations
BHX	Borehole Heat Exchanger
CDD	Cooling Degree Days
CES	City Energy Simulations
CHP	Combined Heat and Power
CPC	Compound parabolic collector
CSP	Concentrated Solar Power
CTC	Cylindrical trough collector
CT	Cooling Tower
CVRMSE	Coefficient of Variance of Mean Root Square Error
DHC	District Heating and Cooling
DHC	District Heating and Cooling
DH	District Heating
DHS	District Heating System
DHS	District Heating Systems
DHW	Domestic Hot Water
ETC	Evacuated tube collector
EU	European Union
FC	Fixed Carbon

FEC	Final Energy Consumption
FLC	Fresnel Lens Collector
FLR	Fresnel Linear Reflector
FPC	Flat plate collector
HDD	Heating Degree Days
HFC	Heliostat field collector
HHV	Higher Heating value
HTF	Heat Transfer Fluid
CV	Heating value
IEA	International Energy Agency
IEEP	Intelligent Energy Europe Programme
LDES	Long Duration Energy Storage
LFR	Linear Fresnel reflector
LHV	Low Heating Value
LHV	Lower Heating value
LMTD	Logarithmic Mean Temperature Difference
LPG	Liquefied Petrouleum Gas
MSM	Modular Simulation Methodology
NMBE	Normalized Mean Bias Error
NO	Nitrous Oxide
NT	Net Temperature
NZE	Net Zero Emissions
PDR	Parabolic dish reflector
PTC	Parabolic trough collector
PVGIS	Photovoltaic Geographical Information System
RACU	Renewable air cooling unit
RER	Renewable Energy Ratio

TB	Target Building
TESS	Thermal Energy System Specialists
TMY	Typical Meteorological Year
TRL	Technology Readiness Level
TRNSYS	TRaNsient SYstems Simulation Program
UBES	Ubes Building Energy Simulations
UCO	Universidad de Córdoba
UNSTPB	Universitatea Națională de Știință și Tehnologie POLITEHNICA București (National University of Science and Technology POLITEHNICA Bucharest)
WeSSun	We Smile with the Sun
WP	Work Package

Greek Symbols

Symbol	Description	Units
α_C	Cooling share factor	-
α	Absorptance	-
β_C	CAPEX cooling share factor	-
ϵ	Emmitance of the receiver to the sky	-
γ	Intercept Factor	-
μ	Viscosity	$\frac{N \cdot s}{m^2}$
ρ	Specular, diffuse reflectance or transmittance of refractor (if refractor)	-
ρ	Density	$\frac{kg}{m^3}$
σ	Stefan-Boltzmann constant $5.67 \cdot 10^{-8}$	$\frac{W}{m^2 \cdot K^4}$
τ	Transmittance	-
θ	Incidence angle	$\circ$

Roman Symbols

Symbol	Description	Units

A_C	Collector Surface	m^2
A_{abs}	Absorber Surface	m^2
C_{ratio}	Concentration ratio	-
$C_{d.C}$	Direct construction costs for the equipment used exclusively for cooling	€
$C_{d.H}$	Direct construction costs for the equipment used exclusively for heating	€
$C_{d.HC}$	Direct construction costs for the equipment used for heating and cooling	€
$C_{p.c}$	Project contingency costs	€
$C_{p.d}$	Project development costs	€
$C_{p.e}$	Project engineering costs	€
$C_{p.f}$	Project finance costs	€
$CAPEX_C$	Total normalized CAPEX for the equipment providing cooling service	€
$CAPEX_H$	Total normalized CAPEX for the equipment providing heating service	€
C_p	Specific Heat Capacity. Constant pressure	$\frac{J}{m^3 \cdot K}$
D_i	Inside diameter	m
D_o	Outside diameter	m
$E_{el.aux}$	Auxiliary electrical energy	kWh
$E_{el.CHP}$	Generated electricity	kWh
$E_{exp.i}$	Exported energy carrier "i"	kWh
$E_{exp.i}$	Exported energy of carrier “i"	kWh
E_{exp}	Net exported electricity	kWh
$E_{i.C}$	Energy input of carrier "i" in cooling technology applications	kWh
$E_{i.C}$	Energy produced for non 100% renewable energy carrier “i" consumed exclusively for cooling generation	kWh
$E_{i.H}$	Energy input of carrier "i" in heating technology applications	kWh

$E_{i.H}$	Energy produced for non 100% renewable energy carrier “i" consumed exclusively for heating generation	kWh
$E_{i.HC}$	Energy input of carrier "i" in equipment used for both cooling and heating applications (shared)	kWh
$E_{i.HC}$	Energy produced for non-100% energy carrier “i" consumed for cooling and heating generation	kWh
E_i	Energy input of carrier "i"	kWh
$E_{i.C}$	Auxiliary electrical energy imported from the grid used exclusively for cooling applications	kWh
$E_{i.H}$	Auxiliary electrical energy imported from the grid used exclusively for heating applications	kWh
$E_{i.HC}$	Auxiliary electrical energy imported from the grid used for both cooling and heating applications (shared)	kWh
$E_{r.C.i}$	Renewable energy produced by energy carrier “i" and consumed exclusively for cooling generation	kWh
$E_{r.H.i}$	Renewable energy produced by energy carrier “i" and consumed exclusively for heating generation	kWh
$E_{r.HC.i}$	Renewable energy produced by energy carrier “i" and consumed for both cooling and heating generation	kWh
F'	Collector Efficiency Factor	-
F''	Collector Flow Factor	-
f_{el}	Non-renewable primary energy factor of electricity mix	-
$f_{exp.i}$	Total primary energy factor of exported energy carrier “i”	-
$f_{nr.el}$	Non-renewable primary energy factor of electricity mix	-
$f_{P.nren.C}$	Cooling non-renewable primary energy factor	-

$f_{P.nren.ext}$	Non-renewable primary energy factor of the external heat input	-
$f_{P.nren.H}$	Heating non-renewable primary energy factor	-
$f_{P.nren.i}$	Non-renewable primary energy factor of the carrier	-
$f_{P.nren}$	Non-renewable primary energy factor	-
F_R	Collector Heat Removal Factor	-
$f_{r.i}$	Renewable primary energy factor for energy carrier “i"	-
$f_{t.i}$	Total primary energy factor for energy carrier “i"	-
h_{fi}	Internal convection heat transfer coefficient of fluid "f"	$\frac{W}{m^2 \cdot K}$
h_w	Convection heat transfer coefficient outside the tube "wind"	$\frac{W}{m^2 \cdot K}$
HHV	Higher Heating Value	$\frac{J}{kg}$
I_b	Beam Irradiance	$\frac{kW}{m^2}$
I_{Bn}	Beam Irradiation on the normal plane	$\frac{kW}{m^2}$
I_{Bt}	Beam Irradiation on the tilted surface	$\frac{kW}{m^2}$
k	Thermal Conductivity	$\frac{W}{m \cdot K}$
L	Lenght	m
$LCoE$	Levelized Cost of Energy	$\frac{€}{MWh}$
LHV	Lower Heating Value	$\frac{J}{kg}$
$\dot{m}_{fuel}$	Fuel mass flow rate	$\frac{kg}{s}$
$O_{F.C.i}$	Fix operational costs for cooling service only	€
$O_{F.H.i}$	Fix operational costs for heating service only	€
$O_{F.HC.i}$	Fix operational costs shared between heating and cooling service	€
$O_{V.C.i}$	Variable operational costs for cooling service only	€

$O_{V.H.i}$	Variable operational costs for heating service only	€
$O_{V.HC.i}$	Variable operational costs shared between heating and cooling service	€
$OPEX_{F.C}$	Total normalized fix operational costs for cooling	$\frac{€}{kW}$
$OPEX_{F.H}$	Total normalized fix operational costs for heating	$\frac{€}{kW}$
$OPEX_{V.C}$	Total normalized variable operational costs for cooling	$\frac{€}{kW}$
$OPEX_{V.H}$	Total normalized variable operational costs for heating	$\frac{€}{kW}$
P_b	Usefull heat generated Boiler	W
P_C	System cooling capacity	kW
$p_{exp.i}$	Price of energy exported by energy carrier "i"	$\frac{€}{kW}$
P_H	System heating capacity	kW
$Q_{C.del}$	Cooling delivered	kWh
$Q_{H.del}$	Delivered heat	kWh
$Q_{HC.del}$	Heat consumed for cooling production at the consumer side	kWh
Q_{ext}	External heat input	kWh
$Q_{j.C}$	External heat input used exclusively for cooling applications	kWh
$Q_{j.H}$	External heat input used exclusively for heating applications	kWh
$Q_{j.HC}$	External heat input used for cooling and heating applications (shared)	kWh
Q_{Loss}	Receiver heat losses	W
Q_{Fuel}^{BO01}	Rate of energy entering the boiler through the fuel combustion	kW
Q_{In}^{CAC01}	Rate of energy entering the cycle through the generator	kW
Q_{L}^{BO01}	Energy loss rate from the boiler	kW

$Q_L^{PI01/PI02}$	Energy loss rate from the pipes	kW
Q_L^{ST01}	Energy loss rate from the storage	kW
Q_{Rej}^{CHI01}	Rate of energy being rejected in the cycle through the condenser	kW
Q_{Source}^{HP01}	Rate of energy being rejected or absorbed by the cycle	kW
q'_u	Useful energy gain per unit of collector length	$\frac{W}{m}$
Q_u^{COL01}	Usefull power from collector	kW
$Q_u^{PU01/PU02}$	energy transmission rate by the pumps into the fluid due to inefficiencies	kW
RER_C	Cooling Renewable Energy Ratio	-
RER_H	Heating Renewable Energy Ratio	-
S	Irradiation per Collector area	$\frac{W}{m^2}$
$\sum_j Q_{del.j}$	Delivered heat	kWh
T_{amb}	Ambient temperature	K
T_{amb}	Temperature ambient	K
T_f	Fluid temperature	K
T_r	Receiver temperature	K
U_{cond}	Heat transfer coefficient conduction	$\frac{W}{m^2 \cdot K}$
U_L	Overall heat loss coefficient	$\frac{W}{m^2 \cdot K}$
W_U^{CAC01}	Work done by the absorber cycle (mostly cycle pump)	kW
W_U^{CHO01}	Work done by the compression chiller cycle (mostly cycle compressor)	kW
W_U^{HP01}	Work done by the heat pump cycle (mostly cycle compressor)	kW

Chapter 1

Introduction

1.1 Actual energetic context

The energy context has suffered a rapid shift in context over the past few years. Following the signing of the Paris Agreement [1], efforts have been made to reduce CO_2 emissions. However, especially from a European standpoint, the rise in natural gas prices has accelerated decarbonization by adding an economic driver to it, apart from its obvious environmental benefits.

Focus will be made on what this study can inflict on, that is, domestic consumption, in particular, those where thermal energy supply can impact, space heating and cooling, and domestic hot water (DHW) generation.

A dual analysis will be made regarding the consumption in Europe and Spain. While quantitatively, Spanish heat demands in the domestic sector are not dominant at a European level, adding up to a total of approximately 5.6% of the total European consumption for this use, the distribution seen in the different applications of this energy follows a trend [2]. It is visible and coherent that space heating in Spain does not account for the same percentage of consumption as in Europe, as Spain is placed more in the hot-weather spectrum of Europe (as visible in Figure 1.1).

Examining the distribution of different fuel sources used for this production has led us to a contrasting scenario. Figure 1.2 illustrates that fossil fuels (natural gas, oil and petroleum products), continue to significantly contribute to energy generation for heating purposes in the residential sector.

From a Spanish standpoint, although renewables play a larger role in heat generation compared to the European percentage average, the significant reliance on fossil fuels (particularly oil and petroleum products, which seem even obsolete at this point) suggests that there is still room for improvement. Moreover, the amount of natural gas consumed for water heating could also be reduced. The decrease of up to 225,000 TJ in greenhouse gas-emitting fuels (90 from oil and petroleum sources and 135 from natural gas) could be offset by the use of renewables and biofuels, as well as other technologies such as heat pumps.

A way of introducing renewables into heat generation is the implementation of district heating (DH), which gives the possibility of planning generation in a centralized manner, which will be further explained in the following section (Section 1.2). An intriguing element

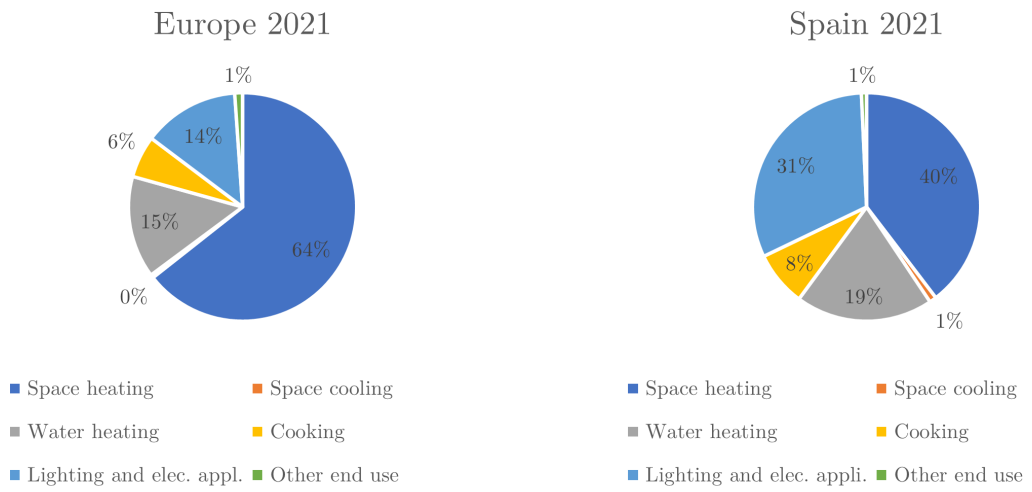

Figure 1.1: End-user energy consumption distribution in EU and Spain by use [2]

of district heating implementation in Spain is its limited adoption, despite the widespread use of renewable energy sources throughout the country. This observation, as highlighted in reference [3] and summarized in Figure 1.3, suggests ample opportunities for the installation and expansion of district heating systems within Spain. Within the Wedistrict project, special attention was put on the evaluation of the socio-economic barriers for District Heating and Cooling (DHC) in Spain and other countries such as Poland.

In the cases of these two countries (Spain and Poland), we find two distinct situations. Spain has an interesting renewable percentage for its lack of district heating implementation, whereas Poland finds itself in a more clear advantage, The Market share of district heating is already high (around 40%) but renewable use is in the order of 20%. This means that while DHNs are already installed in the country, these are not being supplied by renewable means. This phenomenon can be observed in Figure 1.4 which shows the broad use of solid fossil fuels (primarily coal) for the production of said heat. An abnormal situation in Figure 1.3 is visible in Iceland, where a heavy geothermal resource was harvested, this renewable energy shows there is no unique magical solution for all locations, but the real struggle is to find the correct technology for each one.

Currently, District Heating Systems (DHS) are being tracked by the IEA (International Energy Agency) as one of the fifty components of the energy system that are critical for clean energy transitions [4]. The outlook is still not promising, as growth in DHS does not show the expected results to achieve the IEA's Net Zero Emissions by 2050 Scenario (NZE) [5].

Two factors are concerning. First, actual installations of DHS rely worldwide primarily on fossil fuels, still dominating district network supplies globally (about 90% of total heat production). Secondly, the technologies needed to decarbonize heating are readily available and mature (heat pumps, biomass boilers, solar thermal, etc.), which implies that not only existent DHS not sufficiently implementing renewable technologies, but also, new networks are not being built using more environmentally friendly alternatives.

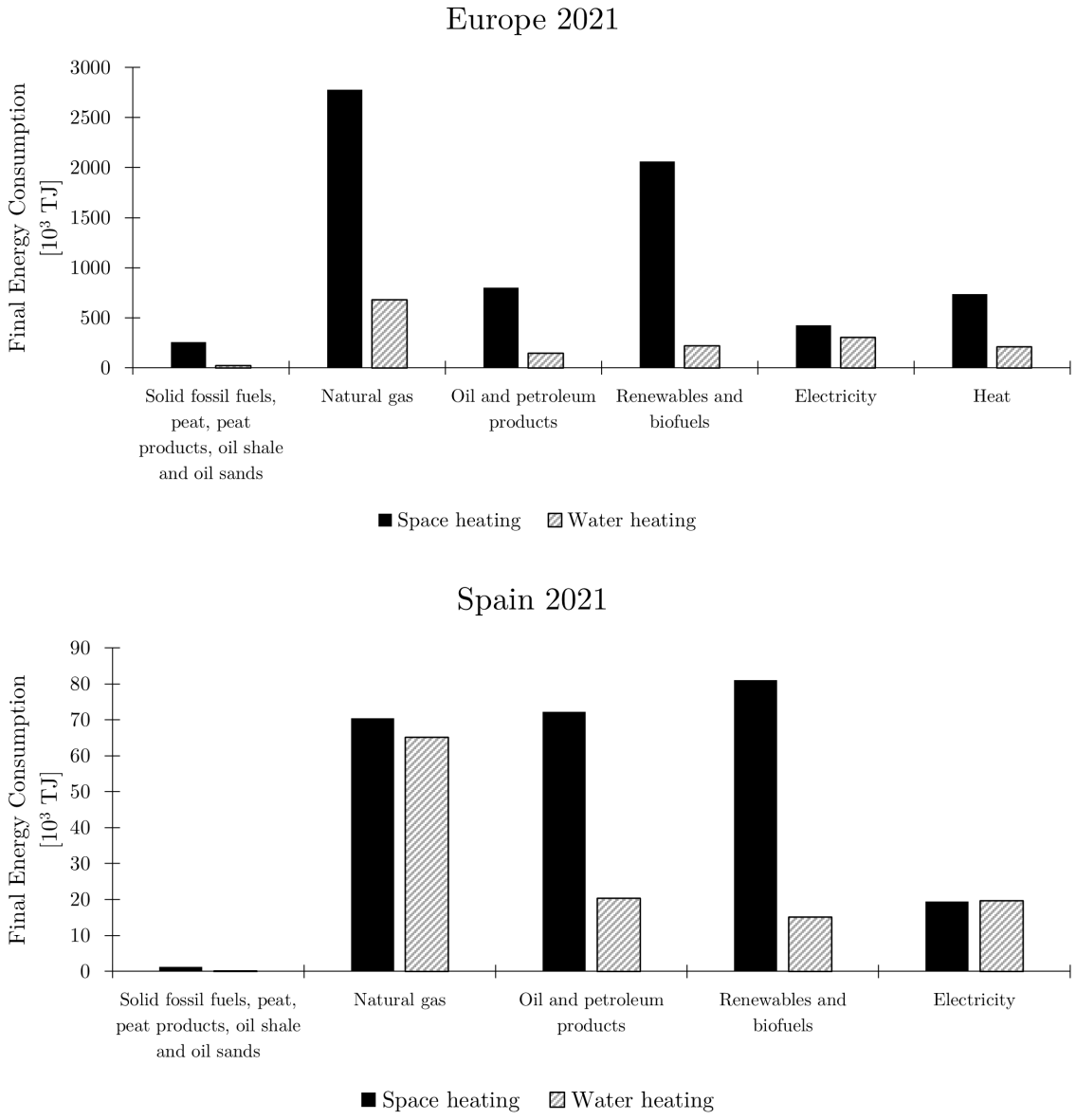

Figure 1.2: Energy consumption distribution in EU and Spain by fuel [2]

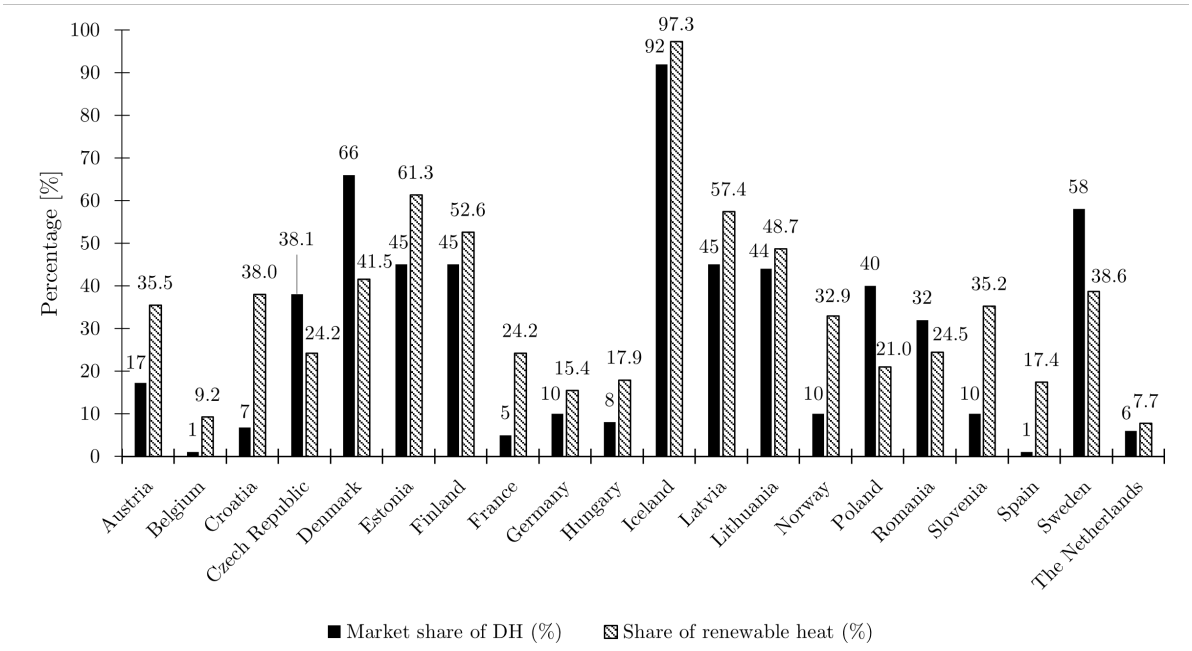

Figure 1.3: Market share of DH vs renewable heat [3]

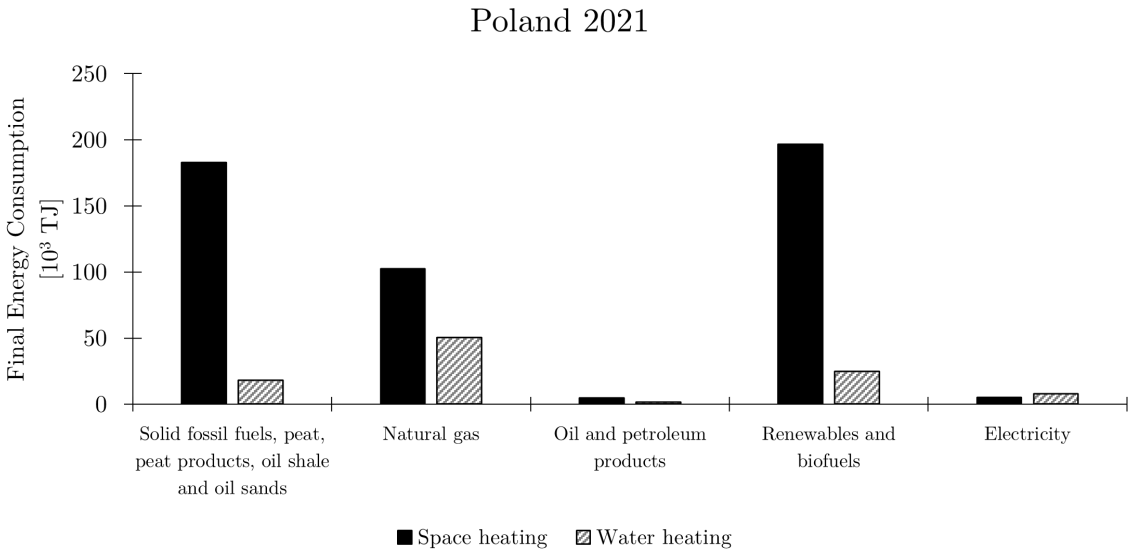

Figure 1.4: End-user energy consumption distribution in Poland by use [2]

1.2 District Heating Systems

Different authors have pinpointed the birth of district heating in different milestones throughout the years, even saying that the Roman baths could be marked as the first one [6]. However, the first district heating network can be dated to France in 1334, but it was not until the late 19th century (the 1870s) in the United States that the term was used for the first time [7]. In this case, thermal distribution was not considered to provide heating per se, but the steam supplied was used to produce electricity in the different buildings connected prior to the installation of electrical networks. In this chapter, what components it takes to consider a district system as such, will be analyzed, along with the evolution of the concept in the last years.

1.2.1 Description

To provide a comprehensive definition of district heating systems, it is important to identify three key components (visible in Figure 1.5).

Firstly, the generation side of these systems has traditionally relied on centralized approaches; however, there have been noteworthy shifts in design principles over time.

Secondly, the network aspect, known as the district heating network, enables the efficient distribution of heat to residential and commercial buildings within a defined area. The connection methods within this network have evolved with technological advancements and enhancements in design and isolation strategies, which reduce heat losses.

Lastly, consumers in the district heating system are transitioning from passive roles of solely relying on the network to becoming active participants. Some consumers now contribute to heat generation through renewable energy sources or heat pumps. The demand pattern set by consumers has a significant impact on the overall generation requirements of the system, emphasizing their critical role in production.

The variation of these three components led to different generations in district heating as described thoroughly by Lund in his articles [8], [9], and summarized in figure 1.6. These generations will be further explained in the following sections.

One of the fundamental concepts of district heating is to utilize and recycle heat that would otherwise be wasted, leading to a more efficient utilization of primary energy and natural resources. In this way, strongly industrialized cities could take advantage of waste heat from metallurgy and other heavy industries. Independent of the source, district heating systems of all types require a method for transferring heat between the distribution network and the consumer. Substations, which can be compared to electric transformers in electricity grids, include heat exchangers and hydraulic components that isolate consumers from the heat distribution network. This allows energy (heat) to be converted from a higher level to a lower level by reducing temperature and related parameters. The efficiency of this heat transfer depends on the design of substations as well as the difference between supply and return temperatures. Current substation technology is designed to operate with annual supply/return temperatures around 69°C/34°C (Δ T = 35°C), and modern district heating systems can typically function within $\pm$ 5°C range near these temperatures [10]. The operating temperatures of district heating networks typically differ according to national

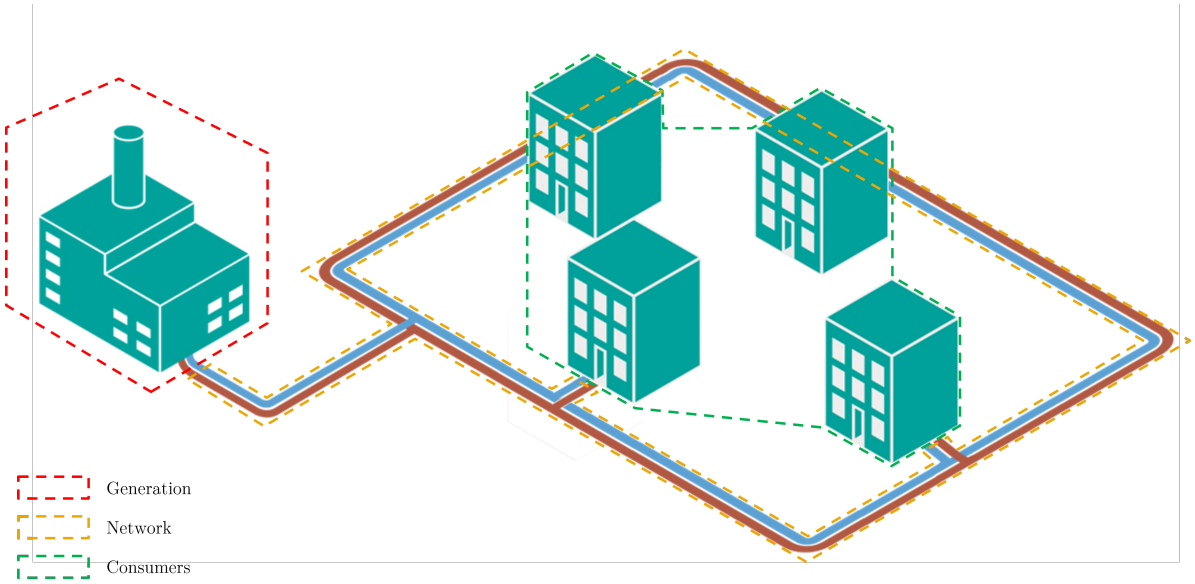

Figure 1.5: District heating components

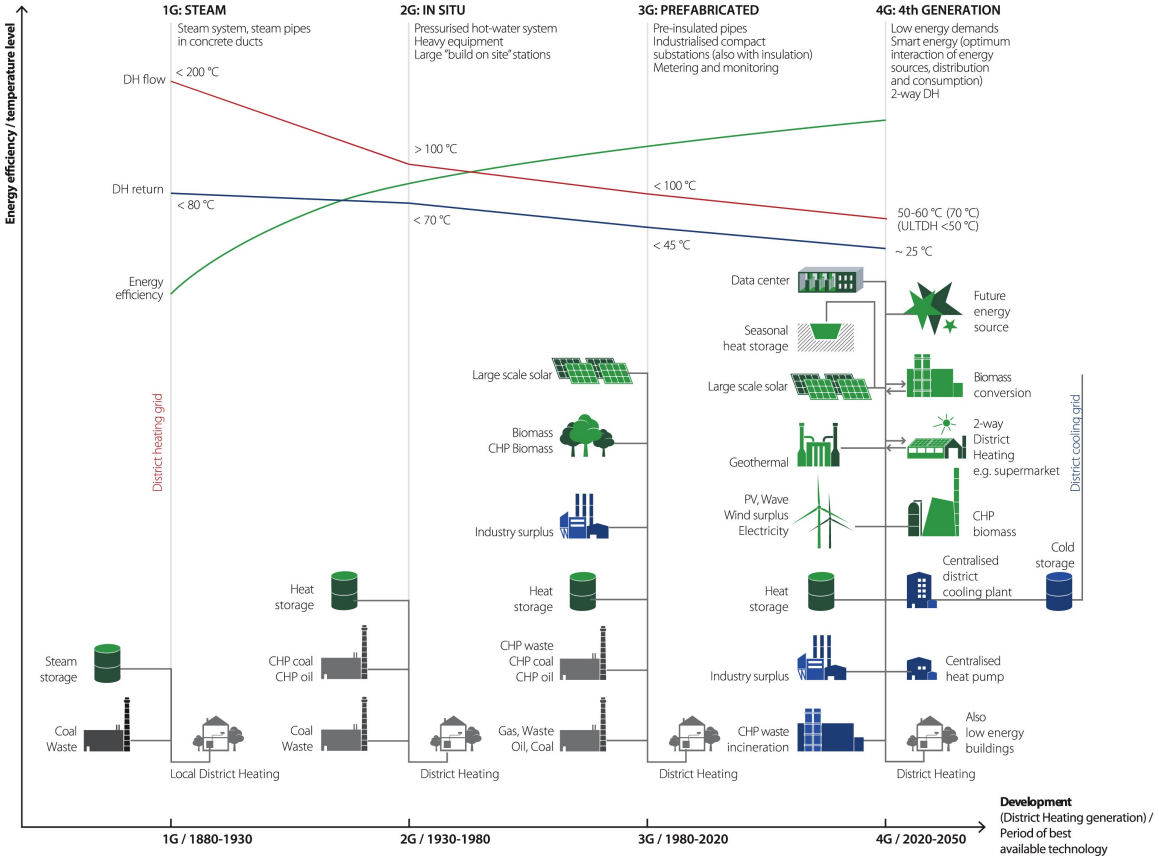

Figure 1.6: Evolution in the generations of District Heating [9].

regulations and design guidelines. Table 1.1 provides an overview of various national design temperatures.

Temperatures [°C]			
Country	Supply	Return	DHW
Denmark	70	4	<60
Finland	70	40	55
Korea	70	50	55
Romania	95	75	-
Russia	95	75	50
United Kingdom	82	70	65
Poland	85	71	55
Germany	80	60	55

Table 1.1: Overview of some example national design temperatures for heating networks [10]

1.2.2 Advantages and Disadvantages

Advantages

District heating offers significant advantages, such as reduced heating costs during periods of high international fuel prices and the ability to internalize environmental impacts by incorporating damage costs into taxes or fees. It is especially beneficial in densely populated urban areas with concentrated heat demands, where distribution costs are minimal [11]. A vast majority of the literature discusses combined heat and power as the most efficient technology for district heating, however, this advantage has also been discussed by Huang in [12] for systems with solar systems. Another interesting comparison has been made against DH actual alternative, which is individual heating, by Dorotic in [13], which returned important favorable results when considering carbon allocation for the actual production for both alternatives.

Once production is centralized, the possibility of adding more renewable sources to the mix becomes attractive. Moreover, the recycling of heat from industrial sources could become an additional input that otherwise would be lost. This advantageous use of priorly wasted energy improves LCoE in a straightforward manner, as mentioned in section 1.2.1, and described in Doracic's paper [14].

The importance of security of supply should also be mentioned [15], as dependence on fossil fuels could lead to failure in supplying energy in unstable political situations as the latest gas crisis has shown.

Disadvantages

Network prices present a big disadvantage for DH systems. In contrast to the advantages discussed for densely populated areas, it is less competitive in suburban and rural areas with dispersed heat demands where distribution costs increase [16]. Another context that hinders

DHC implementation is when international fossil fuel prices are low which makes technologies based on these fuels more economically viable. In addition, the technological complexity concerning intermittency and maintenance availability affects, either due to the implementation of reliable and well-dimensioned storage for long-term supply (energy reserve), or the distance to technical services, especially in rural areas.

1.2.3 District Heating generations

In this section, a summary of the different "generations" of DH will be done. The idea is to comprehend the vital differences between each one of the implementations of DH throughout history to understand where the future of this technology is heading.

First Generation DH

The initial generation of district heating systems utilized steam as the heat transfer medium, as previously mentioned. These systems were first implemented as heat suppliers in the United States during the 1880s. Steam-based technology was commonly employed in both American and European district heating systems established before 1930. Typical components included concrete-encased steam pipes, steam traps, and compensators. However, the modern-day perspective considers such steam-powered systems outdated due to substantial heat losses caused by high temperatures and potential safety hazards like explosions that have resulted in pedestrian fatalities. Additionally, corrosion issues with condensate return pipes often lead to reduced returns and decreased energy efficiency [8]. The main objective of implementing these systems in society was to minimize the risk of boiler explosions and enhance comfort by replacing individual boilers in apartment buildings. In most cases, heat delivery is facilitated through radiators using condensation. While steam remains the primary heat carrier in older systems like those found in Manhattan and Paris, replacement initiatives have been carried out in various European cities.

Second Generation DH

After the realization of the safety hazards, and material decay, that accompany steam transport, the second generation of systems was characterized by the use of pressurized hot water as the heat carrier. The use of pressurized water in these systems involved the use of supply temperatures typically exceeding 100°C. These systems were prevalent from the 1930s to the 1970s and featured components such as water pipes in concrete ducts, large tube-and-shell heat exchangers, and heavy valves that required a lot of material. The specific reasons for adopting this technology varied slightly between countries and cultures but generally focused on achieving fuel savings and improving comfort through combined heat and power (CHP) utilization. The introduction of government policies and planning initiatives aimed to facilitate coordinated expansions of CHP in urban areas.

Third Generation DH

The introduction of the third generation of systems in the 1970s marked a significant shift in district heating technology, and it quickly gained popularity as new installations continued

throughout the 1980s and beyond. In this generation, pressurized water is still utilized as the heat carrier; however, there has been a decrease in supply temperatures which often fall below 100 °C. This innovative approach includes key components such as prefabricated pipes that are directly buried into the ground, compact substations featuring plate stainless steel heat exchangers, and material-efficient equipment. The adoption of this technology extends to Europe and former USSR countries where it replaces old systems. Furthermore, all new developments worldwide utilize this advanced third-generation technology for effective space heating solutions. Typically, the main driving factor behind this generational shift was the desire to ensure a reliable energy supply in response to two oil crises. This led to an increased emphasis on energy efficiency through CHP systems, as well as substituting oil with more affordable local fuels like coal, biomass, and waste. Additionally, in certain locations solar and geothermal heat sources were utilized as supplementary forms of energy.

Fourth Generation DH

In his article, Lund determines five challenges to fulfill in order to consider a system to be part of the fourth generation DHS [8]. Which are,

- The ability to supply low-temperature district heating for space heating and domestic hot water to existing buildings, energy-renovated existing buildings, and new low-energy buildings.
- The ability to distribute heat in networks with low grid losses
- The ability to recycle heat from low-temperature sources and integrate renewable heat sources such as solar and geothermal heat.
- The ability to be an integrated part of smart energy systems (i.e. integrated smart electricity, gas, fluid, and thermal grids), including being an integrated part of 4th Generation District Cooling systems.
- And lastly, the ability to ensure suitable planning, cost, and motivation structures in relation to the operation as well as to strategic investments related to the transformation into future sustainable energy systems.

While these challenges seem numerous, two principles could lead to the fulfillment of them all. The main one is the reduction in the temperature of the network, which would lead to the fulfillment of the first three challenges mentioned, supplying low-temperature district heating for space heating and DHW, being the first. The ability to distribute heat in networks with low grid losses would be fulfilled as a collateral result of the first because by reducing the temperature of the network, losses would ultimately be reduced as well. The ability to recycle heat from low-temperature sources and integrate renewable heat sources such as solar and geothermal heat, would also be possible by reducing the network temperature because the temperature of these new sources would not have to be that high. The fourth and fifth challenges would be solved by the implementation of already existing advanced measurement and control devices.

So the main difference between third and fourth-generation networks would be the temperature setting and the implementation of control strategies and measures already available.

Fifth Generation DH or Neutral Temperature Networks

While often mentioned as fifth-generation District Heating Systems (DHS), some new networks developed at the same time as fourth-generation DHS. While fourth-generation DHS have low temperatures, these new systems lower the temperature even lower than the minimum required to produce space heating in modern buildings (around 40°C with the use of large area exchangers).

In this thesis, we will refer to these systems as Neutral Temperature Networks (NT-DHC) as was done by Calitxo et. al in their article [17]. This is based on the temperatures used by these networks (from 10 to 25°C).

The main reason to differentiate these systems from the aforementioned generations is due to how these systems change the centralized generation to a decentralized approach. This principle benefits from reduced losses in the distribution of higher temperatures but continues to generate a distributed network to supply water to decentralized heat pumps scattered among the different consumers, which would potentially give the system the possibility of generating both heating and cooling. It also requires a significant electricity consumption apart from the thermal heat.

As this approach differs substantially from the one used in the different generations, it seems coherent to address it outside of this terminology.

1.2.4 District Cooling generations

An equivalent analysis will be done for DC systems as it was done for DH generations. Different generations will be analyzed by their characteristics to identify past and future tendencies.

First Generation DC

Cooling systems of the first generation utilized pressurized brine or ammonia networks. The initial implementation of an ammonia system occurred in Denver in 1889, where it made use of an absorption chiller with a capacity of around 105 kW. This system employed a three-pipe distribution setup to generate cold for a storage warehouse with approximately 1400 m^3 capacity. Liquid ammonia was transported through the distribution pipes that were linked to 29 cold boxes within the warehouse. Each box underwent an expansion process at its entrance to lower temperatures suitable for cooling.

The introduction of piped refrigeration systems brought about convenient and cost-effective refrigeration compared to alternatives such as ice deliveries, which required space and emitted moisture into the air while being difficult to regulate and struggling to achieve low temperatures. In contrast, piped refrigeration systems occupied minimal space, provided dry air, could be controlled by adjusting the expansion valve, and even offered freezing capability when necessary.

The Denver system was soon closed, but a similar system established in St. Louis in 1890 survived until the 1960s when it was discontinued due to interference with new highway construction. This system represented the initial use of comfort cooling alongside commercial cooling, although solely for demonstration purposes. The distribution of brine through

underground pipes was pioneered by the Manhattan Refrigeration Company in 1906 within a New York City district that housed a power plant and nine cold storage warehouses. This advancement paved the way for large warehouse cooling, refrigeration of small market buildings, ships, and more throughout New York City, remaining operative until 1979. As a result, these systems primarily offered refrigeration services to concentrated areas within the food supply chain markets. Other pipeline refrigeration systems were also implemented in various cities such as Boston, Los Angeles, Kansas City, Baltimore, Washington DC, Philadelphia, Atlantic City, Seattle, Minneapolis, and Phoenix, characterized by centrally generated cooling potential serving customers with refrigeration demands [18].

Second Generation DC

District cooling technology underwent a significant transformation during the 1960s and 1970s when second-generation systems were introduced. Instead of relying on numerous small chillers, these new systems utilized a combination of larger compression chillers along with absorption or river cooling as supplementary sources to fulfill comfort cooling requirements. The initial implementation of this system took place in Hartford, USA, central business district in 1962, combining both absorption and compression chillers while incorporating cold storage in 1986. These chillers were powered by steam from the company's district steam system, creating a beneficial synergy between heating and cooling operations. In Europe, Paris' western suburbs saw the establishment of the first major district cooling system in 1967. This extensive network serves multiple office buildings across La Defense area through interconnected networks operated jointly by Enertherm and SOC companies. All second-generation systems share a common feature: the predominant use of large compression chillers in the cold supply, with limited utilization of heat recovery and cold storage. In general, second-generation district cooling shifts its focus from the food industry towards providing cooling for comfort purposes. The system is further simplified as the end-user no longer has any part in the cooling generation, unlike it was with a decentralized evaporator [18].

Third Generation DC

Third-generation cooling systems emerged in the 1990s when CFC was initially replaced, and later HCFC (hydrochlorofluorocarbons) refrigerants were substituted as per the Montreal Protocol (1987) [19]. This led to opportunities for DC systems. An early example is the Climespace system established in Paris city center in 1991, which incorporated the central Les Halles cooling plant from 1978 as a significant capacity asset. Subsequently, the Seine River was utilized as a heat sink. Cold is produced at ten cold supply plants with a cold storage capacity of 140 MWh. This system currently boasts one of Europe's highest annual capacities for delivering cold among all DCs, at almost 500 GWh per year [18].

Third-generation DC systems boast a wide array of cold supply options, such as natural cooling, absorption chillers, heat pump cold recovery for heating, compression chillers, and short-term cold storage units. These systems also incorporate synergy with combined cooling, heating and power configurations (trigeneration) by utilizing absorption chillers in some cases. Some third-generation systems emphasize the use of locally available resources

while phasing out refrigerants with high ozone layer depletion characteristics. Additionally, energy efficiency is prioritized by recycling waste heat into local district heating grids in Scandinavian systems.

Fourth Generation DC

The first three generations can mainly be understood through their differences in distribution fluids, cold generation, and storage facilities. As we look ahead to the future and consider the increasing levels of renewable energy, fourth-generation district cooling emerges as a concept. The key driver for this new generation is its integration into smart energy systems across different sectors, leveraging combined heating and cooling synergies where possible. In this approach, surplus heat obtained from cooling during summer can be used to meet heating demands in winter, while surplus cold from heat pump-based heating in winter can offset cooling needs in summer. Fourth-generation district cooling also heavily relies on long-term thermal storage to provide flexibility that enables seamless integration with other energy sectors. This level of smart integration not only accommodates variable renewable energy sources but also supports the transition towards carbon-neutral renewable energy-based systems [18].

It can be summarized that fourth-generation district cooling systems work in coordination with other energy sectors such as electricity and heating. These systems use centralized and/or decentralized technologies like electric heat pumps, absorption heat pumps, ambient sources, and cold storage facilities to fulfill the cooling requirements of residential, commercial, and industrial contexts. The main motivators for this strategy are the smart integration of energy systems and the utilization of combined heating and cooling synergy.

1.2.5 Actual situation

Existing DH networks There is a difference in availability between electrical networks' information and district heating networks' information. As was pointed out by Pelda in his article [20], in 2013, the European Commission implemented Regulation Number 534/2013, which obliged electricity network operators in the European Union to demonstrate transparency across multiple aspects. As a result of this regulation, information regarding the electricity grid, power generation, consumption, and trade has been made available to the public. This scenario is not equivalent in the heating sector, where suppliers are not forced to share their information. Some databases are available but not all have complete information. For example, there are databases focused on different technologies, such as the case of GeoDH [21] which possesses information on geothermal district heating networks up to 2014 with their power, and also information on the presence of DH networks in different cities but without information on the installed capacity or characteristics.

The District Heating Atlas (DHA) [22] presented by Pelda in his article, shows a great advance in this regard. DHA shows information on different district heating networks with, not only their installed capacity, but often temperatures used for the supply and return that may orient the users as to which generation those DHN could belong (Figure 1.8). Unfortunately, it is only available at national level (Germany).

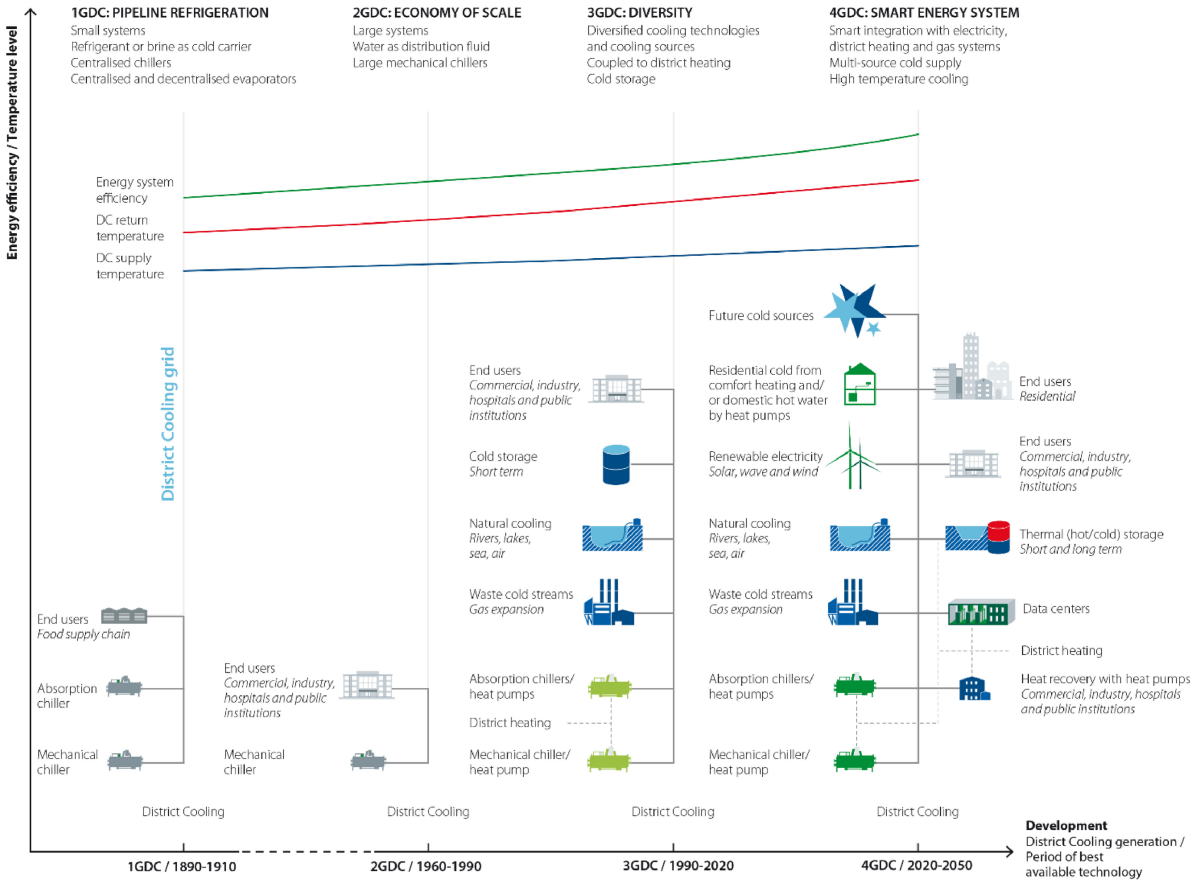

Figure 1.7: Evolution in the generations of District Cooling [18].

Another approach was taken in France, where the association "Via Sèva" has a similar map [23], but instead of installed networks, shows places where installation of networks could be economically interesting to develop, to supply through DHN 90% of France's heating energy.

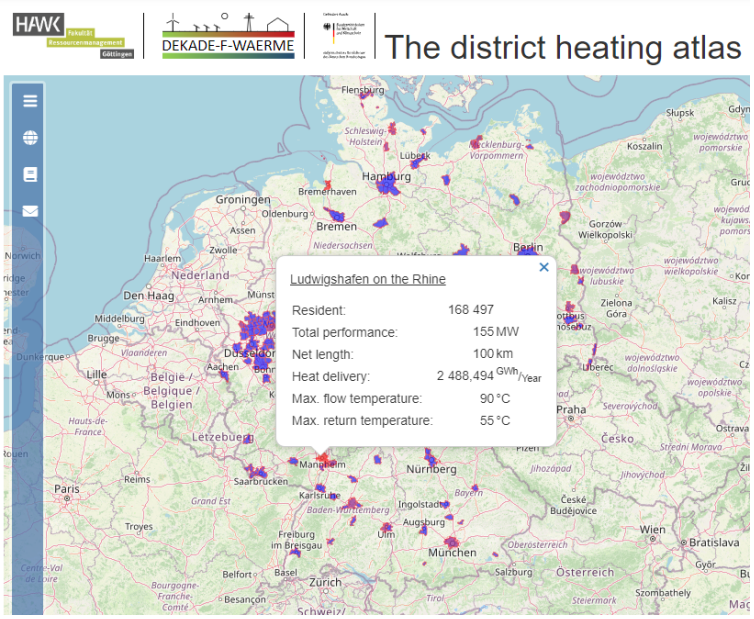

Figure 1.8: District Heating Atlas [22].

The truth on installed DH capacity shows that growth in DHS has not been directed into decarbonizing but more as an advantageous decision when cogeneration plants yielded promising economic results. These results can be observed in the installed capacities for the different countries of the EU (Table 1.2). These capacities are in line with what was shown on market share in Figure 1.3. As mentioned before, information is not as available as it is with electricity, a thorough report was made by the European Union with different sources of information, this is the "Overview of District Heating and Cooling Markets and Regulatory Frameworks under the Revised Renewable Energy Directive" [24]. This document shows technology distribution values as fuel source information on existing DHS. These values depict a grim panorama of DHS. Not only DH systems are not triumphing on a European scale, having only around 9% of market share at this level. But even more, this installed capacity is not as renewable as it could be. Only 27% of this installed capacity could be considered renewable, having 10% of the total production being purely heat generation from renewable sources, and the other 17% CHP generated from renewable sources. The other non-renewable 73% is driven primarily by fossil fuels, either in CHP generation (52% of the total) or heat-only applications (21%).

Different reports show existing plants and overviews of the installed technologies. Between those made by governmental agencies, it is the example of the European Commission METIS studies [25] and Euroheat's Market Outlook [3]. In the METIS study S9 [25], some examples of different generation's installed networks are available as seen in Table 1.3.

Country	CHP Heat Capacity [MW]	Heat Only Boilers [MW]	Geothermal [MW]	Solar thermal [MW]	Heat pumps [MW]	Industrial excess heat [MW]	Total installed capacity [MW]
Austria	3,855	7,266	76	30	3		11,200
Belgium			17				
Bulgaria	2,888	3,253				232	6,373
Croatia	1,568	589	42				2,199
Czech Republic	12,801	29,884	7		6		42,697
Denmark	9,836	15,268	33	1,089	671	362	25,104
Estonia	520	4,914			20		5,434
Finland	8,328	15,206		1	155		23,534
France	4,351	18,036	430	13	23	237	23,067
Germany	49,781	45,315	335	56			95,487
Greece	312			10			312
Hungary	5,914	2,213	230	14			8,371
Ireland							
Italy	2,871	5,812	134	2	45	44	8,908
Latvia	3,247	2,360		15			5,622
Lithuania	1,832	6,850	18				8,700
Luxembourg							
Netherlands	1,595	4,046	208	11	1		5,850
Poland	18,081	37,054	74	16			55,209
Portugal							34
Romania	4,058	3,679	158				7,737
Slovakia	2,484	12,492	22		2		15,000
Slovenia	528	1,164	47				1,739
Spain	-	1,187	3	6			1,190
Sweden	7,902			27	1,244		
EU-27	**142,751**	**216,588**	**1,833**	**1,290**	**2,170**	**875**	**353,767**

Table 1.2: Total installed heat capacity per technology type (MWth) [24].

Location	Construction	Gen.	Heat Demand [GWh]	Observations	Source distribution
Copenhaguen (Denmark)	1923	2-3	10000	93% residential. 6% tertiary. 1% local industry	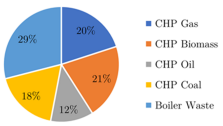
Chemintz (Germany)	1930	3	1000	Heat peak in 2008: 353 MWth Mainly residential and tertiary consumers	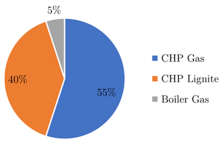
Lyon (France)	1930	3	1000	50 000 households. Residential and commercial consumers.	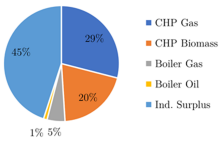
Tartu (Estonia)	1930	3	500	Heat peak in 2015: 328 MW Mainly residential (80 000 buildings)	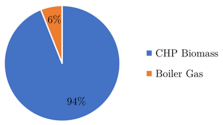
Brescia (Italy)	1972	3	1000	21 000 buildings supplied. 80% residential. 20% tertiary.	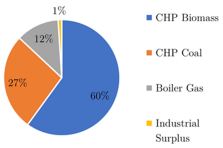
Hamburg Hafen city (Germany)	2014	4	6	Ecodistrict with a low temperature heat demand (30% to 45% below building code requirements)	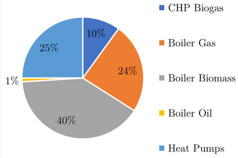
Gram (Denmark)	2015	4	20	1 171 residential buildings. Low temperature. Seasonal storage. 62% solar share.	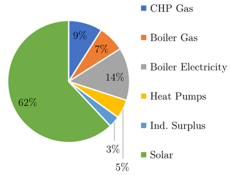
Paris Saclay (France)	2017	4	40	Heat peak: 37 MWth. Mostly tertiary. Two geothermal drills 700m depth at 30°C. Storage.	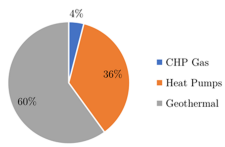

Table 1.3: Existing DHN examples by generation [25].

1.3 Research Methodology

The first state-of-the-art on software available was developed. In this period, the selection was based on which could be versatile enough to simulate all the different technologies that were considered for WeDistrict. TRNSYS was selected, considering that many types were available already in the software's library. All technologies were then translated to the methodology's language while generating corrections in the methodology itself to find a final form to obtain ordered results.

Once these results were achieved, Key Performance Indicators started being calculated through a first methodology, which was still done in a more manual manner, until methodology's development led to a Python script that sped up the procedure.

Communication with other software, such as JEPlus, led to the generation of parametric analysis which made result production faster and automated.

With the automatization of the results, the methodology led to the possibility of generating databases which led to the Tool development.

1.4 Thesis Structure

In the State-of-the-art chapter (Chapter 2), the different situations of the simulated technologies will be described, discriminating between heating, cooling and storage technologies. Then a thorough analysis of the simulation software available will be made. This will lead to differentiating the used software in a wider range of applicable options and singling out the capabilities and limitations of the different software described.

In the Methodology chapter (Chapter 4), the Modular Simulation Methodology is explained, as how the methodology used represented the different technologies. This will cast light on how we went from different technological simulations to complete systems using the different technologies involved in the project. In this chapter, calculations of Key Performance Indicators will be explained, and how were these applied in the project. Also, how the methodology uses these calculations communicating between different software to be able to perform parametric calculations and results.

Technology chapter (Chapter 5), will come as a continuation of the Methodology chapter, showing the implementation of the described methodology to translate the technologies needed for the simulations into TRNSYS and how modeling was done.

Once the theoretical basis has been laid in previous chapters, results are described in their own chapter (Chapter 6). In this chapter, all the different results obtained from the use of the methodology are explained along with which aspect of the methodology made each result possible.

Validation of the results obtained for the constructed demonstration site in NUST (National University of Science and Technology Politehnica) in Romania are discussed in the Validation chapter (Chapter 7).

1.5 Related publications

From this research, different publications and conference participations were produced.

1.5.1 Peer-reviewed journals

One of the first papers published was "Proposal of a Thermocline Molten Salt Storage Tank for District Heating and Cooling" in Applied Thermal Engineering journal [26]. In this paper, the methodology used to replicate the molten salts tank technology in TRNSYS was explained.

"Comprehensive Analysis of Hot Water Tank Sizing for a Hybrid Solar-Biomass District Heating and Cooling" was then published in Results in Engineering journal [27]. In this paper, the methodology's capacity for parametric simulation was tested, looking for optimum design scenarios for a complex network. This paper will be further explained in Section 6.3.

1.5.2 Conference Proceedings

The first conference work to be submitted was 'Development of TRNSYS macros for solar resource integration in a district heating and cooling network: W.E. DISTRICT project" for SolarPACES 2021. In this article, the first development in solar macros was explained for the Alcalá Demo site. This was the first approach to the methodology.

The second conference work to be submitted, in this case as coauthor was 'Proposal of a thermocline Molten Salt Storage Tank for District Heating and Cooling" in Polygeneration 2022. In which the model generated for the molten salts tank was explained. This work was chosen as the best paper of the conference, and led to the paper in Applied Engineering mentioned in 1.5.1.

The third conference work to be submitted was 'Comprehensive analysis of hot water tank sizing for a hybrid solar-biomass district heating and cooling" in CNIT 2022. In which the application of parametric analysis with the MSM was shown. This work then led to the article published in Results in Engineering, mentioned in 1.5.1.

"Analysis of the Experimental District Heating and Cooling Facility in Alcalá in the Framework of the W.E.District Project" was presented in the 16th conference of Heat Transfer, Fluid Mechanics and Thermodynamics (HEFAT) in 2022. This paper describes the work to be done in the Alcalá demo site and how the system was first proposed.

The fourth conference work to be submitted was "Hybrid Solar-biomass with Energy Storage Comprehensive Analysis for District Heating Systems" in SolarPACES 2022. In which the basis of the methodology was first depicted and used for a hybrid case.

There was also "Replacing Fossil Fuels by Renewable Energies in the District Heating Systems: A Case of Study of Mrągowo (Poland)" work, which was based on the work performed for the Demonstration followers described in Section 6.2, and was published in the 11th International Conference On Energy And Environment (CIEM) in 2023.

"Techno-economic assessment of the hybridization of biomass, geothermal heat pumps and PV panels for decarbonizing the Focsani District Heating System" was the work presented for CNIT 2023. In which an economic evaluation was done on one of the solutions proposed for the Demo follower case in Focsani.

"Techno-economic Comparison of a Solar Absorption Chiller and Photovoltaic Compression Chiller" was published for the 36th International Conference On Efficiency, Cost, Optimization, Simulation And Environmental Impact Of Energy Systems, Ecos 2023. In this work, further use of the parametric calculation capacity of the methodology was used but aimed towards cooling networks instead of heating and cooling as was done in previous conferences.

"The WEDISTRICT Tool: An open-access web application to support decisions on district heating and cooling projects around Europe" will be presented in ECOS 2024, as a way of publicly introducing the Tool in an involved environment.

Chapter 2

State of the Art

While district heating systems are becoming increasingly popular, their efficiency and sustainability are highly dependent on the optimization of various parameters such as network dimensioning, heat storage capacity, and integration. However, the design of these systems, while usual in northern European countries is still below European targets in most of the continent. It is essential to meet these targets, to create user-friendly design tools for various demographic settings, such as cities, towns, and villages, in order to cater to a wide range of users beyond just those with a particularly energy-oriented education.

The concept behind the chosen methodology is the use of modules with assigned roles to create complex networks. This chapter will analyze the software available considering the advantages and disadvantages of each one, leading to the final selection for the Modular Simulation Methodology (MSM) case, which will be explained in Section 4. Then, once the possible methodologies have been covered the technologies used in the MSM will be described. In order, heating, cooling, and storage technologies will be covered in the following chapter.

2.1 District Heating Simulation

The simulation of district heating and cooling can be subdivided into the simulation of its different components, already stated in Section 1.2.1. These components are:

1. The generation side (heat/cool source).
2. The energy distribution network.
3. And the consumers (end-users).

These components were also identified in Talebi's et al. article "A Review of District Heating Systems: Modeling and Optimization" [28]. In this article, different limitations in the modeling of these components are approached. These limitations were also underlined by Connolly et al. [29] by stating that one of the possible reasons DHS were being neglected was the lack of tools to analyze them as possible solutions. In this section, the tools used to simulate these different components will be described and compared. The energy distribution network will be left aside, as it will be treated as part of the simulation of the generation side, in case it is simulated in detail, or as a constant loss from standard values and added

to the end-users in most simulations. Also, software developed at the same time this thesis will be described at the end of this section to compare results from a common starting point.

2.1.1 Software Available for Generation Side

More than one commercial software tool exists specifically for modeling DHC networks. Some focus on the individual components of the network such as determining load profile of buildings, although recently researchers have been more motivated to develop a simulation package for the broader system incorporating the distribution network, production sites and thermal loads. However, due to the complexity of modeling heterogeneous systems, no single simulation tool can reproduce the behavior accurately. In Reference [30] Beausoleil-Morrison suggests four approaches for the correct simulation of DHC networks:

- Adding new features to existing tools
- Integrating the source code from one tool into another
- Develop new simulation tools
- Using the co-simulation approach (chosen in the reference)

The first tool to be identified is the simulation program known as TRNSYS [31], which stands for "transient system". TRNSYS was initially created to model solar-based thermal systems for water heating applications. Over time, it has expanded its range of features to include the simulation of larger-scale thermal and electrical energy systems. The software includes a library with various components such as pumps, fans, solar collectors, cogeneration units, and wind turbines that can be used to create detailed models. Each component is defined by a specific set of governing equations. However, it should be noted that TRNSYS is specifically designed for simulating energy systems and may not be suitable for modeling energy flows at broader district or city levels.

Another tool used for simulation is EnergyPRO [32], which is a software tool that enables the optimization of complex energy systems for combined electrical and thermal supply. It offers various technologies, including thermal and battery storage, which can be selected as needed. The modeling approach used in EnergyPRO is simplified, with building heat demand based on degree days and manual input of network heat losses calculated separately. The software allows for operational cost optimization to ensure the most economical electricity consumption within the system; however, it does not include a retail market pricing module.

A more utilized software is EnergyPlus simulation tool [33], which is primarily designed for building-level simulations, but it can also be utilized to simulate district networks, renewable technologies, and external airflow. However, these simulations may involve some level of simplification. In cases where the interactions between buildings are limited, multiple EnergyPlus models can be used to represent different buildings within the district. If simulating all buildings in a large district becomes impractical, representative archetype buildings can be simulated instead with results extrapolated for other buildings.

A different tool is PLEXOS [34], a versatile software that allows for the modeling of various systems, including electric power, water, and gas. While it does not have specific

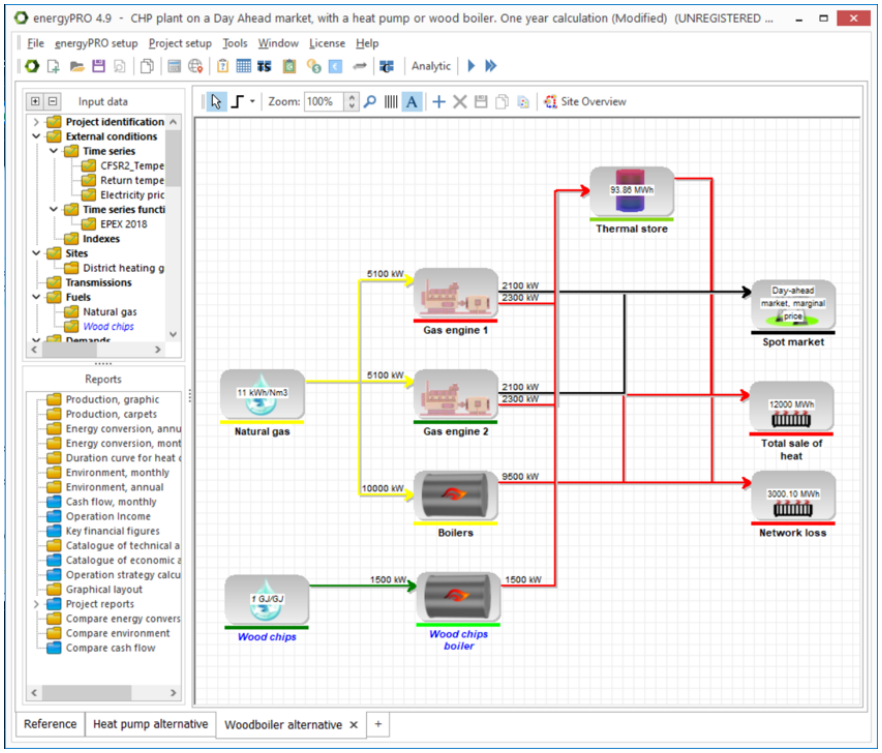

Figure 2.1: EnergyPRO example screen.

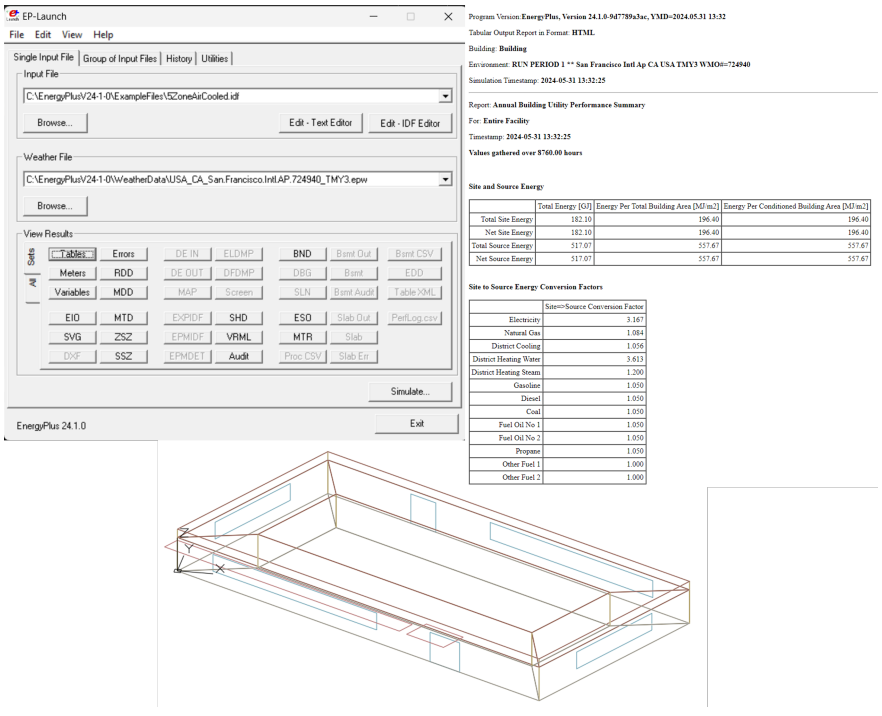

Figure 2.2: EnergyPlus screen.

functionality for hydraulic continuous networks, approximations can be made using its gas features combined with constraints. Gas pipelines are modeled similarly to water pipes due to hydraulic transients. However, PLEXOS falls short when it comes to considering both thermal and hydraulic properties in the case of hydraulic continuous networks. Nevertheless, one notable feature of this tool is its ability to perform market modeling, pricing analysis, and network optimization.

Even though it was not specifically designed for network simulations, the software Polysun [35] (Figure 2.3) offers in-depth hydraulic modeling capabilities that can simulate energy flows and pumping power requirements for district heating networks with decentralized pumps. While the approximation of building load is used, there are some limitations on the available selection of technologies.

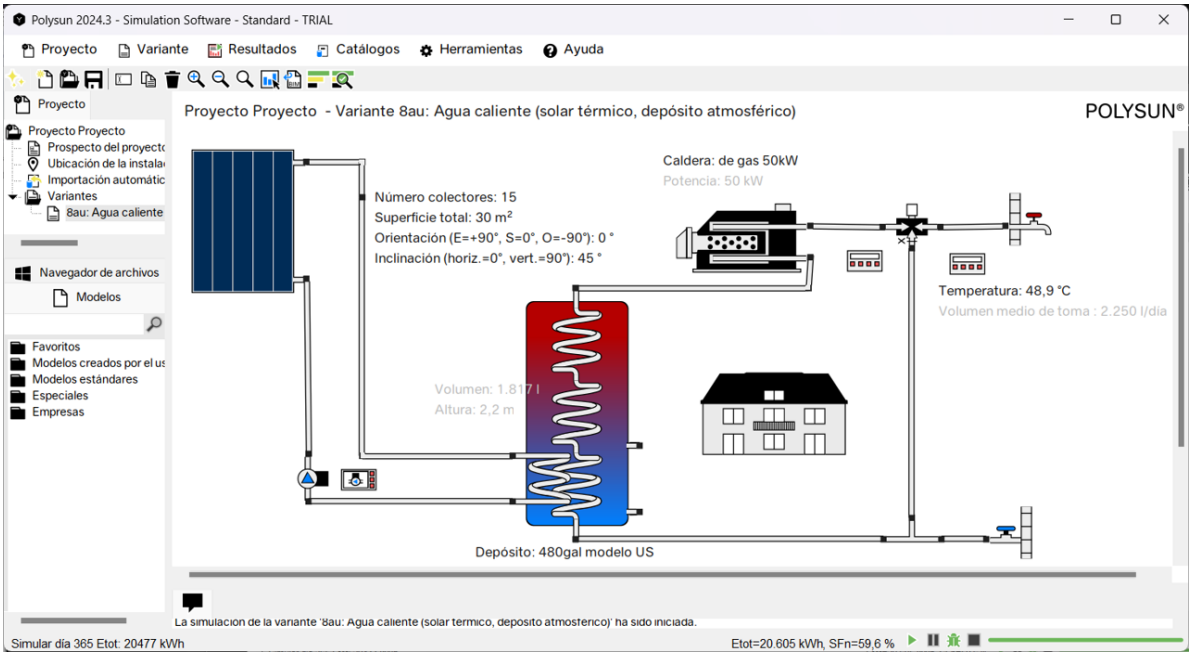

Figure 2.3: Polysun example file screen.

Last but not least, EnergyPLAN [36] is a versatile simulation tool (Figure 2.4) that allows users to analyze and compare different energy systems using various fuel sources and technologies. Users can conduct technical simulations without considering electricity market structures or pricing, as well as market-economic simulations. EnergyPLAN offers several advantages, including the ability to model entire systems with multiple sectors, aggregating units into representative ones to reduce data requirements, and quickly simulate user-defined scenarios. To optimize scenarios, users should have some level of experience and expertise, since detailed operation of individual units is not included in order to save computational time.

In Reference [37], Brown does a good job identifying these different tools and evaluating them for their capabilities. The tools which were singled out as most useful have been summarized in Table 2.1.

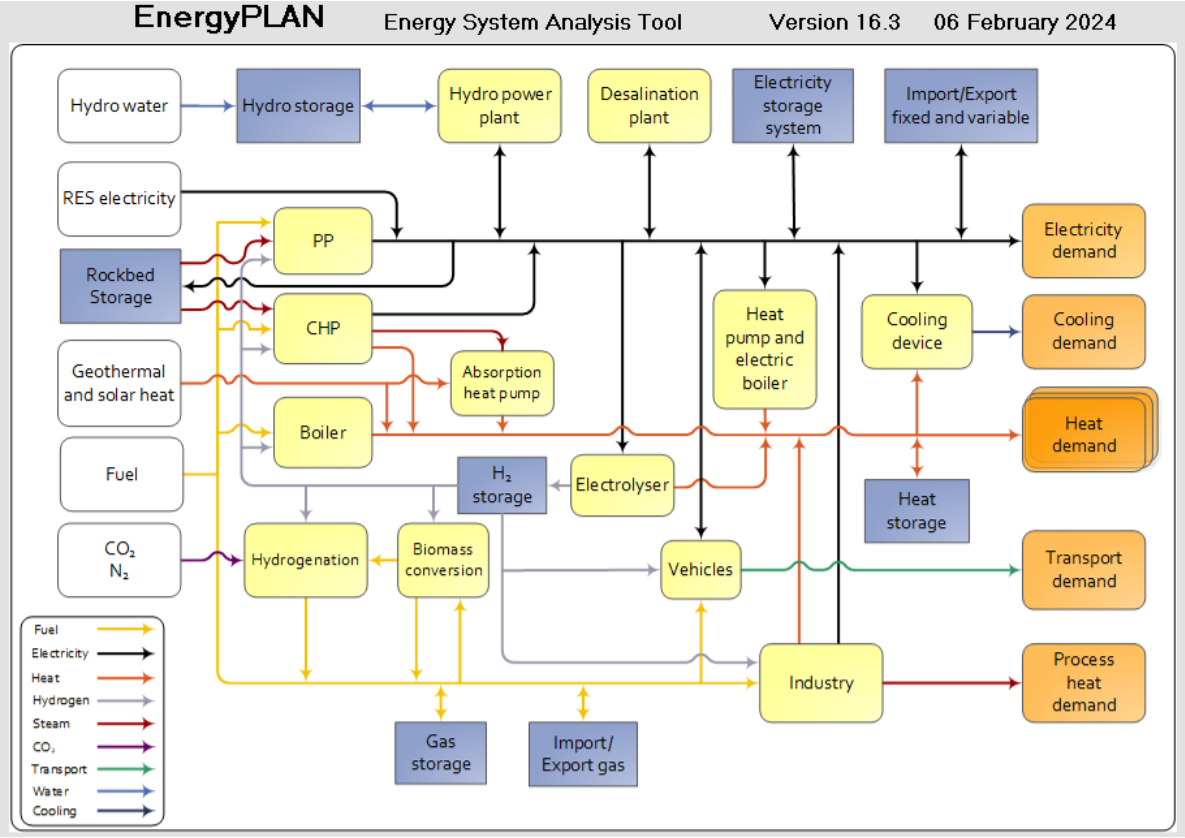

Figure 2.4: Energyplan home screen.

Modelling tool	Limitation
TRNSYS	Designed for energy system simulations and unsuitable for general energy flows at district or city levels.
EnergyPRO	Retail market pricing module is not incorporated.
EnergyPLUS	It is simplified. Not designed for DHN although can adapt.
PLEXOS	Cannot consider thermal and hydraulic properties.
Polysun	Limited Selection of technologies.
EnergyPlan	Detailed operation of individual units is not captured in order to lower computational time. Experience is required to identify the optimal scenario.

Table 2.1: Software used for DHC simulation and their limitations.

2.1.2 End-users

When simulating demand for district heating two approaches are available. Detailed simulation of all buildings involved in the district. Or the estimation of the demand considering the district as a whole using models. These two approaches can also be subdivided by methodologies shown in [28].

- Historical methods: Historical data from both the demand and supply sides is used to model the demand profile of the system.
- Deterministic methods: Deterministic methods, also known as simulation-based techniques, utilize mathematical representations of the physical behavior of buildings. Depending on the information input into these models, they can be categorized into simplified models and complex models that account for more detailed and specific characteristics of the buildings.
- Predictive time-series methods: these models rely on mathematical curve fitting relations to predict the demand profile.

Prediction error for district			Prediction error for individual buildings		
Reference	Country	Error(%)	Reference	Country	Error(%)
Shimoda et al. (2004) [38]	Japan	18	Sehrawat and Kensek (2014) [39]	USA	11–23
Heiple and Sailor (2008) [40]	USA	10–13	Theodoridou et al. (2011) [41]	Greece	12–55
Dall'O'and Galante et al. (2012) [42]	Italy	10	Nouvel et al. (2013) [43]	Germany	5–50
Caputo et al. (2013) [44]	Italy	4	Nouvel et al. (2013) [43]	Germany	18–31
Filogamo et al. (2014) [45]	Italy	8	Koene et al. (2014) [46]	Germany	1–60
Nouvel et al. (2013) [43]	Germany	21	Orehouniget al. (2014)	Switzerland	6–88
Nouvel et al. (2013) [43]	Germany	7	Fonseca and Schlueter (2015) [47]	Switzerland	8–99
Orehounig et al. (2014) [48]	Switzerland	8			
Fonseca and Schlueter (2015) [47]	Switzerland	9–66			

Table 2.2: Prediction error for different methods [28]

Another outlook of these methodologies based on their scale is given by Fryssinet in his article [49]. This division generates three groups BES (Building Energy Simulations), UBES (Urban Building Energy Simulations), and CES (City Energy Simulation) (see Figure 2.5).

Considering the prediction error between estimating the demand in district heating networks and individual buildings, taking into account also the advantage of reducing simulation times. A combination of approaches has been considered for this thesis which will be explained in Section 5.10.6 which results in a CES. Considering a mixture of historical methods, using both Heating Degree Days methodology, combined with measured data from the Hotmaps toolbox [50], and considerations from Stratego Project [51]. For heat losses two different approaches will be taken. One, considering a constant heat loss based on standards, which will also be explained in Section 5.10.6, or the possibility of simulating it as an additional part of the system.

Deterministic methods for demand estimation become difficult to consider for a large number of buildings. Bearing in mind that individual buildings present wide ranges of error, the addition of this error and the improbability of having all the information for the different buildings inside a district network add to an almost inviable variability.

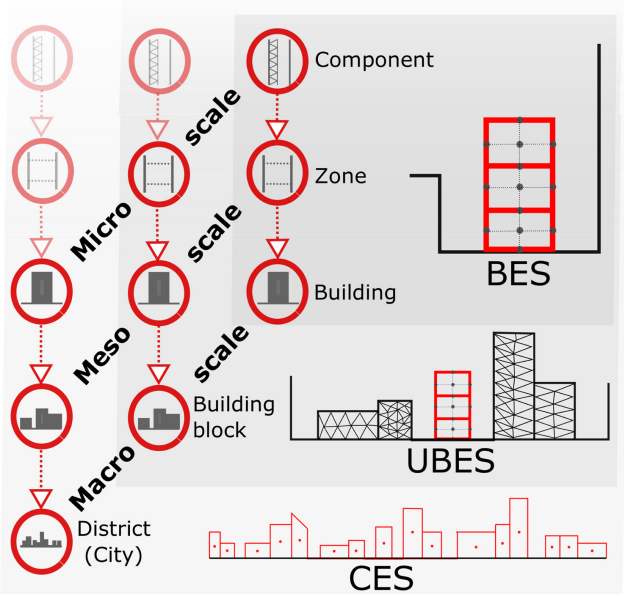

Figure 2.5: Different categories of demand simulation based on scale [49].

Considering that one of the main objectives of the calculation of the DHS is to account for its peak yearly consumption to size the equipment, the error seen in district demand simulations seems coherent for a first approach to estimating equipment which can have a cost estimate error of -15 to -30% and +20 to +50% in the feasibility stage of a project as a Class 4 estimate [52], [53].

During the development of this thesis, other tools were generated which contribute to the new state of the art. One of the most interesting ones, analyzing the possibility of developing new software mentioned in the previous section, is nPro tool [54].

This tool excelled in dissecting one of the main problems also detected by this thesis, which is the need for a more approachable tool in order to be able to calculate DHS networks without the need for detailed information upfront. The main advantage of this software is the visualization of the network as a whole, considering electricity, heat, and even hydrogen exchange within the network. This tool performs exceptionally well considering demand as part of the calculation. Generating the profile inside the tool limits the input data to reduce the possibility of errors when introducing the profile. This consideration was also made in the MSM but was made independently, calculating the profiles and leaving the yearly demand as input for the Tool calculation. But without constraining in the case of the combinations of technologies to allow the load of any demand profile by file when performing new parametric analyses.

This tool provides a wide range of technologies to cater to the demand (Figure 2.6), having some assumptions that make sense for a first calculation. Some of these calculations are the positioning of the storage units to simplify the number of combinations and gathering the fuels in a single hub.

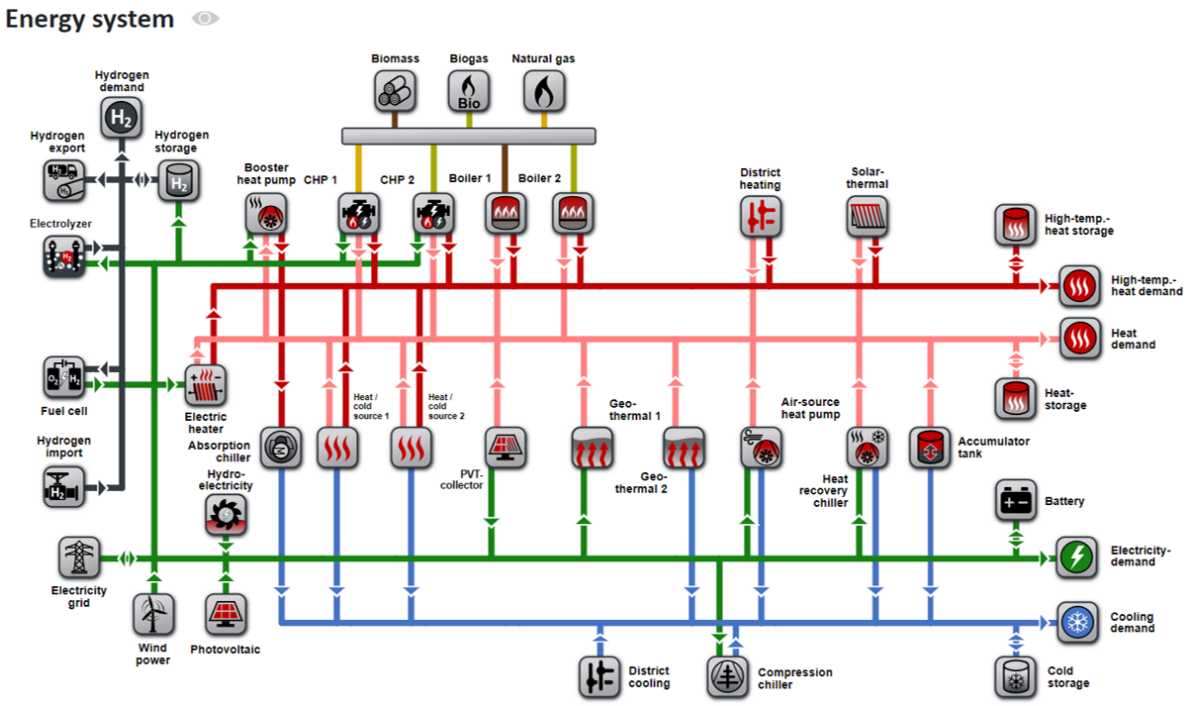

Figure 2.6: Energy-hub screen from the nPro tool [55].

2.2 Objectives

Most software analyzed during the state of the art has proven to be difficult to approach by non-specialist personnel. This generates serious problems for the DHN to achieve visibility, considering that implementation has to be encouraged by estate representatives to overcome regulatory obstacles. Another detectable flaw in the latest software is the lack of versatility to add new technologies, making these solutions stationary in front of the generation of new energy sources in the upcoming years.

The use of MSM aims to make the calculation of networks easy enough for any potential user to acquire enough information to, at least, take into account this solution in the design stage. And by implementing the whole methodology, be able to integrate new technologies as they become available in the market.

The objectives of this methodology, and therefore of this thesis are:

1. To make a methodology open to new technologies to be able to keep up with technological changes.

2. To obtain clear indicators or KPIs for policymakers to consider DHN.

3. To obtain results rapidly, for the user to have them available at the time of tender.

4. To make DHN available for non-specialists, therefore, applicable for future constructions.

A positive factor of this methodology is that it is specially prepared to generate modules for new technologies, broadening the range of possible combinations to be simulated. Also, changing performance maps of some technologies such as boilers or chillers, which undergo technological improvements over time.

One consideration that would improve the availability of district networks is the measurability of the proposed solutions. To reduce this distance, values must be generated for comparison. Key Performance Indicators will be calculated by the methodology to be able to compare with existent solutions available in the market, to make it possible for the user to make a value-based decision. Generating a methodology able to simulate different combinations while acquiring these results makes it appealing for the most result-oriented user.

If the results obtained take large amounts of time to be produced, the user could be deterred from following this path, as time is usually appreciated as money. In light of this consideration, the reduction of simulation times seems crucial for DHS to thrive, making the efficiency of the methodology a key aspect. The methodology developed in this thesis reduces data input for simulations greatly, reducing the amount of time invested by the user for a network simulation.

One of the principal obstacles when considering district networks is the availability. This thesis aims to bridge the divide between potential users and district heating and cooling networks. As mentioned in previous sections, technology to reduce CO_2 emissions is available, and DHS is a mature technology. The missing link could be in a series of factors:

- economical: values are not adding up to a desired value.
- awareness: decision-makers do not evaluate this possibility.
- trust: economic values are promising, but not enough for related parties to take the risk of changing the usual construction procedures.
- novelty: new technologies or improvements over existing technologies are arising constantly. Tools should be prepared to adapt to new equipment or new technologies.

Chapter 3

MSM Technologies

This chapter will cover the state-of-the-art and theoretical frame for the technologies used in the MSM. As previously mentioned, the technologies will be shown in the following: heating, cooling, and storage technologies.

3.1 Heating generation

This section will discuss heating technologies, with a focus on those integrated into the proposed solutions within the Wedistrict project framework. It will address factors that affect technology performance, offering insight into their impact and how they were factored into the MSM calculation.

3.1.1 Solar Technologies

The most evident heat source that humanity has stumbled upon from its first "day" is the sun. It could also be called the source of sources, as its energy was involved in the production of other known fuels such as coal, oil, natural gas, and wood itself, generated through photosynthesis processes, and then transformed by chemical decomposition reactions in a specific context. Even wind has a solar background as temperatures vary between different regions and currents are generated [56].

The reason why this energy is available is the existence of the sun itself. The sun acts as a constant and massive fusion reactor continuously converting hydrogen to helium maintaining its surface temperature at around 5500/5700 K [56], [57]. Although solar radiation is a source of high temperature and energy at origin, with a high radiosity of 63 MW/m^2, sun–earth geometrical constraints lead to a dramatic dilution of flux. As a result, the irradiance available for terrestrial use is only slightly higher than 1 kW/m^2, depending on the location.

Humanity has developed many ways of harvesting this energy. Two primary methods have been utilized to harness this radiation: one for heating purposes through thermal solar collectors, and the other for electricity generation using photovoltaic panels.

Solar collectors can be classified into two types, non-concentrating or stationary, and concentrating. Non-concentrating collectors have a uniform area for capturing solar radiation, while sun-tracking concentrating solar collectors use concave reflecting surfaces or refraction

lenses to redirect and concentrate the sunlight onto a smaller receiving area, increasing its intensity. Concentrating collectors are preferred for high-temperature uses. The irradiation concentrated in this type of collector is specifically direct irradiation. This concentration is affected by the cosine effect, see Equation 3.1. This means that the irradiation on the tilted surface is affected by the incidence angle.

$$I_{Bt} = I_{Bn} \cdot \cos\theta \tag{3.1}$$

Where,

- I_{Bt}:Beam Irradiation on the tilted surface $[\frac{kW}{m^2}]$.
- I_{Bn}:Beam Irradiation on the normal plane $[\frac{kW}{m^2}]$.
- θ: Incidence angle [°].

Additionally, solar collectors differ based on the type of heat transfer fluid (HTF) employed (water, non-freezing liquid, air, or heat transfer oil) as well as whether they are covered or uncovered. Performance variation in the different collectors will be analyzed to understand how simulation is developed for these different collectors.

Concentrating

Solar concentration enables the collection of "higher-grade" energy by achieving higher temperatures, which results in greater potential for generating mechanical work. As stated by the second law of thermodynamics, a heat engine's efficiency (such as the one used in a CSP plant) improves with increasing operating temperature. The solar receiver or absorber outlet temperature directly determines the operating temperature of the heat engine. Solar concentration enables the reduction of the receiver-absorber aperture area, minimizing losses from infrared radiation. Additionally, it allows for the development of a smaller absorber surface which has potential cost-reduction benefits. Solar concentrating systems utilize devices such as mirrors or lenses to redirect and concentrate incident solar radiation onto a specific collector surface A_C, resulting in a higher geometric concentration ratio ($C_{ratio} = \frac{A_c}{A_{abs}}$), achieved by concentrating it onto a smaller absorber surface A_{abs}. Values of C_{ratio} are shown in Table 3.2 and a representation for different types of collectors is shown in Figure 3.1.

Special attention will be paid to parabolic concentrators (d) and Fresnel collectors (f), which will be modeled in the context of Wedistrict project. And also to plane receivers with plane reflectors (c) that are similar to the functioning principle of "We Smile with the Sun" (WeSSun) technology developed by Seenso for the Wedistrict project.

Parabolic Trough Parabolic trough collectors are a cost-effective option for heat applications up to 400°C. These collectors utilize a reflective material bent into a parabolic shape, which effectively concentrates sunlight onto a black tube placed at the focal line of the receiver. To ensure optimum performance, single-axis tracking can be employed to orientate the collector in an east-west or north-south direction based on sun movement throughout the day. By utilizing PTCs, systems with light structures and affordable technology can efficiently produce heat within temperature ranges of 50 to 400 °C. One of the benefits of

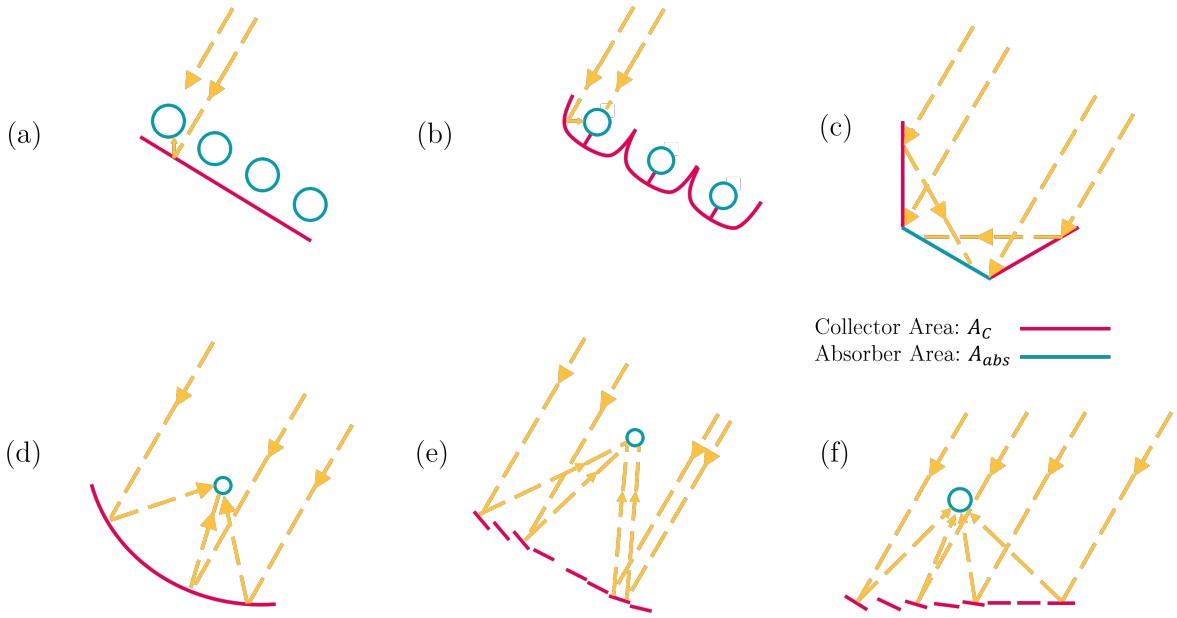

Figure 3.1: Possible concentrating collector configurations: (a) Tubular absorbers with diffuse back reflector; (b) tubular absorbers with specular cusp reflectors; (c) plane receiver with plane reflectors; (d) parabolic concentrator; (e) Fresnel reflector; (f) array of heliostat with central receiver. From [57] modified.

using a tracking mode in solar collectors is that there are fewer adjustments needed throughout the day, and the entire aperture always faces the sun at noon. However, this mode may result in reduced collector performance during early morning and late afternoon hours due to large incidence angles which lead to cosine loss. PTCs oriented in the north-south direction experience their highest cosine loss (see equation 3.1) at noon but have lower losses during mornings and evenings when the sun is positioned east or west, respectively [58]. PTCs will be a part of the methodology used in this thesis, as it is a technology supplied by Soltigua within the Wedistrict project.

Fresnel There are two distinct types of Fresnel collectors, the Fresnel Lens Collector (FLC), shown in Figure 3.2, which uses plastic lenses to concentrate the incident radiation to the receiver. And the linear Fresnel Reflector (FLR), shown in Figure 3.1 (e), which uses stripes of mirrors to reflect the radiation, the configuration of these stripes resembling the shape of a parabola. The clear advantage of these stripes is that they do not need to be parabolic (flat or elastically curved), saving big amounts of costs in construction. Also, being these stripes mounted at ground level, which also results in reduced installation costs [56]. For this thesis, only FLR will be taken into account, as it is more commonly applied and technologically available. Besides, one of Soltigua's proposed technologies is a FLR. Soltigua's model replaces the standard cabled solution with an innovative wireless system that eliminates the need for both communication and power supply cables. The power supply utilizes a stand-alone system consisting of a photovoltaic module and battery, while for communication, a Sub-GHz radio system has been developed and installed. The use of Sub-GHz frequency enables wide signal coverage over long distances, allowing the signal to reach the receiver directly

without having to hop between different nodes. This enhances the reliability and speed of the system.

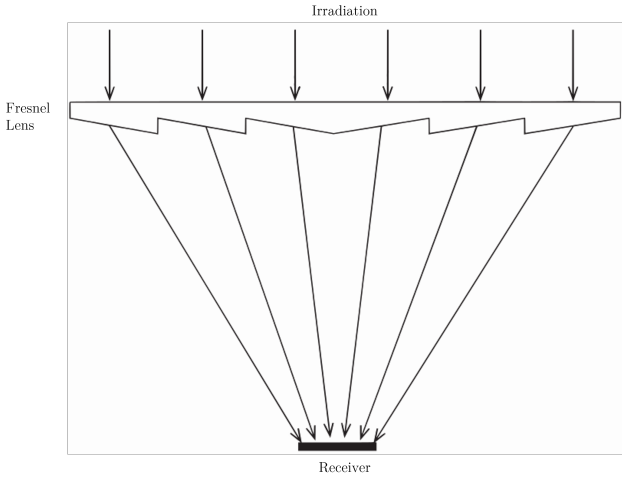

Figure 3.2: Fresnel Lens Collector diagram. From [56].

We Smile with The Sun (WeSSun) The WeSSun is a cylindrical concentrator that does not focus light and has a cross-section in the shape of a truncated cone. It uses moving flat mirrors that rotate around an axis parallel to the cylinder's axis, providing low concentration levels (usually C$\leq$ 2). Its design allows for easy connection with standard solar thermal collectors, including those available commercially, thus improving their energy efficiency without requiring changes to the tilt angle. One unique aspect of this device is its capability to evenly distribute sunlight across the aperture by adjusting the positions of its reflective plane mirrors according to the sun's apparent movement. This feature prevents high local concentrations which are common in focusing concentrators and CPCs, ensuring uniform illumination of the absorber.

These characteristics give WeSSun advantages that are for example, improved thermal collector performance, meaning that the solar productivity per m^2 of aperture has been enhanced, along with the implementation of automatic and simple protection against wind overloads and excessive temperatures which is given by the ability to close the mirrors on top of the collector in such situations. However, there is a larger land use capacity compared to conventional tracking collectors, whether equipped with mirrors or without them. Additionally, safety during operation has been improved through reduced structural and stagnation temperature-related requirements. This was achieved by allowing the mirrors to be folded to prevent overheating, and also, providing resistance against strong winds. This system can also be adapted to existing thermal products that are manufactured in large series such as flat plate collectors and ETC collectors. It utilizes well-proven components including solar collectors with Solar Keymark certification, tempered glass/silver mirrors, as well as tracking devices used for PV trackers aided by Programmable Logic Controllers (PLCs) for tracking and installation control. Furthermore, this innovative approach results in cost reduction, larger scalability, simplification of the primary circuit, and ultimately lowers energy production costs.

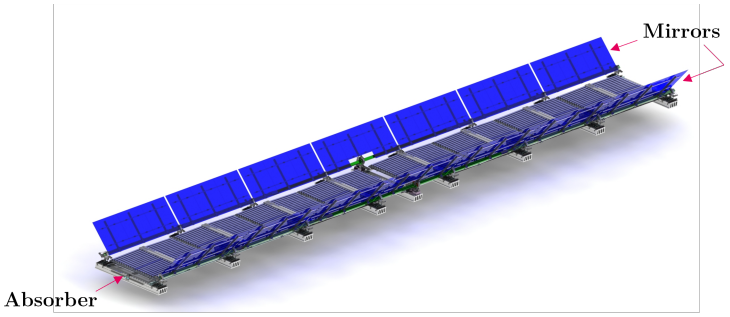

Figure 3.3: WeSSun collector diagram.

Heat Transfer Fluids

Solar systems have different needs depending on the final application of the energy harnessed, while all thermal collectors gather energy, the thermal level will vary depending on the application. It is important to highlight that higher energy levels imply higher thermal losses and lower collector efficiencies, as will be explained in the following section 3.1.1.

Depending on this temperature level, HTF should accommodate different requirements. Desirable properties of a heat transfer fluid comprise a low melting point, high boiling point, thermal stability, low vapor pressure at elevated temperatures (<1 atm), minimal corrosion with metal alloys used in HTF containment, low viscosity, high thermal conductivity and heat capacity for efficient energy storage. Additionally, cost-effectiveness is an important factor to consider [59]. In the search for these properties, different fluids have been used, which can be classified into six groups based on their type:

- air and other gases
- water/steam
- thermal oils
- organics
- molten-salts
- liquid metals

Some of these fluids' characteristics are outlined in Table 3.1. It is noteworthy that while the costs differ among these fluids, the material cost significantly influences their overall utilization cost.

For applications intended for district heating, high temperatures are not often needed, which is why the use of water, or occasionally thermal oils, is sufficient.

Performance

Performance for solar collectors will depend on a series of factors, both geometrical and physical. The estimation of absorbed radiation per area of aperture (S) is of utmost importance and requires examination of both the optical properties and level of radiation involved in the

Name	Melting point (C)	Stability limit (C)	Viscosity (Pa s)	Thermal conductivity ($\frac{W}{m \cdot K}$)	Heat capacity (kJ kg-1 K-1)	Cost ($/kg)	Corrosion		
							Rate (micro m/year unless specified)	Alloy	Temp. (C)
Air	-	-	0.00003 (at 600°C)	0.06 (at 600 C)	1.12 (at 600 °C)	0	7–14 g/mb	Fe–Al (5.8–16.2 wt%) – Cr (1.9–9.7 wt%)	1100
Water/Steam			0.00133 (at 600°C)	0.08 (at 600 C)	2.42 (at 600 °C)	∼0	1.3-3.5	In600	300
Thermal Oils									
Mineral oil	-20	300	N/A	∼0.1	N/A	0.3	N/A		
Synthetic oil	-20	350	N/A	∼0.1	N/A	3	N/A		
Silicone oil	-20	400	N/A	∼0.1	N/A	5	N/A		
Xceltherm 600 (paraffinic)	N/A	315	0.001085 (at 300 °C)	∼0.1	2.436 (at 300 °C)	N/A	N/A		
Organics									
Biphenyl/Diphenyl oxide	12	393	0.00059 (at 300 °C)	∼0.1 (at 300°C)	1.93 (at 300 °C)	100	N/A		
Molten-salts									
Solar Salt	220	600	0.00326 (at 300 C)	0.55 (at 400 C)	1.1 (at 600 C)	0.5	5	A36	316
							6–15	304	570
							15.9/4	316	600/680
							60	321	600/680
							10.4/4	347	600/680
							47	Ha230	600/680
							19.8/6	In625	
Liquid Metals									
Na	98	883	0.00021 (at 600 C)	46.0 (at 600 C)	1.25 (at 600 C)	2	N/A		
Na-K	-12	785	0.00018 (at 600 C)	26.2 (at 600 C)	0.87 (at 600 C)	2	N/A		
Pb-Bi	125	1533	0.00108 (at 600 C)	12.8 (at 600 C)	0.15 (at 600 C)	13	25-250	Ferritic SS	800
							>250	Austenitic SS	
							>250	Nickel Alloy	

Table 3.1: Thermal and physical properties of commonly used HTFs [59]

concentrator and absorber (receiver), in the case of concentrating collectors. Sections that follow will be dedicated to elaborate on how one can estimate S effectively for the different collectors. Thermal losses from the receiver are often estimated via an established loss coefficient U_L, which depends upon the surface area of said absorber (A_{abs}). Consideration for temperature gradients along the length of the absorber is managed utilizing a flow factor known as F_R; this way actual inlet fluid temperatures might still be implemented in energy balance evaluations. This text focuses on detailing methods for estimating values like U_L and F_R accurately.

For models in the Wedistrict project, the performance of the collectors will be simulated by applying Equation 3.2 according to American and European standards (ASHRAE and ISO) [60], [61].

$$\eta_i = a_0 - a_1 \frac{\Delta T}{I_T} - a_2 \frac{(\Delta T)^2}{I_T} \tag{3.2}$$

Where,

- η_i: solar thermal collector efficiency [-].
- a_0:Intercept (maximum) of the collector efficiency [-].
- a_1: Negative of the first-order coefficient in collector efficiency equation $[\frac{W}{m^2 \cdot K}]$.
- a_2: Negative of the second-order coefficient in collector efficiency equation $[\frac{W}{m^2 \cdot K^2}]$.
- ΔT: Inlet temperature of fluid to collector minus ambient temperature $[K]$.
- I_T: Global radiation incident on the solar collector (Tilted surface) $[\frac{W}{m^2}]$.

This equation summarizes how efficiency has a theoretical limit, and how fluid temperature has a linear and a quadratic factor on the efficiency. This implies that low-temperature collectors will have a higher efficiency than those working at high temperatures.

To arrive at this simplified equation a thorough analysis of the characteristics aforementioned, that determine the performance of the collector, must be followed. The comprehensive thermal examination of a concentrated collector draws parallels with that of a flat-plate collector. While not obligatory, it proves helpful to derive suitable expressions for the efficiency factor F, loss coefficient U_L, and heat removal factor F_R of the collector. Once values for F_R and U_L are established, one can determine useful gain from an expression mirroring that used in flat-plate collectors. A notable discrepancy between these two types is the higher temperatures usually found in concentrating collectors; this scenario implies thermal radiation's significance which results in temperature-dependent loss coefficients [57]. U_L calculation is based on the calculation of the heat loss linearly through the collector. Considering all means of heat transfer (conduction to the supports, radiation to the ambient, and convection to the surroundings) Q_{loss} can be seen in Equation 3.3.

$$\begin{aligned} \frac{Q_{loss}}{A_{abs}} &= h_w(T_r - T_{amb}) + \epsilon\sigma(T_r^4 - T_{sky}^4) + U_{cond}(T_r - T_{amb}) \\ &= (h_w + h_r + U_{cond})(T_r - T_{amb}) \\ &= U_L(T_r - T_{amb}) \end{aligned} \tag{3.3}$$

With h_r (linearized radiation coefficient):

$$h_r = \frac{\epsilon\sigma(T_r^4 - T_{sky}^4)}{T_r - T_{amb}} \tag{3.4}$$

Where,

- Q_{loss}: receiver heat losses $[W]$.
- A_{abs}: Area absorber (receiver) $[m^2]$.
- h_w: convection heat transfer coefficient outside the tube "wind" $[\frac{W}{m^2 \cdot K}]$.
- T_r: temperature receiver $[K]$.
- T_{amb}: ambient temperature $[K]$.
- ϵ: emmitance of the receiver to the sky $[-]$.
- σ: Stefan-Boltzmann constant $5.67 \cdot 10^{-8}$ $[\frac{W}{m^2 \cdot K^4}]$.
- U_L: overall heat loss coefficient $[\frac{W}{m^2 \cdot K^2}]$
- U_{cond}: heat transfer coefficient conduction $[\frac{W}{m^2 \cdot K}]$.

Using iterative methods, Q_{loss} can be calculated, considering it equal in its different mediums. Once Q_{loss} is calculated, U_L can be solved from Equation 3.3.

Once U_L is available, let us examine the temperature gradient factors in the flow direction. The process is similar to that for flat-plate collectors, but modified procedures are necessary for different geometries. Furthermore, to deal with linear concentrating systems with cylindrical receivers, the heat transfer resistance from the outer surface of the receiving tube to the fluid in the tube should include the tube wall since the heat flux in a concentrating system can be high. The overall heat transfer coefficient (determined by the external diameter of the receiver tube) between the environment [57].

$$U_o = \left(\frac{1}{U_L} + \frac{D_o}{h_{fi} D_i} + \frac{D_o \ln (D_o/D_i)}{2k} \right)^{-1} \tag{3.5}$$

Where,

- D_o: receiver tube outside diameter [m].
- D_i: receiver tube inside diameter [m].
- h_{fi}: convection heat transfer coefficient inside the tube $[\frac{W}{m^2 \cdot K}]$
- k: the thermal conductivity of the tube $[\frac{W}{m \cdot K}]$.

The useful energy gain per unit of collector length q_u, expressed in terms of the receiver temperature T_r and the absorbed solar radiation per unit of aperture area S, is:

$$q'_u = \frac{A_{col}S}{L} + \frac{A_{abs}U_L}{L}(T_r - T_{amb}) \tag{3.6}$$

Where,

- q'_u: useful energy gain per unit of collector length $[\frac{W}{m^2}]$
- A_{col}: Collector area $[m^2]$.
- S: Irradiation per Collector area $[\frac{W}{m^2}]$.
- L: Collector lenght [m].

In terms of the energy transfer to the fluid at temperature T_f:

$$q'_u = \frac{(A_r/L)(T_r - T_f)}{\frac{D_o}{h_{fi}D_i} + \left(\frac{D_o}{2k}\ln\frac{D_o}{D_i}\right)} \tag{3.7}$$

Simplifying T_r from both equations 3.6 and 3.7, the following equation is obtained

$$q'_u = F'\frac{A_{col}}{L}\left[S - \frac{A_{abs}}{A_{col}}U_L(T_f - T_{amb})\right] \tag{3.8}$$

Where F', the collector efficiency factor, is:

$$F' = \frac{1/U_L}{\frac{1}{U_L} + \frac{D_o}{h_{fi}D_i} + \left(\frac{D_o}{2k}\ln\frac{D_o}{D_i}\right)} \tag{3.9}$$

$$F' = \frac{U_O}{U_L} \tag{3.10}$$

The concepts behind these equations and those from flat plate collectors are identical. If the same procedure is followed as it is used for flat-plate collectors relating the useful flow to the collector's heat removal factor, the following equation is obtained. The heat removal factor "F_R" is a quantity that relates a collector's actual useful energy gain to the useful gain if the whole collector surface were at the fluid inlet temperature. In equation form, it is:

$$F_R = \frac{\dot{m}c_p(T_{fo} - T_{fi})}{A_{col}\left[S - U_L(T_{fi} - T_{amb})\right]} \tag{3.11}$$

$$Q_u = F_R A_{col}\left[S - \frac{A_{abs}}{A_{col}}U_L(T_i - T_{amb})\right] \tag{3.12}$$

And in the same manner, collector flow factor F'' is:

$$F'' = \frac{F_R}{F'} = \frac{\dot{m}c_p}{A_{abs}U_L F'} \left[1 - \exp\left(-\frac{A_{abs}U_L F'}{\dot{m}c_p} \right) \right] \tag{3.13}$$

At last, to be able to perform these calculations on the useful energy of the collector, the value of S should be available. To calculate it for the different concentrating collectors, the following equation is available.

$$S = I_b \rho (\gamma\tau\alpha)_n K_{\gamma\tau\alpha} \tag{3.14}$$

Each component in this formula implies unique considerations different from those of flat panel collectors, and their handling depends upon the geometry of the collector. The efficient incident irradiation recorded on the plane's aperture, symbolized by I_b, incorporates only direct solar rays for all concentrating collectors excluding those with a low concentration ratio ($C_{ratio} \leq 10$ as per Table 3.2). For systems with low concentration ratios, some scattered light might bounce back at the absorber, an amount dependent on the angle of acceptance of the concentrator. Generally ρ signifies specular reflectance of concentrator but will stand for diffuse reflectance when cylindrical absorbers with diffuse reflectors are used. And it will stand for the transmittance of the refractor if refractors are used as concentrators. The following variables, γ,τ, and α, are calculated in correspondence to the angle of radiation incidence on the aperture. The influence of this angle on these parameters can be examined individually or incorporated as suggested by Equation 3.14 into an incidence angle modifier ($K_{\gamma\tau\alpha}$). Evacuated tubular absorbers have covers that are optically non-symmetrical. As recommended by Mclntire and Read (1983), biaxial incidence angle modifiers are used, and should be implemented as shown in the following equation [57].

$$K_{\tau\alpha} = (K_{\tau\alpha})_t (K_{\tau\alpha})_l \tag{3.15}$$

Where the suffix "t" corresponds to the transversal plane and "l" to the longitudinal plane, respectively. Herein, the intercept factor γ is characterized as a fraction of reflected radiation that arrives at the absorptive surface of the receiver.

Having determined these variables, using Equation 3.12, an instantaneous efficiency for the collector (η_i) can be determined.

$$\eta_i = \frac{Q_u}{A_{col} I_T} = F_R(\tau\alpha) - \frac{F_R U_L (T_i - T_{amb})}{I_T} \tag{3.16}$$

and

$$\eta_i = \frac{\dot{m}c_p (T_o - T_i)}{A_{col} I_T} \tag{3.17}$$

European standards [61] tend to use average temperatures as a base in their tests, so Equation 3.16 is rewritten as:

$$\eta_i = \frac{Q_u}{A_{col} I_T} = F_{av}(\tau\alpha) - \frac{F_{av} U_L (T_{f,av} - T_{amb})}{I_T} \tag{3.18}$$

As with the differential equation of temperature for the node, a more accurate expression may be obtained by taking into account a quadratic temperature-dependent loss term as well:

$$\eta_i = F_{av}(\tau\alpha) - \frac{F_{av}U_L(T_{f,av} - T_{amb})}{I_T} - \frac{F_{av}U_{L/T}(T_{f,av} - T_{amb})|(T_{f,av} - T_{amb})|}{I_T} \tag{3.19}$$

Where,

- $U_{L/T}$: quadratic loss coefficient $[W/m^2/K^2]$

Equation 3.19 can also be rewritten as the efficiency used in the Wedistrict project, shown in equation 3.2:

$$\eta_i = a_0 - a_1\frac{\Delta T}{I_T} - a_2\frac{(\Delta T)|\Delta T|}{I_T} \tag{3.2}$$

Motion	Collector type	Absorber type	Concentration ratio	Indicative temperature range (°C)
Stationary	Flat plate collector (FPC)	Flat	1	30–80
	Evacuated tube collector (ETC)	Flat	1	50–200
	Compound parabolic collector (CPC)	Tubular	1–5	60–240
Single-axis tracking	Linear Fresnel reflector (LFR)	Tubular	10–40	60–250
	Parabolic trough collector (PTC)	Tubular	15–45	60–300
	Cylindrical trough collector (CTC)	Tubular	10–50	60–300
Two-axes tracking	Parabolic dish reflector (PDR)	Point	100-1000	100-500
	Heliostat field collector (HFC)	Point	100-1500	150-2000

Table 3.2: Solar Collectors.
Note: Concentration ratio is defined as the aperture area divided by the receiver/absorber area of the collector [58]

3.1.2 Boilers

Considering life as a never-ending cycle, we could establish that all commonly used fuels come from a biological source. If photosynthesis is the main mean of transformation from solar energy into a stable form (chemical) in our world, the growth of plant-based individuals can be determined by it. Being those life forms, the principal sustaining driver for all other life forms, even if those do not make this transformation but then through decaying reactions become fossil fuels, we could find a link to determine that all fuels are biofuels, even solar fuels. But to establish a limit, the material of plants and animals, including their wastes and residues, will be defined as biomass [62].

While there are different methods to obtain energy from biofuels (see [62]), in this section, direct combustion of solid biomass will be prioritized as it is the main technological boiler application used in the Wedistrict project.

Boilers have different designs regarding their shapes and applications. A main classification can be made as to what flows through the boiler tubes. Three mayor classifications arise [63]:

- Fire tube, flue tube or shell type boilers. Where the products of the combustion flow through the tubes (Figure 3.4).
- Water tube when water flows through the tubes (Figure 3.5).
- Combination type. Where both flue gases and water flow through tubes and the furnace is external. This type has the shell boiler after the furnace.

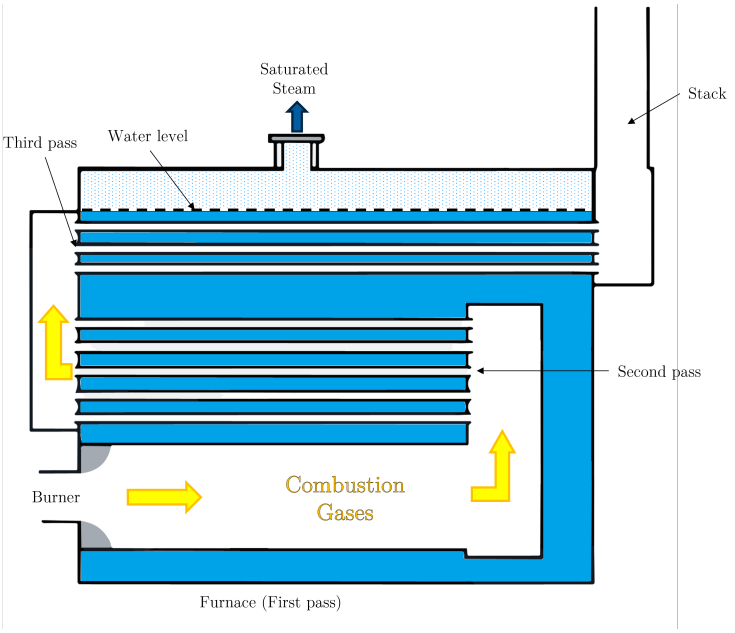

Figure 3.4: Schematic representation of a typical three-pass fire-tube boiler from [64] modified.

At the end of this section, how performance varies in the boilers will be analyzed for the simulated cases.

Biomass

Researchers classify different types of biomass in various ways, and one straightforward approach is to categorize them into four main groups: woody plants, herbaceous plants/grasses, aquatic plants, and manures. Among these categories, herbaceous plants can be further subdivided based on their moisture content - high or low. For this thesis, the focus will be on investigating biomass types with lower moisture content such as woody plants and herbaceous species due to their prevalence in commercial activities unless specific applications call for other types [66].

The selection of the appropriate conversion process for biomass is influenced by its inherent properties and any potential processing challenges. Similarly, the choice of biomass

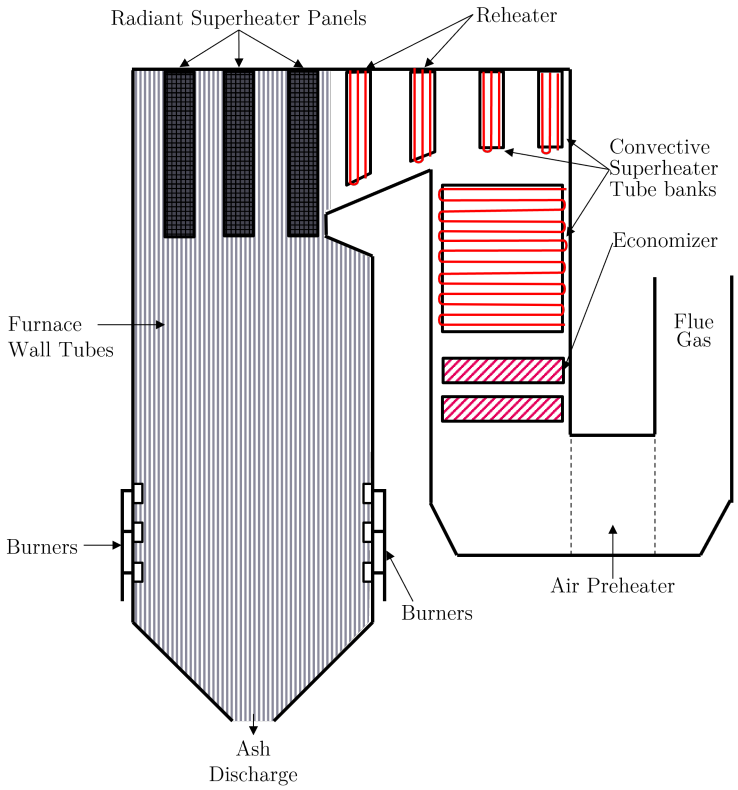

Figure 3.5: Pulverized coal-fired power-generation water-tube boiler. from [65] modified.

source depends on the desired form of energy utilization, allowing for flexibility in using biomass as an energy source. This study focuses on woody and herbaceous species, which are commonly examined by researchers and technology providers in the field of biomass. The specific material properties become crucial during subsequent processing depending on the chosen energy conversion method. During the subsequent processing of biomass as an energy source, the primary material properties of importance are:

- Moisture content, which can be divided into two categories: intrinsic and extrinsic. Intrinsic moisture refers to the moisture content that is not influenced by weather conditions, while extrinsic moisture is influenced by prevailing weather conditions during harvesting, affecting the overall biomass moisture content.
- Heating value, as previously discussed.
- Volatile and Fixed Carbon (FC). The composition of a solid fuel can be determined by analyzing its fixed carbon and volatile proportions. Volatile matter refers to the portion that is released as gas, including moisture, when heated at 950 °C for 7 minutes. On the other hand, fixed carbon content represents the mass that remains after volatiles are released, excluding ash and moisture contents.
- Ash/residue content. The solid residue in biochemical conversion processes refers to the non-biodegradable carbon content present in biomass. This residue exceeds the

ash content as it consists of recalcitrant carbon that cannot be further biologically degraded, but can potentially be burned during thermo-chemical conversion.

- Alkali metal content. The presence of alkali metals in biomass, such as Na, K, Mg, P and Ca, is particularly crucial for thermochemical conversion processes. When these metals react with silica found in the ash during combustion or gasification, it produces a sticky liquid phase that can cause blockages in furnace and boiler systems. It should be noted that even if the initial silica content of a biomass source is low, contamination from soil during harvesting can significantly increase the overall silica content. This increased total silica content may then lead to operational challenges despite any concerns about intrinsic silica levels in the material itself.

- Cellulose/lignin ratio. The relative amounts of cellulose and lignin in biomass play a critical role specifically in biochemical conversion methods. Cellulose has higher biodegradability compared to lignin, resulting in more effective conversion of the carbon-containing plant material when it consists mainly of cellulose. This aspect becomes significant when considering which species of biomass plants are suitable for biochemical processing.

When considering the conversion of dry biomass, it is important to focus on the first five properties mentioned. On the other hand, when dealing with wet biomass conversion processes, priority should be given to the first and last properties listed. See property values listed in Table 3.3.

Biomass	Moisture (%)	VM (%)	FC (%)	Ash (%)	LHV (MJ/kg)
Wood	20	82	17	1	18.6
Wheat straw	16	59	21	4	17.3
Barley straw	30	46	18	6	16.1
Lignite	34	29	31	6	26.8
Bituminous Coal	11	35	45	9	34

Table 3.3: Proximate analysis of some biomass feedstocks (wt%) [66]

Performance

For all types of boilers, efficiency is defined as [67]:

$$\eta_b = \frac{P_b}{\dot{m}_{fuel} HV} \tag{3.20}$$

Where,

- P_b: useful heat generated [W].
- $\dot{m}_{fuel}$: fuel mass flow rate [kg/s].

- HV: is the heating value (Lower or Higher) [J/kg].

North American standards tend to use Higher Heating Value (HHV) as basis, while European standards tend to base boiler's efficiency on Lower Heating Values (LHV) [67]. Its main losses come from the stack loss, which is the heat that leaves the boiler in the flue gases. Stack losses respond to:

$$Q_{StackL} = \dot{m}_{flue} c_{p.flue} (T_{flue} - T_{amb}) \tag{3.21}$$

Where,

- Q_{StackL}: stack heat losses [W].
- $\dot{m}_{flue}$: flue gas mass flow rate [kg/s].
- $c_{p.flue}$: mean specific heat of flue gas [J/kg/K].
- T_{flue}: stack flue gas temperature [K].

The efficiency of a boiler, as explained before, can be calculated by subtracting the heat lost in the exhaust gases from the fuel energy input, divided by the energy input. The overall efficiency takes into account additional losses such as heat radiated from the boiler and off-cycle energy losses, and is obtained by dividing the steam or hot water energy output by the energy input. In a natural-gas-fired boiler with an overall efficiency of 82%, approximately 4% of the energy input is radiated from the boiler, 4% is lost as sensible heat in exhaust gas, and 10% is lost as latent heat (water vapor) in exhaust gas that hasn't condensed. To achieve high efficiency, it's important to condense water vapor in order to utilize released latent heat. One possible approach is to preheat either the combustion air or the return water using the combustion gases. However, this method can be more costly and may lead to increased NO (nitrous oxide) emissions. Another option is to use the return water, but it requires its temperature to be lower than the dewpoint of the exhaust gas (approximately 55°C for natural gas boilers with 10% excess air). Traditionally, hot water for space heating has been supplied at around 80°C and returns at about 70°C, which prevents condensing boiler usage. Nevertheless, advancements in thermal envelopes (to decrease peak heating requirements) and radiant heating panels allow for significantly lower supply and return temperatures. The colder the returning water entering into the boiler inlet, the greater the amount of vaporized water that can be condensed resulting in higher boiler efficiencies which are visible below the dew temperature of the flue gas (around 55°C). At higher temperatures, heat can no longer be recovered, efficiency curve resembles the behaviour of a non-condensing unit (see Figure 3.6) but with lower performances. Non-condensing boilers typically have combustion efficiencies of 75-85 % under full load (with some as low as 68 percent), while condensing boilers achieve combustion efficiencies of 88-95%. The latent heat in the exhaust gas from oil-fired boilers is lower compared to natural gas due to the smaller hydrogen-to-carbon ratio in heating oil, making it less favorable for the construction of condensing oil-fired boilers. To maximize efficiency, highly efficient condensing boilers are well-insulated to minimize heat loss from the boiler walls and also recover heat from water used during flushing to remove impurities, which can account for an additional energy input of 1-3%. Condensing boilers

have traditionally been expensive due to the use of corrosion-resistant materials and their reliance on clean-burning fuels like natural gas. However, recent advancements have led to a decrease in cost, making them more accessible. While condensing boilers previously accounted for only 2% of the boiler market in the US, newer models are now available at a premium ranging from 25 to 100%. It is also possible to reduce costs by installing fewer condensing units with one as backup instead of using two equally sized non-condensing boilers. As demand increases and technology improves, the price gap between traditional boilers and condensing boilers is expected to narrow through learning-by-doing processes. Condensing boilers are widely used in Europe [68].

Part-load ratio Part-load operation of boilers can occur through on/off cycling (with a greater fraction of time off the lower the load, but full output when on), by modulating the fuel flow without adjusting the airflow, or by modulating both the fuel and airflow. Non-condensing boilers typically use on/off cycling because reducing fuel flow may cause condensation for which they are not designed. On/off cycling is inefficient as heat is lost during off-cycles and reheating is required at each start of an on-cycle. As a result, overall efficiency decreases with decreasing load in non-condensing boilers below approximately 80% of full load (where peak efficiency occurs in some cases). Similar to furnaces, boilers can utilize natural draft or fan-assisted draft; however, the former tends to have larger standby heat loss. With modulation capabilities for both fuel and airflow implemented in modern condensing boilers, efficiency improves at part loads. The efficiency of a boiler decreases significantly at lower loads, as the ratio of heat exchanger surface area to heat flow increases. This leads to on/off cycling and a sharp decrease in efficiency. Since boilers operate at part load most of the time, this difference in seasonal average efficiency between condensing and non-condensing boilers is amplified, with condensing boilers showing higher levels of overall efficiency. It has been observed that condensing boilers are more efficient at lower loads but experience a significant decrease in efficiency at very low loads. To minimize energy consumption, it is advisable to use multiple small boilers instead of one or two large boilers and distribute the heat load across these boilers. This approach not only reduces capital costs by minimizing backup capacity but also optimizes energy usage [68].

3.2 Cooling generation

This section will discuss cooling technologies, with a focus on those integrated into the proposed solutions within the Wedistrict project framework. It will address factors that affect technology performance, offering insight into their impact and how they were factored into the MSM calculation.

3.2.1 Compression-driven

While this title has been purposefully set in the cooling generation section due to its history as a supplier of this type of demand, equipment such as the ones that will be described in this section have the possibility of generating both heating and cooling. The specific ability to upgrade the temperature level of a heat source finds itself useful in modern district heating,

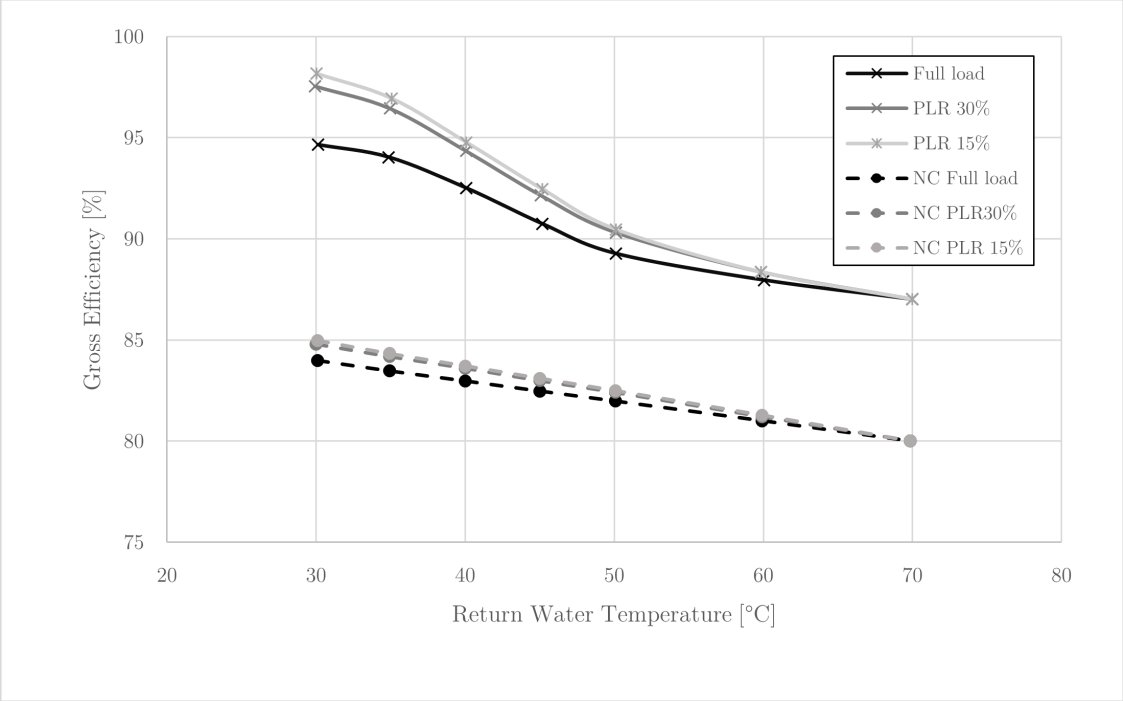

Figure 3.6: Condensing and non-condensing boilers efficiencies vs inlet temperature [69] modified.

where efficiency attempts to extract lower and lower quality heat (lower temperatures), and even more so, lower distribution temperatures are expected.

Figure 3.7 illustrates a schematic and a T-s diagram for the fundamental Carnot vapor compression cycle, which can be utilized for heating, cooling, or both, as has been priorly stated. Traditionally used mainly for cooling purposes, the working fluid is commonly referred to as a "refrigerant" irrespective of its intended function.

A compressor increases the temperature along line A-B in a reversible manner (at constant entropy s) from a lower level T_L to a higher level T_H. Subsequently, the refrigerant releases heat Q_{OUT} along line B-C at constant temperature in a heat exchanger. Then, it undergoes temperature reduction back to T_L through vertical line C-D at constant entropy s and reversibly in a small turbine. Finally, it absorbs heat Q_{IN} at constant temperature through line D-A in another heat exchanger. The rectangular path is followed counterclockwise, unlike the clockwise path of a Carnot cycle that generates power as in power plant [67].

Note that when generating cooling W_{IN} is bigger than W_{OUT}, thus W_{IN} is inserted through an electrical engine.

When generating heat, the Coefficient of Performance (COP) for an ideal Carnot cycle is given by:

$$COP_H = Q_{OUT}/W_{IN} = T_H/(T_H - T_L) \tag{3.22}$$

When generating cooling, however, the COP for an ideal Carnot cycle is defined as:

$$COP_C = Q_{IN}/W_{IN} = T_L/(T_H - T_L) \tag{3.23}$$

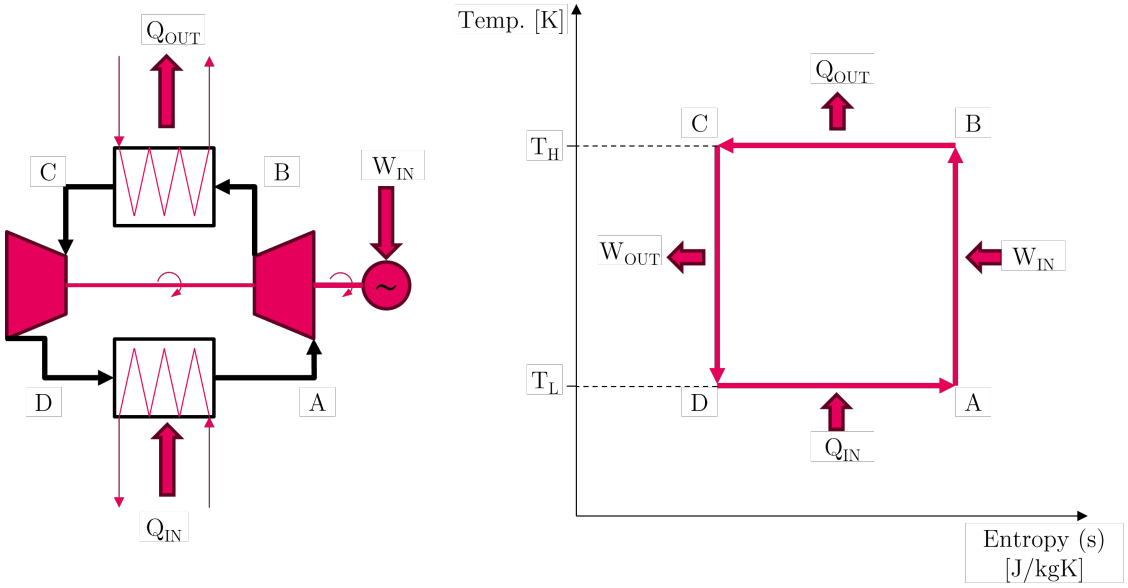

Figure 3.7: Idealized carnot vapor compression heat pump/chiller with T-s state diagram [67] modified.

However, an actual compression cycle differs from the one in Figure 3.7. Figure 3.8 depicts a simplified vapor-compression unit and its thermodynamic cycle. The refrigerant evaporates along path D-A, is desuperheated along path B-C (at constant pressure), and then condenses. The Coefficients of Performance from Equations 3.22 and 3.23 apply here, but temperature-based calculations are not applicable. In this practical unit, expansion occurs through throttling in a valve along line C-D instead of in a turbine as in the ideal plant. Although this increases the demand for electrical power slightly, it is more cost-effective and simpler to operate than using a turbine, especially for small units economically speaking [67].

In reality, the differences between this compression cycle (Figure 3.8) and the ideal Carnot cycle can be identified. Firstly the occurrence of superheating. The prevention of any liquid presence in the vapor upon entry into the compressor is crucial to avoid potential damage. To ensure this, a slight heating of the refrigerant occurs before it reaches the compressor, as an added safety measure. Second, non-isentropic compression. The compressor is responsible for the energy required to facilitate the compression-expansion cycle. In an ideal heat pump, the compressor contributes precisely the amount of energy necessary to compress the working fluid. However, due to thermal transfer from the compressor to the working fluid and other factors, more energy than required is typically introduced, leading to a higher discharge temperature. The comparison between necessary and actual added energy is termed as isentropic efficiency, which commonly stands at around 0.7. Thirdly, compressor mechanical losses can be quantified by the ratio of power input to the compressor against the work delivered to the working fluid, with typical efficiency levels of approximately 95%. Moreover, pressure losses through the condenser and evaporator which translate into a temperature loss in the cycle. Lastly, the occurrence of subcooling. A slight cooling of the working fluid leaving the condenser is necessary to prevent vapor formation before reaching the expansion

valve. Utilizing a heat exchanger, it is possible to use cold refrigerant from the evaporator for this purpose while also providing superheating of the cold refrigerant before entering the condenser. This method minimizes the impact on COP caused by both superheating and subcooling [68].

A more detailed scheme is depicted in Figure 3.9. In (a), "Cooling mode" is shown, demonstrating how the reversing valve works, giving the role in which the outside coil and the internal coil will work. In cooling mode the indoor coil works as an evaporator, removing heat from the building and returning it with a lower temperature, while "dumping" this heat to the exterior. However, in (b) ("Heating mode"), the reversing valve changes the sense of the flow of the cycle, which makes the internal coil work heating the indoor air as a condenser, while taking this desired heat from the outside air, which is returned to the exterior colder.

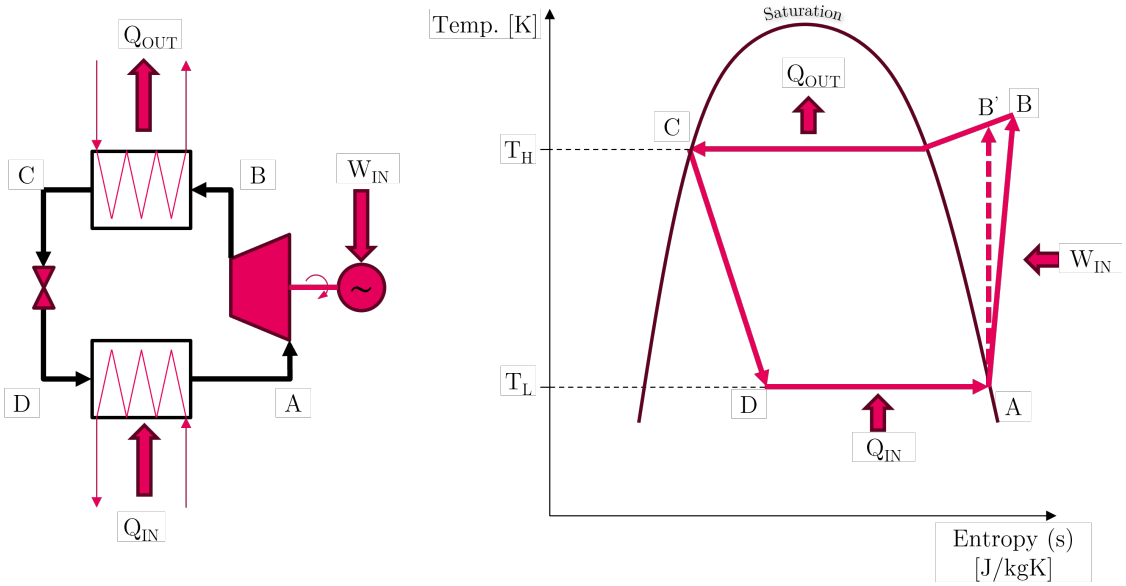

Figure 3.8: Simplified compression heat pump/chiller cycle with T-s state diagram [67] modified.

The explanation given in this section serves for both heat pumps and chillers. The differences between these two pieces of equipment reside principally in their application and refrigerant used. Chillers are more cooling generation-oriented, while heat pumps are designed to fulfill both applications (heating and cooling).

COP variation When modifying conditions in the heat pump, performance varies respecting for once the cycle (if heat entering or leaving varies, the operating points follow this behavior), and from another point design values (variation in flows cannot deliver the same amount of heat due to heat exchangers' design points). To give a clear example, in cooling mode, if the temperature delivered is warmer (higher temperature in the evaporator), the temperature difference is decreased, and therefore, as seen in equation 3.23, COP would increase. This behavior is visible in Figure 3.10.

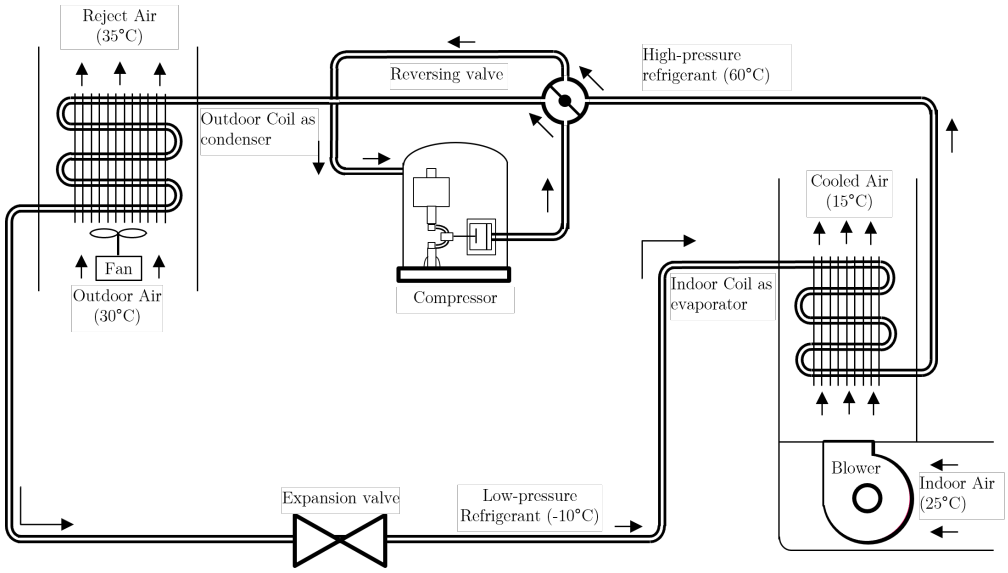

(a) Cooling Cycle

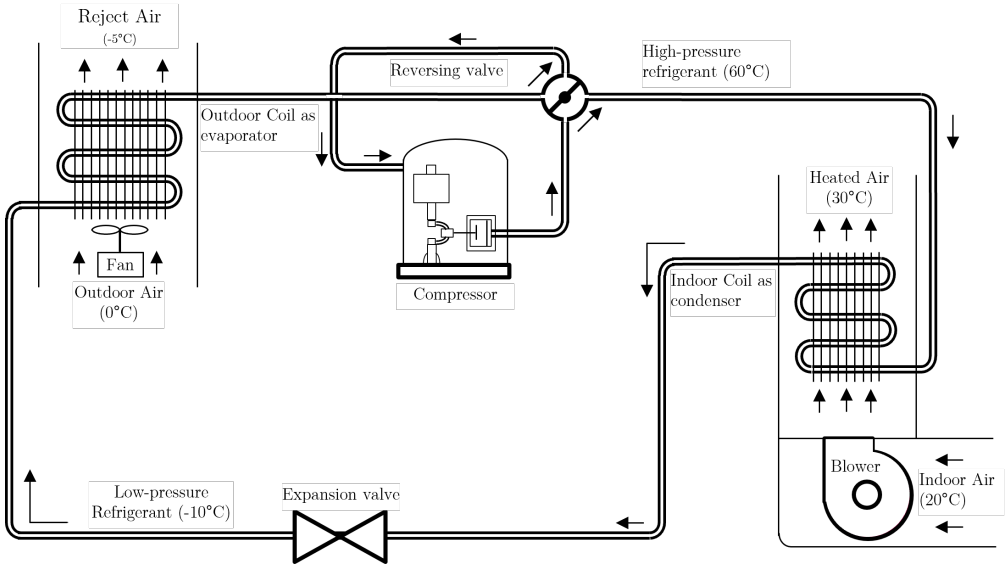

(b) Heating Cycle

Figure 3.9: Compression cycle from [68] modified. (a) Cooling Cycle. (b) Heating Cycle.

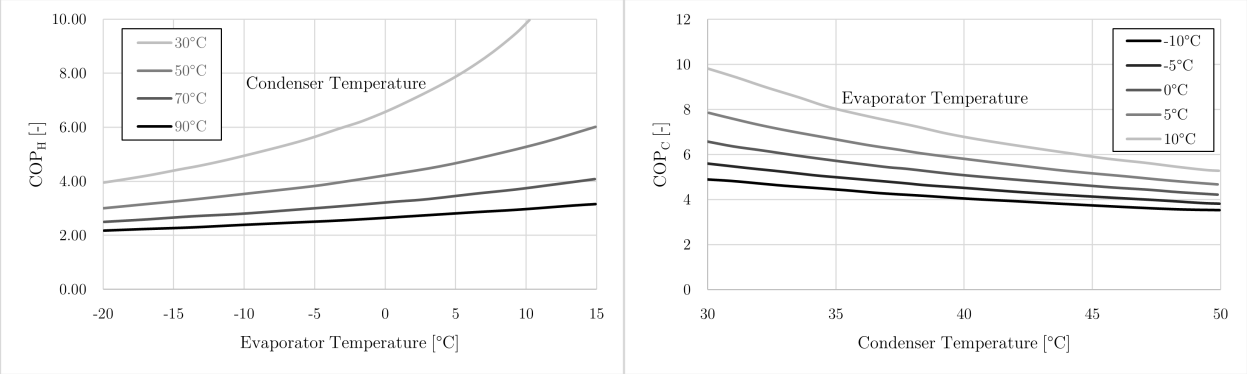

(a) (b)

Figure 3.10: Variation in the COP of a heat pump in heating mode (a) and in cooling mode (b) for various evaporator–temperature combinations, assuming a Carnot efficiency (ratio of actual to ideal COP) of 0.64 [70].

COPs also vary with the variation from the design flow supplied to both the condenser and evaporator. However, this variation is limited by the exchangers' design and does not have the impact that the external conditions do. For the models used in TRNSYS, these different COPs at different conditions are mapped and fed to the model from vendor information.

3.2.2 Absorption

One of the technologies used in the Wedistrict project involves utilizing absorption thermodynamic cycles to produce cooling energy using solar thermal energy as the primary heat source.

Absorption refrigeration has been in existence since 1859 when Carré successfully produced ice using the first ammonia-water absorption machine. Nowadays, the most commonly employed fluid in absorption water cooling systems is a solution of water and lithium bromide. Water serves as the refrigerant while LiBr acts as the absorbent. One notable advantage of this technology is its environmentally friendly nature, especially when compared to $NH_3 - H_2O$ technology. LiBr, which is similar to common salt (NaCl), exhibits a strong affinity for water and readily absorbs it.

To explain the operation in cooling mode, the scheme from Figure 3.11 (a) will be addressed. The cycle will be followed from the generator which is located at the top left of the graph, where the aqueous solution contains 52% LiBr, the nominal inlet temperature of the hot water being 88°C and the outlet temperature 83°C, while the absolute internal pressure is 8 kPa. As an effect of the heat supplied at this ambient pressure, the water in the solution boils and the vapor formed is routed to the adjacent vessel which is the condenser. Due to this vapor separation, the remaining solution is concentrated to 56% LiBr and is then directed to the heat exchanger located at the bottom of the scheme. Meanwhile, in the condenser, the water vapor is cooled down to 36°C thanks to the water circuit coming, for example, from a cooling tower and entering the machine at a temperature of 29.5°C, condensing the vapor and converting it into water. Simultaneously, the 56% concentrated LiBr

solution is directed from the generator into the absorber. The absorber and evaporator share space and pressure, causing water vapor in the absorber to be absorbed by LiBr due to its strong affinity for water. This enables continuous removal of water vapor as it is generated while maintaining a pressure of 0.9 kPa within the shared space. The absorption process generates heat which is subsequently eliminated by the cooling circuit prior to entering the condenser. The solution, after being diluted with steam absorption to a concentration of 52% LiBr, is then returned to the generator for the cycle to restart. Before returning, it passes through a heat exchanger in order to enhance cycle efficiency.

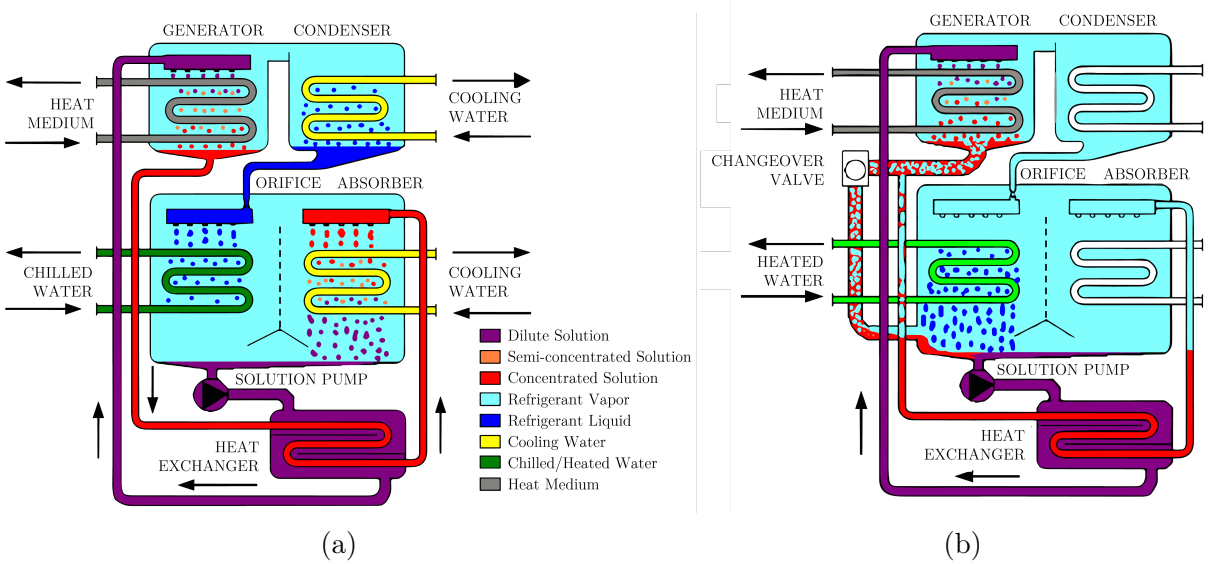

Figure 3.11: Absorption cycle from [71] modified. (a) Cooling Cycle. (b) Heating Cycle. Note that in (b) there is no cooling water flow in the condenser nor the absorber.

During the heating cycle shown in Figure 3.11 (b). When the temperature of the heat medium inlet surpasses 68°C, a dilute solution is pumped into the tubing bundle of the generator. This causes the solution to boil on the surface of the generator, resulting in refrigerant vapor being released. The vapor then ascends and moves towards the condenser. As a consequence of this process, the solution becomes more concentrated while it descends into the generator sump where it flows through the heat exchanger before returning to the absorber section.

In the evaporator hot refrigerant vapor condenses on the surface of the evaporator coil and an amount of heat equivalent to the latent heat of the refrigerant is transferred into the hot water circuit. The recirculating water is heated to the selected set point. Refrigerant liquid mixes with concentrated solution and the resulting dilute solution returns to the generator where the cycle is repeated.

In absorption, COP calculations work similarly to what it was described for heat pumps in equations 3.23 and 3.22, the main difference is that for absorption cycles the cycle does not undergo its processes only between vaporization of the mixture but through concentration, and as the fluid used is a salt, this concentration has to be below the concentration point. This difference in this cycle makes it so, that instead of the compression of a gas (as was the case for heat pumps), the fluid compressed is a liquid through a pump, which makes the

electrical costs much lower for these cycles. For this reason, COP calculations pay special attention to the heat necessary to vaporize and concentrate the solution in the evaporator, as visible in Equation 3.24. This cycle is shown in Figure 3.12 for lithium bromide. In this figure, it is visible that all the system is under vacuum, being the hight pressure of the cycle around 8 kPa and the low pressure side of the cycle at 0.9 kPa, this is necessary to have evaporation temperatures of water around 3°C at the low pressure side. In this specific cycle the inlet temperature of the heat medium to the generator is around 88°C with a ΔT=5°C. The temperature inlet for the chilled water is at 12°C and ΔT=5°C, which makes sense with the evaporation temperature previously mentioned.

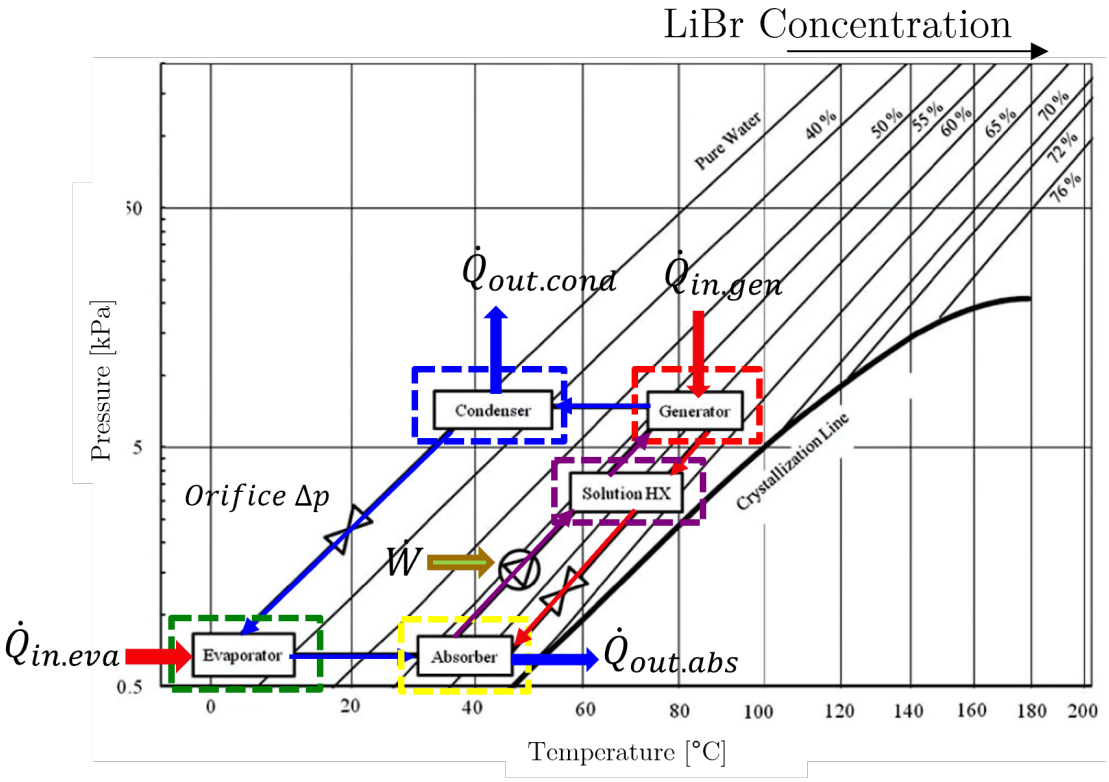

Figure 3.12: Absorption cycle in Dühring diagram for LiBr [72].

$$COP_C = \frac{\dot{Q}_{in.eva}}{\dot{W} + \dot{Q}_{in.gen}} \tag{3.24}$$

COP variation Variation of the absorption COP with different conditions has been studied by Kaushik [73] in his paper, and validated experimentally as well by Tahaineh some time later [74]. In their studies, analysis has also been performed for double-effect absorption chillers, but for this thesis, single-effect is going to be considered (due to the lower temperatures needed, which are more in line with DH application). Different variables affect dissimilarly naming generator, absorber, and evaporator temperatures, to point the most important ones. As a first analysis an increment of COP is observed at first while increasing

the temperature of the generator, but it reaches a maximum value around 91°C and becomes stable or even reduces its COP. This is due to the increment in the outlet temperature of the generator that heats the surrounding absorber and condenser, thus saturating its beneficial impact on COP after a certain value. The solution circulation ratio (ratio of mass flow rate of strong solution required per unit mass flow rate of refrigerant) is another important factor for this behaviour of COP. A rise in generator temperature leads to a decrease in the solution circulation ratio (SRC) and, consequently, reduced heat duties in the generator, condenser, and absorber. For a constant cooling load, the decrease in generator heat duty initially increases the COP. However, at higher generator temperatures, the rate of reduction in SCR slows down while the temperature difference between the generator and sub-cooled solution entering the generator increases. This causes an increase in irreversibility within the generator (reduction in overall efficiency). As a result, although there is a positive effect from decreasing solution circulation ratio it is balanced by a negative effect from increasing temperature difference between the generator and sub-cooled solution entering it. Therefore, as the generator heat duty levels off, the COP curve turns nearly flat, showing a marginal drop in COP [73], as shown in Figure 3.13.

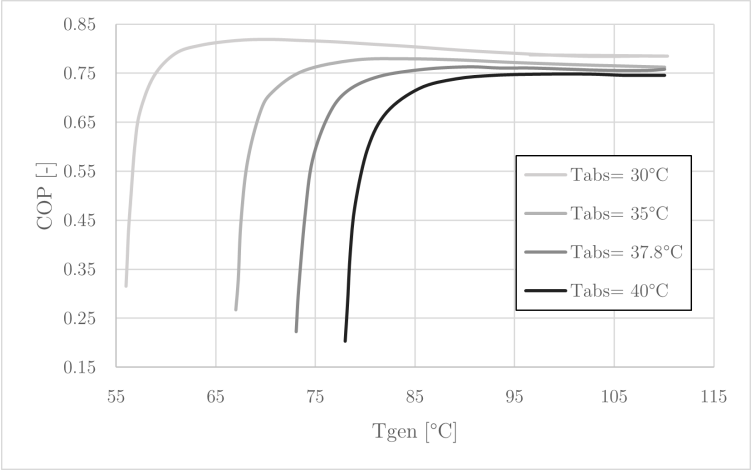

Figure 3.13: Variation of COP with generator temperature ($T_{eva} = 7.2°C$, $T_{cond} = T_{abs}$) [73].

Effect of COP variation due to absorber temperature is tied to the effect on the SCR (Equation 3.25). With the rise in absorber temperature (at a constant evaporator temperature and constant absorber pressure), the strong solution concentration Xs decreases, while weak solution concentration Xw stays the same because generator temperature and generator pressure remain constant. As a result, the numerator remains unchanged, while the denominator decreases, leading to an increase in the SCR. This rise results in higher generator heat duty and pump work. The evaporator load is kept constant as the mass flow rate of refrigerant is assumed to remain constant. Consequently, the COP decreases with a rise in absorber temperature as visible in Figure 3.14.

$$SCR = \frac{X_w}{X_w - X_s} \tag{3.25}$$

Where,

- SCR: solution circulation ratio.
- X_w: concentration of the weak solution.
- X_s: concentration of the strong solution.

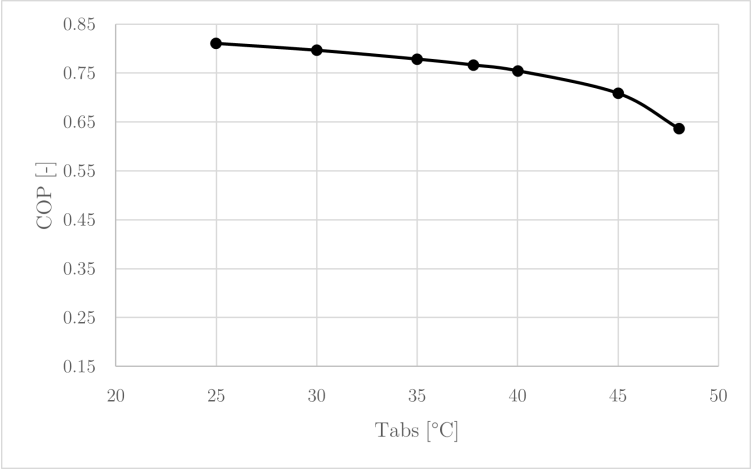

Figure 3.14: Effect of absorber temperature on COP ($T_{gen} = 87.8°C$, $T_{cond} = 37.8°C$, $T_{eva} = 7.2°C$) [73].

With evaporator temperature, there is an improvement in COP with the increase in the evaporator temperature but not an especially significant one in the single-effect absorption chillers that are being analyzed in the thesis, as visible in Figure 3.15.

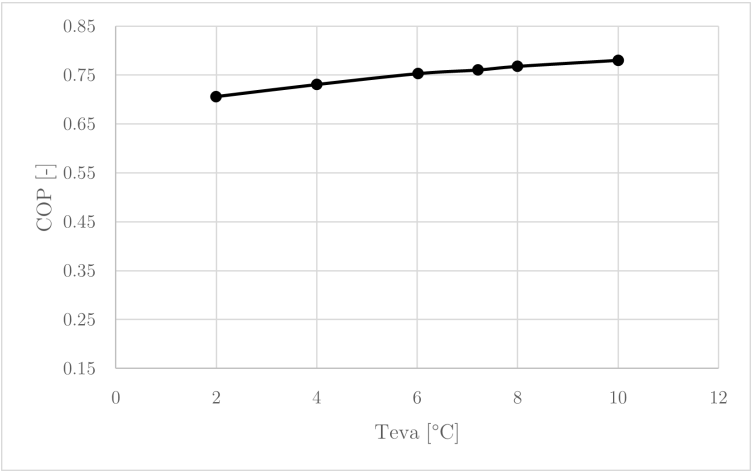

Figure 3.15: Effect of evaporator temperature on COP ($T_{cond} = T_{abs} = 37.8°C$ $T_{gen} = 87.8°C$) [73].

For models in the Wedistrict project, the variation of these values along with the PLR are mapped in an external file (made from developer information) which the TRNSYS type interprets to deliver a more accurate value of the performance.

3.3 Storage technology

The importance of heat, firstly as a food consumption transformer and later, as an enabler of human survival in different environments, is reason enough as to why the discovery of fire is regarded as one of humanities most remarkable events, as it is described by Alva in their paper [75].

There is no need to highlight the sun's importance in human life, but it is important for the purpose of this thesis, to understand the effect and distribution of this contribution along the day. Although irradiation has a fairly normal distribution surrounding noon, actual heating demand does not follow this pattern around climates, on the contrary while cooling demand does follow this distribution, heating tends to evade these hours, as the hours that the sun supplies most of the energy required (3.16).

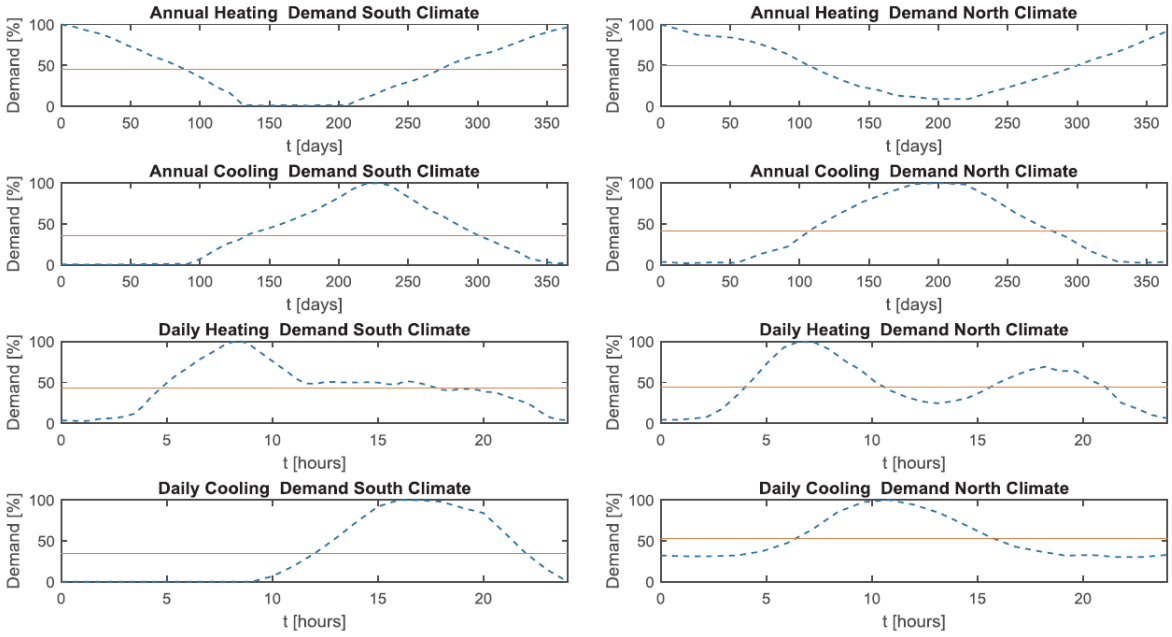

Figure 3.16: Heating and cooling demand distribution in northern and southern climates, on an annual and daily basis [76]

While much can be said about the different storage technologies, three main steps can be singled transversely in all of them. Charging, supplying heat to the source (or extracting in case cold storage is being done). Storing, which is keeping that heat inside the storage (as adiabatically as possible). And lastly discharging, in which energy stored is delivered to consumer [77].

For these steps to be possible, a series of criteria should be fulfilled:

- From a thermal standpoint, it is necessary for the temperature at the energy source to either match or exceed the temperatures of both the energy storage system and its sink.
- in terms of power transfer, there must be a sufficient amount of heat transferred during both charging and discharging processes over a specified time period.

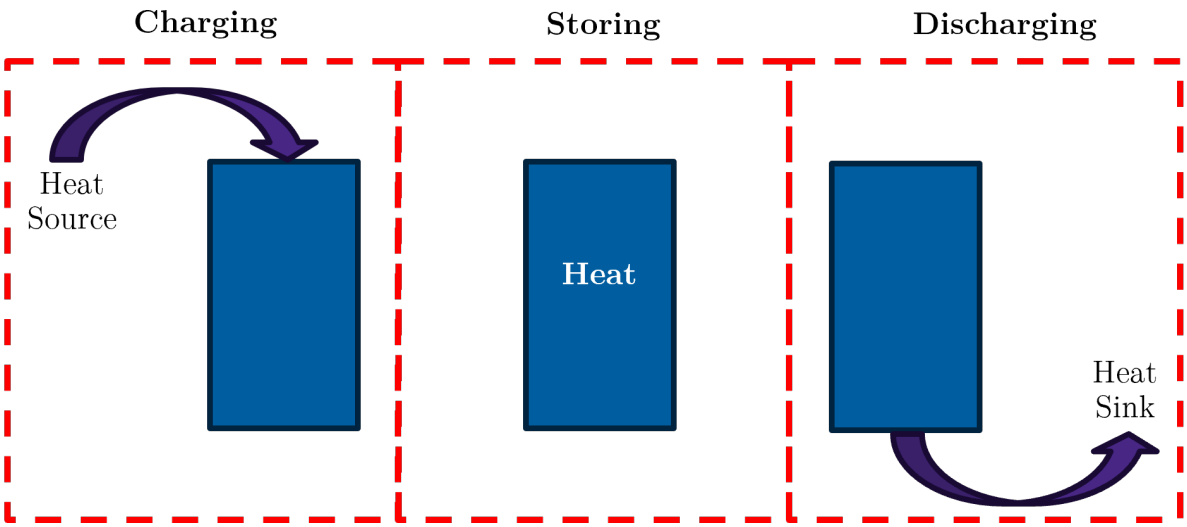

Figure 3.17: Storage Phases

- in certain applications, one must consider the heat transfer fluid and how it moves through free or forced convection.

In the variation of how and for how long this heat is stored different methods arise.

3.3.1 Methods for thermal energy storage

Sensible Heat Sensible heat, as its name addresses, stores heat by variating the temperature of the heat transfer fluid (HTF). This heat can be calculated by considering the first law of thermodynamics:

$$\Delta U = Q - W = Q - P_e \Delta V = \Delta H - \Delta(PV) \tag{3.26}$$

Reorganizing terms:

$$Q = \Delta U + P_e \Delta V = \Delta H - \Delta(PV) + P_e \Delta V \tag{3.27}$$

Considering an incompressible flow and a constant heat capacity along the two temperatures:

$$Q = \Delta U = m \cdot c_p \cdot (T_{out} - T_{in}) \tag{3.28}$$

Being m the mass inside the tank [kg], c_p the mass heat capacity at constant pressure $[\frac{kJ}{kg \cdot K}]$, and T_{out} and T_{in} the temperatures at the outlet and inlet of the tank considering the tank storing heat ($T_{out} > T_{in}$) [K].

While there are various HTFs, this thesis will focus particularly on water, which among inexpensive materials, is the one that shows the highest values of volumetric thermal capacity, property that is key for sensible heat storage. There are other materials which show higher thermal conductance, such as iron, but for the temperatures intended to be used, these materials show higher prices and the possibility of high temperatures for district heating are not appealing for this study, considering how new generation's district heating systems tend to lower their temperature to increase their efficiency [8][78].

Material	Density (kg/m^3)	Specific heat ($J/kg{\cdot}K$)	Volumetric thermal capacity ($10^6 J/m^3{\cdot}K$)
Clay	1458	879	1.28
Brick	1800	837	1.51
Sandstone	2200	712	1.57
Wood	700	2390	1.67
Concrete	2000	880	1.76
Glass	2710	837	2.27
Aluminum	2710	896	2.43
Iron	7900	452	3.57
Steel	7840	465	3.68
Gravelly earth	2050	1840	3.77
Magnetite	5177	752	3.89
Water	988	4182	4.17

Table 3.4: Thermal capacities at 20°C of some common TES materials [79]

Latent Heat When a substance retains heat during its phase transition, it is referred to as latent heat storage. In this methodology, the heat stored is calculated by:

$$Q = \begin{cases} m \cdot (h_f - h_s) = m \cdot \Delta h_f = m \cdot \lambda_f, & \text{if melting/fusing} \\ m \cdot (h_s - h_f) = m \cdot \Delta h_s = m \cdot \lambda_s, & \text{if solidifying} \end{cases} \tag{3.29}$$

Where Δh or λf is the melting enthalpy or heat of fusion or latent heat if the substance is going from the solid state to the fluid state, and in the negative value of this latent heat if going from fluid to solid. m is the mass of the storage material. Note that Q>0 when fusion occurs and Q<0 when solidification occurs, meaning heating is necessary for the solid to turn into a fluid, and cooling is necessary for the fluid to turn it into a solid.

The process of melting and solidification in the solid-liquid phase change allows for the significant absorption and release of heat energy if an appropriate material is used. During the melting process, while heat is being transferred into the storage material, there remains a constant temperature called the phase change temperature or melting temperature. This characteristic distinguishes latent heat from sensible heat (Figure 3.18). Although research primarily focuses on studying solid-liquid phase changes, certain applications also consider specific solid-solid transitions.

As the intention of this thesis is to operate in a low-temperature range, as explained in previous sections due to how district heating temperatures are evolving, by seeing Figure 3.18 the emphasis can be established where the temperature profile of latent heat TES and sensible TES overlap, but, by considering the cost of water storage much lower than those of the materials used for low-temperature latent heat TES (paraffins, and such), the focus will still be set on sensible water TES.

Chemical Heat Storage Chemical heat storage systems can be grouped by their principle, in one side, those which have chemical reversible reactions, and those which depend on

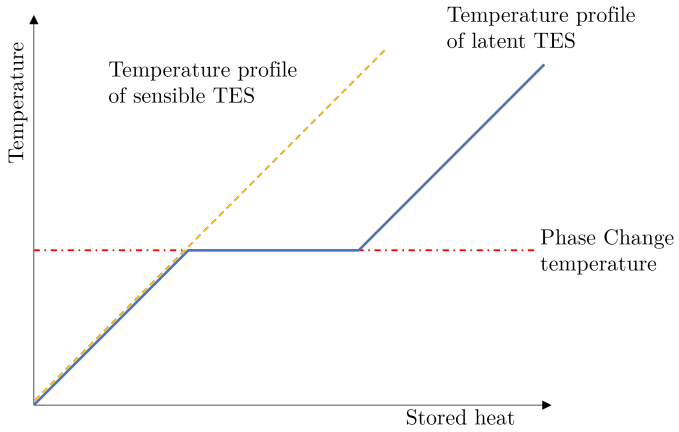

Figure 3.18: Heat storage as sensible and latent TES [77]

absorption and adsorption phenomena:

Absorption, creating a new material in the surface of the solid to which the gas is being absorbed. And adsorption, in which no new material is created in the bonding of this gas and solid, which depends mostly on superficial developments.

This methodology of storage exhibits two appealing factors, those are the volumetric energy density of the storage, having double the amount of energy per m^3 compared to water sensible heat, with a thermal difference of 50 K. This implies that chemical heat storage can accommodate more energy within the same volume as compared to conventional methods using water for storing sensible heat. The other appealing factor is the minimal energy losses to the ambient due to the possibility of storing it at ambient temperature [80].

Even though, these technologies seem promising, this thesis will not elaborate on them given that they still are in a low Technology Readiness Level (TRL), from level 4 to level 6 [76]. Which means that the system has been tested as a prototype in a ground environment but is not yet available in a commercial level [81]. In Commercial Readiness Index (CRI), this can be aligned with a technology that is still not ready to be taken to the market [82].

3.3.2 Time classification for storage

As stated in section 1.2, one of the key steps in the storage process is known as "storing". This step consists in the amount of time which the energy is stored and can be categorized into two distinct types based on the duration involved which was further explained by Twitchell [83].

Short-term storage In district heating systems, short-term energy storage is commonly employed to manage the fluctuations in load that arise throughout the day. Water-filled tanks are widely utilized as thermal energy storage for short-term applications in district heating, with a TRL of 9.

From a pressure point of view, there are two different situations to be considered:

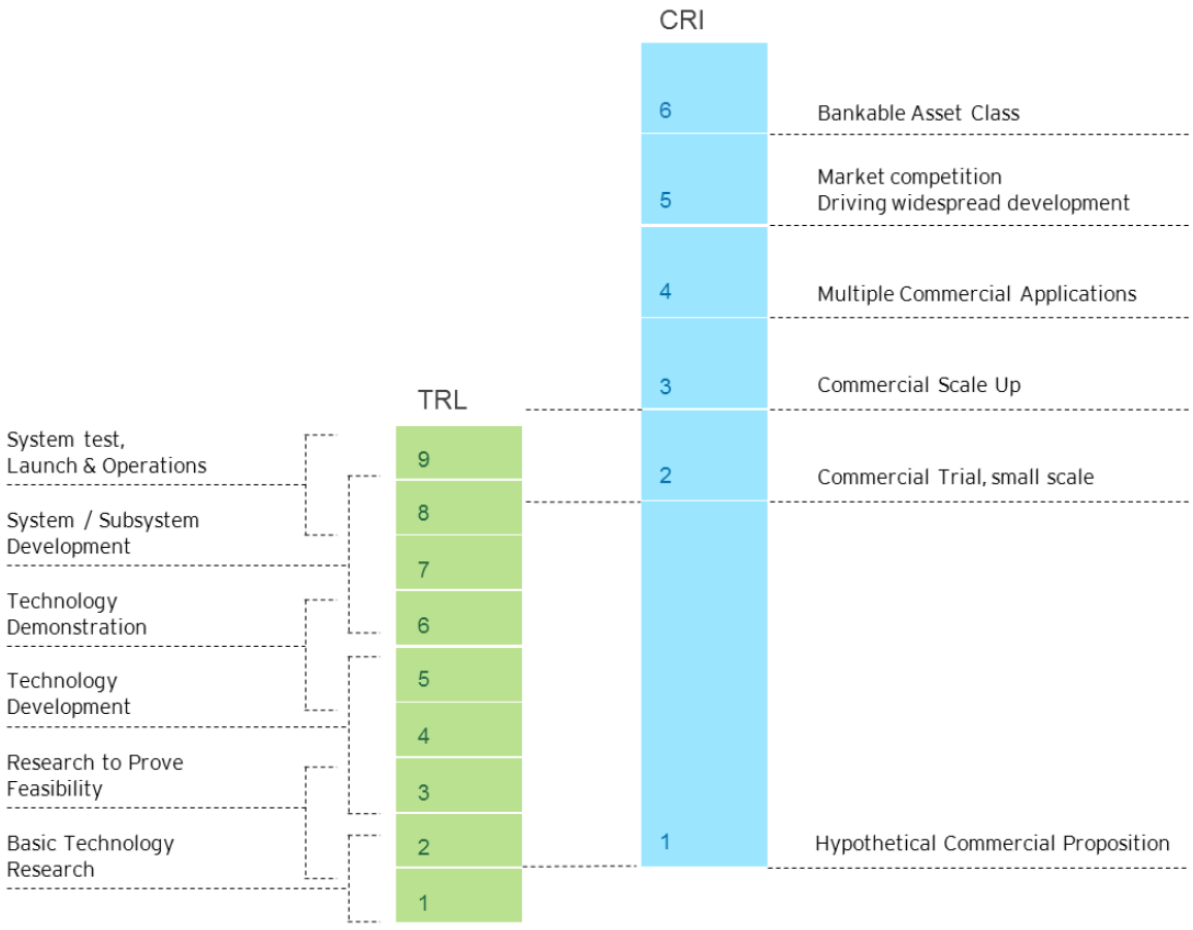

Figure 3.19: TRL levels according to NASA aligned with CRI values

- **High pressure**
  For high temperature systems where temperatures rise above 100°C, a pressure above atmospheric pressure is required to avoid evaporation. An advantage of pressurised TES systems is that, when directly connected, they can act as a pressurisation vessel. This is an essential component in DH networks, especially when regulation is achieved by varying the flow temperature, causing changes in specific volume. In the case of direct connection, the installation of a dedicated pressurised vessel can be avoided by using the TES.

- **Atmospheric pressure**
  The integration of thermal energy storage in low temperature district heating systems, with maximum storage temperatures below 100 °C and temperature differences not exceeding 30-40 °C, is common practice. Atmospheric TES are indirectly connected to the district heating network due to the pressure difference compared to the pipeline.

Long-term storage Long-term storage or long duration energy storage (LDES) has been widely installed used by many authors, but has a lack of a standard definition as to from which period of time this can be refered as "long". An acceptable reunion of different standards is provided in [83], where is denoted that an emerging consensus is being reached at 10 hours. Several types of LDES are shown in [84]. But even in these articles, another subdivision protrudes, which takes into account when these "long periods" involve one or more weeks between the charging of this energy and the actual use.

- **Long-term but diurnal storage**
  While this storage is above the aforementioned 10 hour limit, it is still below the 20 hour limit on a weekly basis, according to Twitchell [83], but considering those 20 hours as net hours, the use of that within a weekly basis could be established as part of this subcategory.

- **Seasonal storage**
  There is a need to capture surplus generation during seasons (e.g. solar) where storage capable of holding this energy is deemed necessary.

3.3.3 Simulation

Storage volume simulation is often based on the discretization of the storage volume into nodes, and applying conservation laws to genreate differential equations to reach its solution.

Simplified equations used by TESS Type 534 are:

$$\frac{dT_{Tank}}{dt} = \frac{(\dot{Q}_{In,Tank} - \dot{Q}_{Out,Tank})}{C_{Tank}} \tag{3.30}$$

$$C_{Tank,j} = \frac{C_p * V_{Tank} * \rho_{Tank}}{n} \tag{3.31}$$

where,

- C_p: specific heat of tank fluid [$\frac{J}{kg \cdot K}$]
- V_{Tank}: volume of tank [m^3]
- ρ_{Tank} = tank fluid density [$\frac{kg}{m^3}$]
- n: number of tank nodes.

Where $\dot{Q}_{In,Tank}$ and $\dot{Q}_{Out,Tank}$ depend on the ambient temperature, inlet fluid conditions, and flow rates. Although there are other methods available to solve coupled differential equations, the TESS model offers an approximate analytical solution. This type of solution has several inherent advantages over numerical solutions. Firstly, this subroutine solves its own mathematical problem without relying on non-standard numerical recipes that need to be attached separately. It can therefore be imported into any FORTRAN compiler without issues. Secondly, unlike some other solution methods (mainly numerical ones), which are highly dependent on the simulation timestep, and may not converge under certain circumstances commonly encountered in storage tank systems (such as high flow rates), the analytical solution is independent of time step but does require an iterative approach within the subroutine to solve the coupled differential equations. While solving two coupled differential equations iteratively can lead to convergence problems at times for some models, this doesn't seem to occur with this specific model under almost all operating conditions.

For achieve this type of analytical solution, Equation 3.30 is put in the form:

$$\frac{dT_{Tank}}{dt} = aT + b \tag{3.32}$$

Node properties are determined by deriving a and b values for each node. The b term encompasses the temperatures of other tank nodes and heat exchanger nodes, which are assumed to remain constant while solving the nodal differential equations at their average value over the timestep. Subsequently, the nodal differential equation is solved (as previously described), leading to new final and average nodal temperatures being calculated. This entire process is iterated until a converged solution is achieved. Following this, the calculations for heat exchanger nodes are repeated until all tank and heat exchanger nodes converge.

If temperature inversions are observed between adjacent nodes, mixing may begin during the timestep. The time at which the nodal temperatures become unstable is calculated if this is the case. The results at this point are stored and a new solution is generated with mixing occurring between the two involved nodes. Temperature inversions are checked again and a new time for inversions to occur may be determined. This process continues until no new temperature inversions are found, at which point the results from the model are reported. As with all TRNSYS components, the outputs from the model are assumed to be average values over the timestep [85].

Chapter 4

Modular Simulation Methodology

4.1 Simulation

4.1.1 Software

TRSNYS (TRaNsient SYstems Simulation Program) software has been used [31], following the modular methodology developed specifically for the Wedistrict project (4.1.2). The Wedistrict project studies integrating innovative technologies for DH and District Heating and Cooling (DHC) networks to develop solutions for fully renewable energy delivery in climatization services.

4.1.2 Modular Simulation Methodology

The Modular Simulation Methodology (MSM) as a whole with its final results is depicted in Figure 4.1. In this section of the thesis, the focus will be on outlining the initial phase up to the first obtaining of results, and their use to the subsequent key performance indicators calculation. Further explanation of the parametric studies and the use of the results obtained from these will be provided in section 4.1.2.

The concept behind MSM is the use of modules with assigned roles to create complex networks. This step is represented as "Technologies and System Modeling" (step 1) in Figure 4.1. These modules are represented by macros, which is the name used by Simulation Studio (TRNSYS graphic interface) to represent a set of TRNSYS Types. TRNSYS Types are Fortran-written modules, which represent a piece of equipment or calculation sequence, that, with the use of inputs and parameters, produces an output (see Figure 4.2). The main difference between inputs and parameters is that inputs are taken as time-dependent, while parameters are to remain constant during the simulation [86].

The use of macros in Wedistrict pursuit to replicate the model used for the Types on a bigger scale, generating whole technologies that could be able to be defined by a set of parameters and interconnected by their inputs and outputs which, from that moment on, would be organized in specific elements inside the macro. To streamline the use of technologies, efforts have been made to minimize the number of parameters required to run them by correlating these parameters externally using code outside TRNSYS. This distinguishing

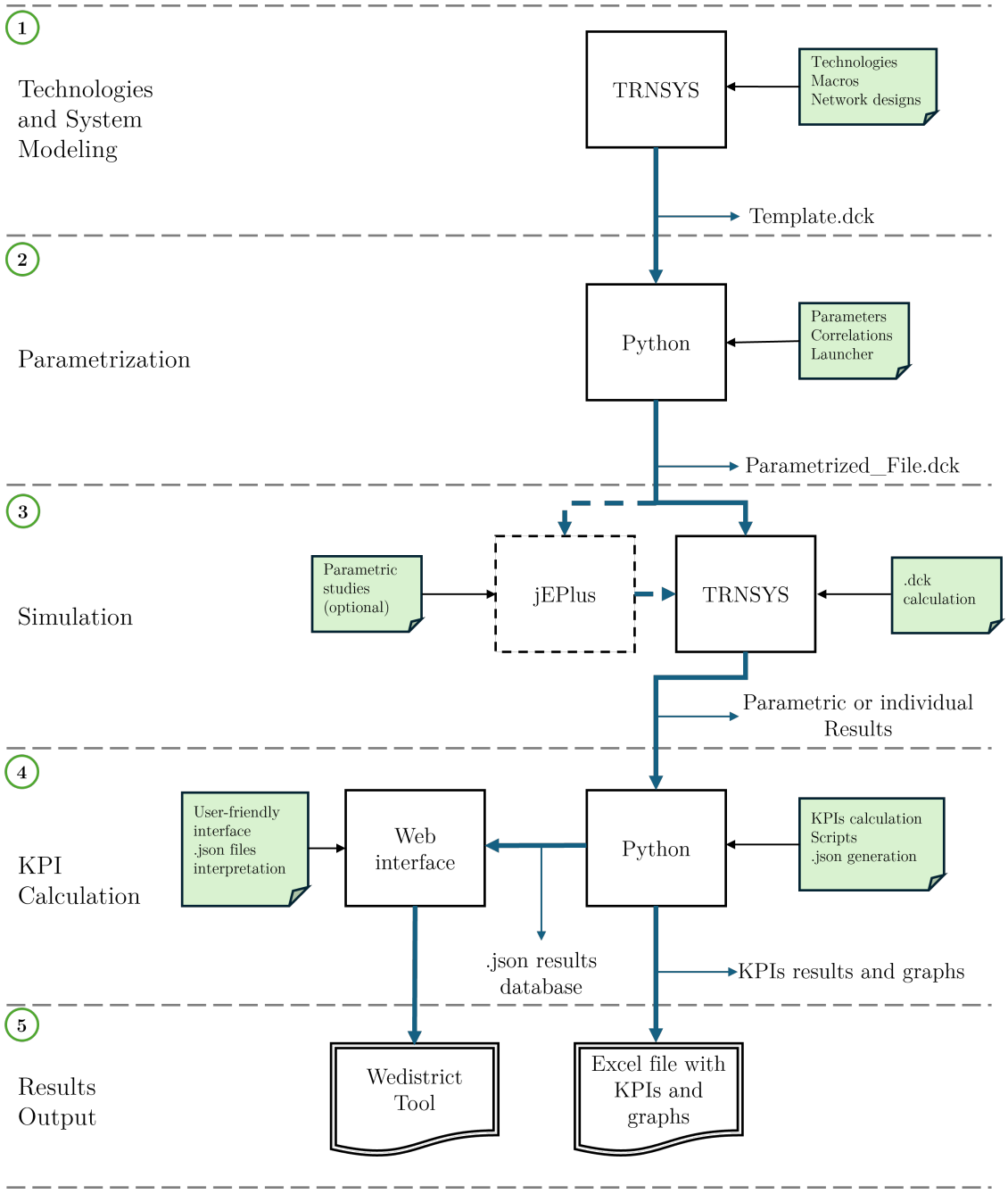

Figure 4.1: Simulation workflow at Wedistrict project using MSM.

feature is what differentiates this approach. Numerous existing tools are capable of simulating DHN, and many others can do so efficiently with minimal steps, simplifying the model. However, the exceptional aspect of this methodology lies in its capacity to perform dynamic simulations for the entire year with minimal input requirements.

To ensure effective organization, modular control has been implemented in each macro, allowing them to produce desired results and calculate outputs based on their inputs. Although, external controls were added as inputs for more complex strategies.

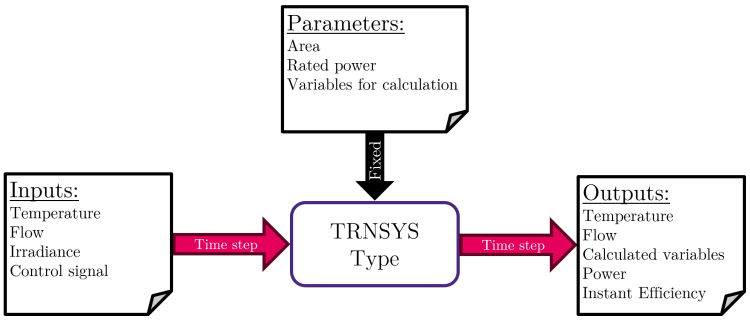

Figure 4.2: TRNSYS Type.

To summarize, Wedistrict macros have characteristics to improve their modularity and flexibility. These characteristics are illustrated in Figure 4.3 :

- Nomenclature: A standard nomenclature for macros, types, and variables
- Input and Output interfaces: Input and output variables are transmitted in and out of the macro by equation blocks. This method simplifies and reduces connections, and allows replacing a macro with another more efficiently (Only a few connectors should be modified).
- Parametrization procedure: The parameters are variables that remain constant during the simulation time. A Python script has been developed to make this more fluent (from specific values calculate the majority through correlations).
- Control strategy: Each macro has its own control strategy based on the technology represented. This method allows adding the same macro into different systems reducing the amount of control parameters to be set.
- Results: Each macro displays its own set of results and its internal calculations, such as energy and mass balance.

TRNSYS types used for the different macros are shown in Table 4.1.

With macros available interconnection between them to generate diverse technology combinations is possible as shown in Figures 4.4 and 4.5. In TRNSYS, the input file read is called "deck". TRNSYS Studio software serves as a graphical interface that aids the user in creating decks. These decks can also be generated by script and run by TRNEXE, which will allow us to generate parametric studies later on.

At first, DH networks were generated for simplicity, in these it is visible, as shown in Figure 4.4 that not all generations will need storage, and combinations will vary with the technologies selected. The real TRNSYS deck will not look like the figure, as each macro will have a unique code. This aspect of the methodology will be further explained in the following section (4.1.2).

Once the system is selected, a ‘Parametrization” step occurs (step 2). This step involves integrating the minimum number of necessary parameters by automating those that are connected. This step is further explained in Section 4.1.2.

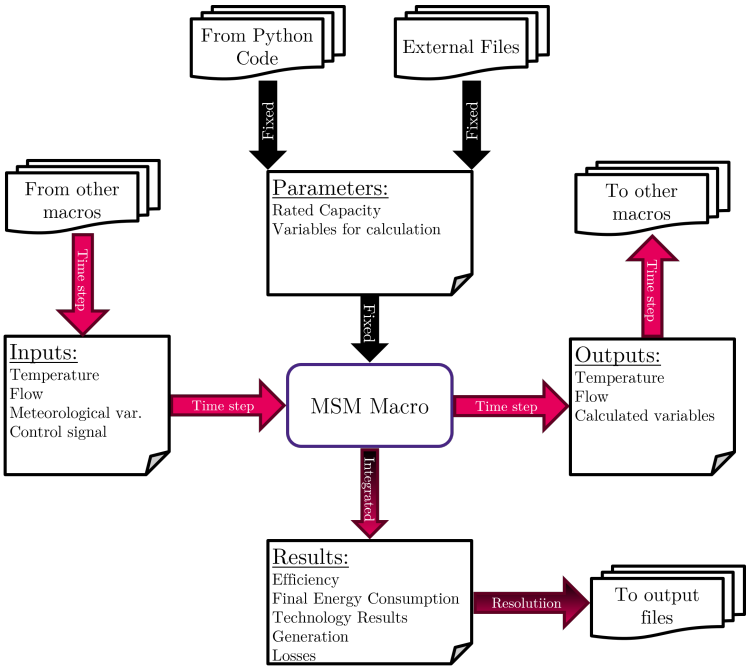

Figure 4.3: MSM macro Scheme.

M0100- METEO	
15-6	Meteo Data
77	Ground Data
M1200 – PTC/FRESNEL COLLECTOR	
1245	Ext. Concentrating Parabolic Collector
709	Pipes
110	Pump
5b	Heat exchanger
2d	Control
67/1262	Shading
M2100 - HOT WATER STORAGE	
534	Tank
709	Pipes
M7200/7300 - COLD/HOT DISTR.	
11f/11h	Diverter/Mixer
709	Pipes

M3100 - BOILER	
751	Boiler
709	Pipes
110	Pump
647/649	Diverter/Mixer
2d	Control
M4200 - ABSORPTION CHILLER	
107	Abs. Chiller
709	Pipes
110	Pump
534	Tank
128	Cooling tower
2d	Control
M8100/8200 - HEAT LOAD	
9c	Data Reader
M9100 - INTERCONNECTION MACRO	
647/649	Diverter/Mixer

Table 4.1: TRNSYS types used for different macros.

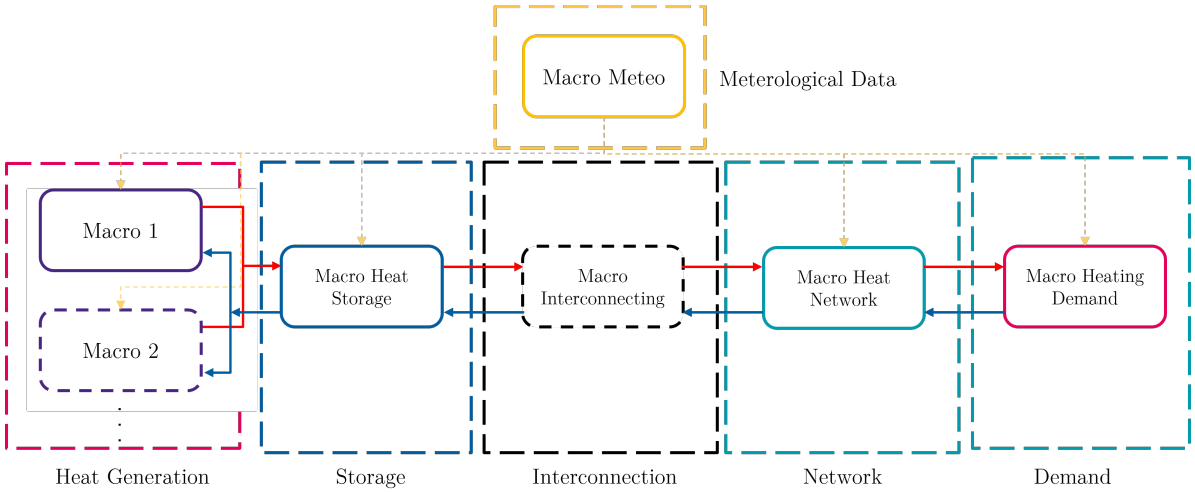

Figure 4.4: Macros connected to generate a DH network

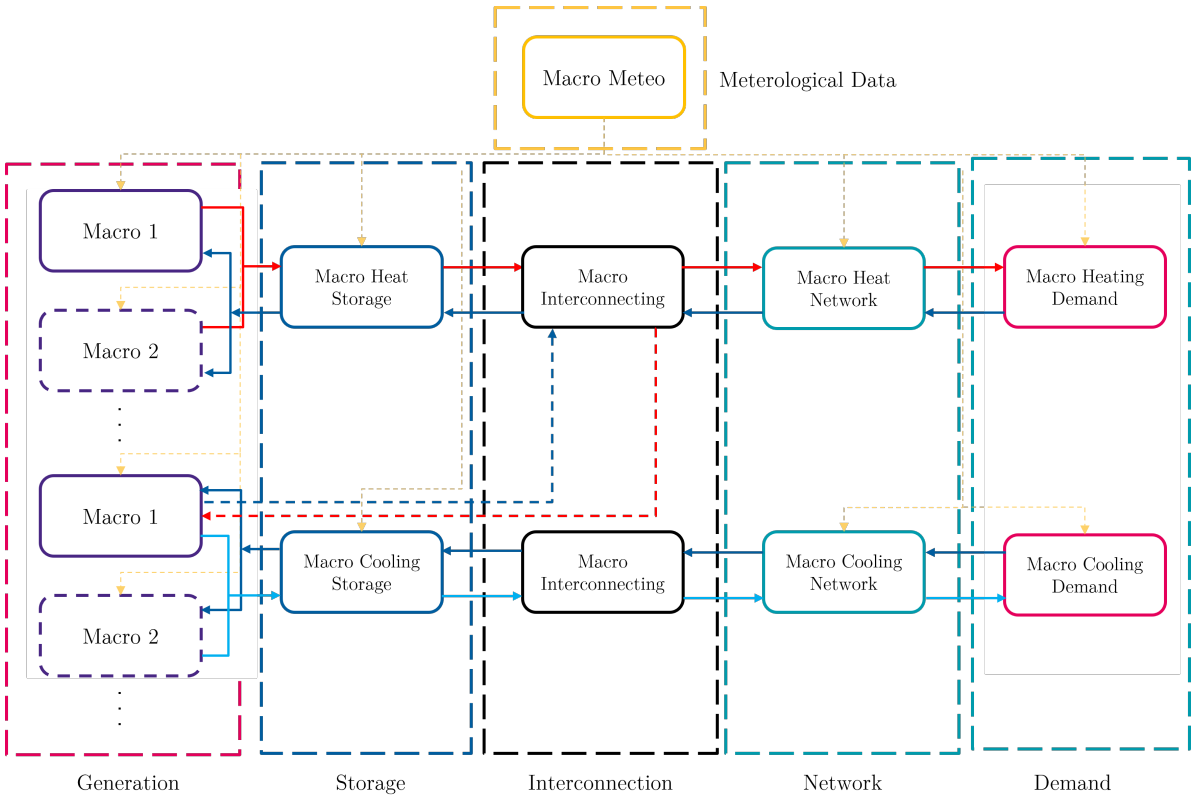

Figure 4.5: Macros connected to generate a DHC network.

With the defined system, "Calculation" is next in order (step 2 in Figure 4.1). In this step, TRNSYS will act, with jEPlus (as an intermediary or not), to obtain results of either one specific system or a parametric study held on one system. This will be expanded in Section 4.1.2.

With a wide range of results obtained from the simulations, a need for order and visualization arises, where the "KPI Calculation" step becomes relevant (step 4). The selection and calculation of the KPIs involved are thoroughly explained in Section 4.1.3. Summarizing, with the results obtained in each macro of each system, technical, environmental, and economic indicators will be calculated and analyzed [87], this has been implemented through another Python script to analyze each particular combination of technologies.

At last, all KPIs obtained will be displayed in a more user-friendly manner through the use of an output Excel file created through the use of Python script, or by generating different ".json" databases to be able to implement these results inside a Web interface. This step, called "Results Output" (step 5), represents the last step in the MSM methodology, supplying the user with the sought information.

Nomenclature and Codes

The MSM is based on TRNSYS macros and decks. Macros are a series of TRNSYS types that are used together to reduce the number of connections to be done, as explained in 4.1.2. The code to describe them has the letter "M" for "macro", followed by four numbers, the first three represent the code of the technology used, separated by the thousands in types of technologies (solar, storage, boilers, etc.), by the hundreds in different technologies between the same family 4.3, by the tenths in variations of the same technology. The unit is left in case the technology repeats itself in the same deck, due to the fact that TRNSYS, as many other software, does not allow variable name repetition (Figure 4.6).

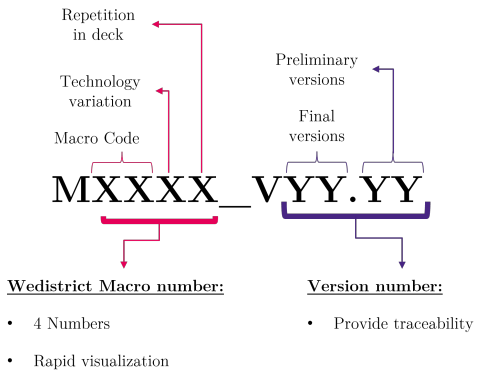

Figure 4.6: Macros coding developed

A similar approach was conducted inside and outside the macros with the variables present in the deck. To be able to identify parameters, inputs, and outputs rapidly from different macros which could be named similarly, or even repeated, special attention was paid to their name assignment. Following the macro code assignment previously described, components were defined paying attention to repetition and assigning a name that could indicate what part of the technology was being represented with two letters if possible or

three if necessary. Being the most used "PU" for pumps, "PI" for pipes, "TK" for tanks, etc. After arriving at the components definition, to clearly identify the variables, some guidelines were set on regard to which letters to use for the most common ones (Table 4.2).

Letter	Description
T	Temperature
M	Mass Flowrate
Q	Thermal Energy Flowrate
W	Electric energy flow
G	Radiative energy Flowrate: with appropriate sub-indexes. t (total), h (horizontal), d (diffuse), b (beam), g (ground)

Table 4.2: Letters used for variables

An additional piece of information was added for inlets and outlets were possible, and the letters "In" or "Ou" were introduced to identify the sense of the variable if it was coming in or out of the macro. To give an example, Figure 4.7 shows how simple is to identify a variable with all the guidelines being used.

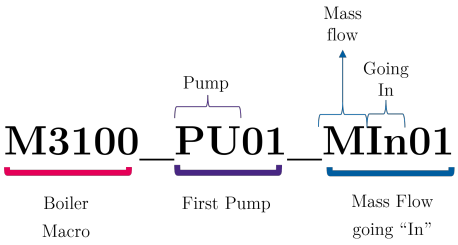

Figure 4.7: Variable code for the mass flow going in the first pump of the boiler

Code	Description of macro family	Macro Start Nº MXX	Code	Description of macro family	Macro Start Nº MXX
MET	**Meteo**	0000s	MSC	**Miscellaneous**	5000s
MEF	Meteonorm File reader	01	GTH	Geothermal	51
STC	**Solar Technologies**	1000s	DCT	Dry Cooling Tower	52
PTC	Parabolic Through Collector	11	WCT	Wet Cooling Tower	53
FRE	Fresnel Collector	12	DCS	Submerged Datacenter	54
FTC	Flatplate Tracking Collector	13	DCA	Air Cooled Data Center	55
FPC	Flatplate Collector	14	HRV	Heat Recovery	56
PVP	Photovoltaic Panels	15		**Tailor Made**	6000s
PVT	Photovoltaic Thermal Hybrid Solar Collector	16	GHP	Geothermal + Heat Pumps	61
STO	**Thermal Storage**	2000s	FCL	Fuel cell + Waste Heat Recovery	62
WST	Water Storage Tank	21	FCL	Fuel cell + Waste Heat Recovery	62
MST	Thermal Storage Tank (Molten Salts)	22		Distribution	7000s
CWS	Cold Water Storage	23	EPW	Power Distribution	71
WPT	Water PTES	24	CDI	Cold Distribution	72
COM	**Combustion Technologies**	3000s	HDI	Heat Distribution	73
BOB	Boiler (Different fuels)	31		**Demand**	8000s
COG	Cogeneration	33	LDH	Heating Load	81
TDC	**Thermodynamic Cycles**	4000s	LDC	Cooling Load	82
AAC	Advanced Absorption Chiller	41	LDL	Variable Load	83
CAC	Conventional Absorption Chiller (2 stage)	42		**Auxiliaries**	9000s
CAW	Chiller A/W	43	INT	Interconnecting Macro	91
CWW	Chiller W/W	44			
HAW	Heat Pump A/W Heat	45			
HWW	Heat Pump W/W Heat	46			
RAC	RACU (Indirect evaporation with desiccant wheel)	47			

Table 4.3: Macro Codes for different technologies. First two numbers of macro code

Parametrization

After identifying all the decks, macros, types, and variables in this methodology, an important advantage emerges, parametrization. During the initial stages of the project, significant effort was dedicated to determining the essential variables necessary for characterizing each technology. These minimum sets of parameters were then used to populate the extensive array of parameters necessary for the execution of a dynamic simulation. The primary aim is to utilize this select group of variables as a foundation for extrapolating all other parameters through correlations when the latter are not readily accessible, as occurs in preliminary design phases.

Common fluids are defined in a general parametrization file called "PAR_MWD" (parameters macros Wedistrict), where its specific heat (C_p), density (ρ), thermal conductivity (k) and viscosity (μ) are defined at constant values considering that DHN will have working temperatures not higher that 100°C and even lower if higher generation DHN are considered ($T \leq 60°C$).

Diameters for piping are set considering the relationship between flow and recommended velocities, considering a minimum value with commercially sold pipes. With this internal diameter, wall thickness is then correlated with pressures used in standard systems, which leads to the obtaining of the external diameter. Through temperature and outside diameter, standards such as ASHRAE 90.1, recommend insulation thicknesses which were used as the basis for generating a correlation, specifically Table 6.8.3-1 and 6.8.3-2 Minimum Piping Insulation Thickness for Heating Systems and for Cooling Systems, respectively [88].

For example, Solar fields in general in this project are calculated with three main parameters (area, ΔT, and temperature setting), through those parameters and selecting the appropriate technology (Parabolic Trough and Fresnel collectors are simulated through the same macro through the selection of a parameter called “PAR_STC”), all other parameters are set to common values (for example, solar Azimut is set to zero), unless the user desires to change them. Further explanation will be given on the individual macros as to how the parameters relate to each other in chapter 5.

Parametric Studies

To be able to design systems, the capability of simulating several cases at the same time and obtaining graphical results automatically is key. To obtain this feature using TRNSYS the use of jEPlus software (Figure 4.8) was proposed [89]. JEPlus is a Java-based tool, firstly intended to be used for EnergyPlus software [33], it was adapted to be used with TRNSYS files in August 2012 (three years after its first release in July 2009).

The Python interface for the MSM was prepared with consideration for the requirement that all files had to be available in the path of the TRNSYS ".dck" file to enable independent simulation runs once jEPlus generated different cases. Another efficiency-enhancing characteristic of this methodology is the utilization of separate result files for each technology, facilitating direct retrieval when calculating Key Performance Indicators (explained in the following section). This approach enables Python to handle multiple cases simultaneously (parametric study cases) and also accommodate diverse configurations.

Different options lay once KPIs are calculated, prioritization of environmental indicators

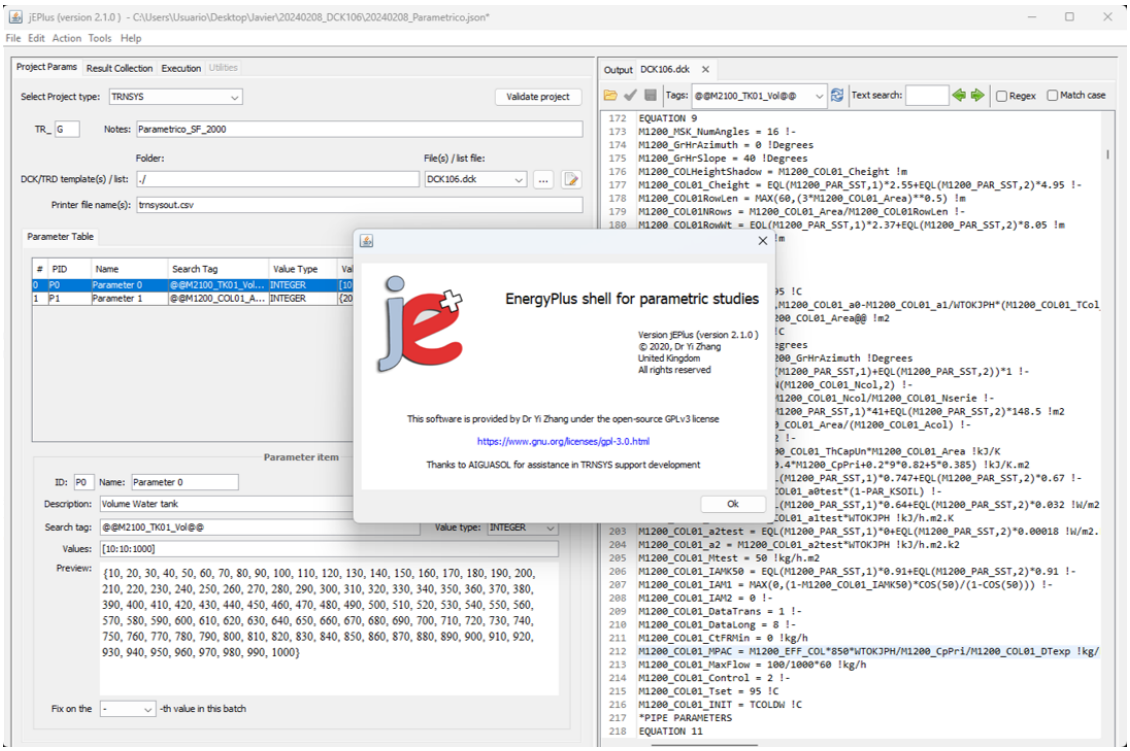

Figure 4.8: jEPlus user interface.

over economic ones is possible, for theoretical purposes, it is better to find an optimal point, where variation in investment and operation costs have a positive impact on emission, and evaluate if this impact is worth the inversion is up to the designer.

4.1.3 Key Performance Indicators (KPIs)

Using the aforementioned MSM, text files are obtained from the results of the different macros, one for each. This information proves to be abundant and difficult to interpret in a rapid manner. That is why a procedure to calculate the Key Performance Indicators set for the project [87], was implemented using Python along with Microsoft Excel. In this section KPIs calculation will be explained, and in the following section, implementation of this operations in python will be discussed.

KPIs Definition

The following KPIs were defined in the framework of the Wedistrict project [87].

Cooling Share α_C The Wedistrict project is focused on developing networks for distributing heating and cooling, as well as exploring technologies for converting energy from heating to cooling on the demand side. In order to ensure a fair and comprehensive evaluation of the project's performance, the system KPIs must be calculated separately for heating and cooling. However, due to the interconnected nature of the heat generation, cooling conversion, and distribution elements, it can be challenging to distinguish the economic, energy,

and environmental impact of each. To address this challenge, a cooling share parameter has been proposed, representing the percentage of the energy, environmental, or economic impact attributed to the cooling service of the shared elements. The division between cooling and heating impact is determined by the energy balance of the system. It is calculated using Equation 4.1, for which variables can be observed in Figure 4.9.

$$\alpha_C = \frac{Q_{H-C}}{Q_{H-C} + Q_{H.dis}} \tag{4.1}$$

Where,

- Q_{H-C}: Heat supplied from the heating network to the cooling network, used for cooling energy generation [kWh].
- $Q_{H.dis}$: Heat injected into the heating network for its distribution [kWh].

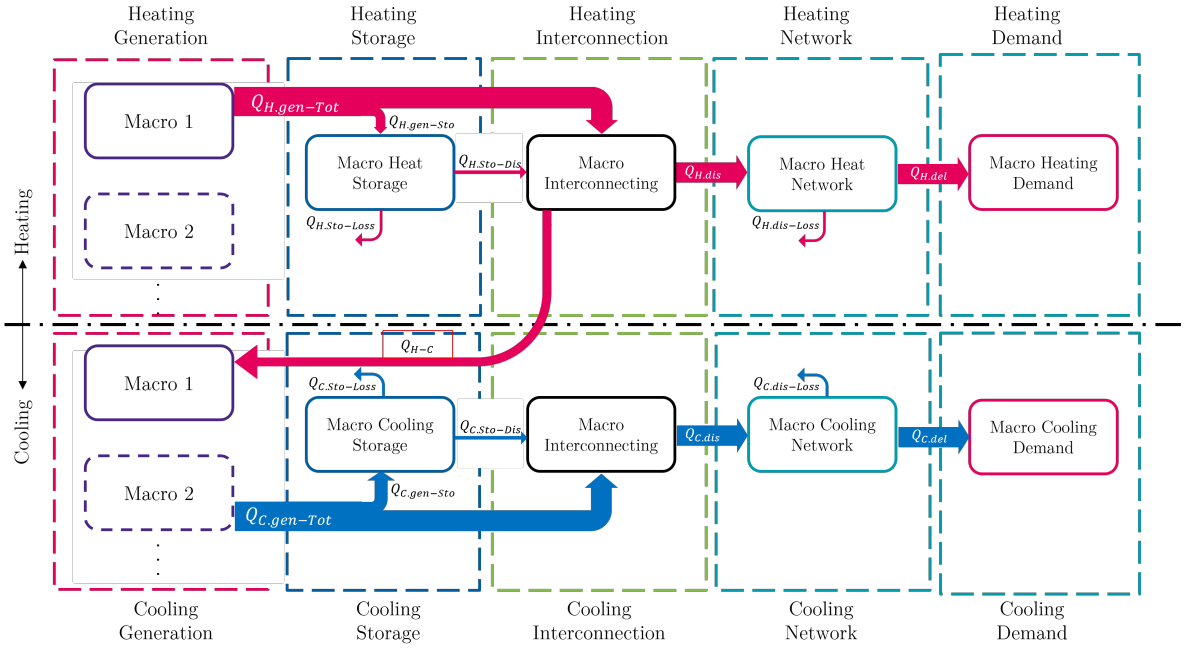

Figure 4.9: Wedistrict Energy variables shown using Figure 4.5

Renewable Energy Ratio (RER) The renewable energy ratio, also known as the share of renewables, refers to the proportion of renewable primary energy utilized by the network in relation to the overall primary energy consumed for meeting heating and cooling requirements. The definition of the Renewable Energy Ratio for buildings, as established by the Energy Performance of Buildings Directive (EPBD), is based on ISO 52000-1 [90]. This definition has been adapted to District Heating and Cooling systems, taking into account the analysis boundaries depicted in Figure 4.9. The calculation of RER includes inputs such as fuel, electricity imports, solar radiation, and external heat sources while subtracting electricity exports. Equation 4.2 provides a general description of how RER is calculated.

$$RER = \frac{E_{Pren}}{E_{Ptot}} \tag{4.2}$$

Where,

- E_{Pren}: Renewable primary energy used by the district energy
- E_{Ptot}: Total primary energy used by the district energy network.

Equation 4.4 and Equation 4.3 describe the calculation of the RER within the Wedistrict project for respectively cooling (RER_C) and heating (RER_H) generation.

$$RER_C = \frac{\sum_i E_{r.C.i} + \sum_i (f_{r.i} E_{i.C}) + \alpha_C [\sum_i E_{r.HC.i} + \sum_i (f_{r.i} E_{i.HC})]}{\sum_i E_{r.C.i} + \sum_i (f_{t.i} E_{i.C}) + \alpha_C [\sum_i E_{r.HC.i} + \sum_i (f_{t.i} E_{i.HC}) - \sum_i (f_{exp.i} E_{exp.i})]} \tag{4.3}$$

$$RER_H = \frac{\sum_i E_{r.H.i} + \sum_i (f_{r.i} E_{i.H}) + (1-\alpha_C) [\sum_i E_{r.HC.i} + \sum_i (f_{r.i} E_{i.HC})]}{\sum_i E_{r.H.i} + \sum_i (f_{t.i} E_{i.H}) + (1-\alpha_C) [\sum_i E_{r.HC.i} + \sum_i (f_{t.i} E_{i.HC}) - \sum_i (f_{exp.i} E_{exp.i})]} \tag{4.4}$$

Where,

- RER_C: Cooling renewable energy ratio [-].
- RER_H: Heating renewable energy ratio [-].
- $E_{r.C.i}$: Renewable energy produced by energy carrier “i" and consumed exclusively for cooling generation [kWh].
- $f_{r.i}$: Renewable primary energy factor for energy carrier “i" [-].
- $E_{i.C}$: Energy produced for non 100% renewable energy carrier “i" consumed exclusively for cooling generation [kWh].
- α_C: Cooling share factor [-].
- $E_{r.HC.i}$: Renewable energy produced by energy carrier “i" and consumed for both cooling and heating generation [kWh].
- $E_{i.HC}$: Energy produced for non-100% energy carrier “i" consumed for cooling and heating generation [kWh].
- $f_{t.i}$: Total primary energy factor for energy carrier “i" [-].
- $f_{exp.i}$: Total primary energy factor of exported energy carrier “i” [-].
- $E_{exp.i}$: Exported energy of carrier “i" [kWh].
- $E_{r.H.i}$: Renewable energy produced by energy carrier “i" and consumed exclusively for heating generation [kWh].

- $E_{i.H}$: Energy produced for non 100% renewable energy carrier “i" consumed exclusively for heating generation [kWh].

Renewable energy carriers like solar, wind, hydro, and ambient energies are taken into account as on-site sources for harvesting renewable energy. These sources are assigned a primary energy factor of "1" to represent their renewable nature. On the other hand, biofuels and electricity are considered to have a non-renewable component, so their corresponding renewable and total primary energy factors are used from Table 4.4. Additionally, any excess PV energy from the Wedistrict project is exported to offset the total primary energy consumption of the DHC system using a primary energy factor equivalent to that of the network carrier.

Non-renewable primary energy factor (f_{nr}) In addition to the previously mentioned Renewable Energy Ratio, another key performance indicator, known as the Non-renewable primary energy factor (f_{nr}), comes into play. This particular indicator takes into account primary energy sources that have not undergone any conversion or transformation processes. In the context of District Heating and Cooling systems, this is particularly useful for directly comparing them with individual heating and cooling systems, as it factors in all energy chains. The non-renewable primary energy factor effectively consolidates all delivered and exported energy from various sources into a single indicator by assigning appropriate weighting factors based on their respective contribution to primary energy consumption. A value of zero would indicate a DHC network that relies entirely on renewable sources. Equation 4.5 demonstrates the calculation of the non-renewable primary energy factor as per the guidelines outlined in Ecoheat4cities [91] used by Ivancic and Romaní in [87].

$$f_{P.nren} = \frac{\sum_i E_i \cdot f_{P.nren.i} + (Q_{ext} \cdot f_{P.nren.ext}) + (E_{el.aux} - E_{el.CHP}) \cdot f_{el}}{\sum_j Q_{del.j}} \tag{4.5}$$

Where,

- $f_{P.nren}$: Non-renewable primary energy factor [-].
- E_i: Energy input of carrier "i" [kWh].
- $f_{P.nren.i}$: Non-renewable primary energy factor of the carrier [-].
- $f_{r.i}$: Renewable primary energy factor for energy carrier “i" [-].
- Q_{ext}: External heat input [kWh].
- $f_{P.nren.ext}$: Non-renewable primary energy factor of the external heat input [-].
- $E_{el.aux}$: Auxiliary electrical energy [kWh].
- $E_{el.CHP}$: Generated electricity [kWh].
- f_{el}: Non-renewable primary energy factor of electricity mix [-]
- $\sum_j Q_{del.j}$: Delivered heat [kWh].

This equation has to be adapted to Wedistrict technologies as has been done for RER in the following equations, which distinguish between the non-renewable primary energy factors for heating service and cooling service.

$$f_{P.nren.C} = \frac{\begin{array}{c}(\sum_i E_{i.C} \cdot f_{P.nren.i} + \sum_i Q_{j.C} \cdot f_{P.nren.j} + E_{imp.c} \cdot f_{nr.el}) + \\ \alpha_C(\sum_i E_{i.HC} \cdot f_{P.nren.i} + \sum_i Q_{j.HC} \cdot f_{P.nren.j} + (E_{imp.HC} - E_{exp}) \cdot f_{P.nren.el}\end{array}}{Q_{C.del}} \tag{4.6}$$

$$f_{P.nren.H} = \frac{\begin{array}{c}(\sum_i E_{i.H} \cdot f_{P.nren.i} + \sum_i Q_{j.H} \cdot f_{P.nren.j} + E_{imp.H} \cdot f_{nr.el}) + \\ (1-\alpha_C)(\sum_i E_{i.HC} \cdot f_{P.nren.i} + \sum_i Q_{j.HC} \cdot f_{P.nren.j} + (E_{imp.HC} - E_{exp}) \cdot f_{P.nren.el}\end{array}}{Q_{H.del} + Q_{HC}} \tag{4.7}$$

Where,

- $f_{P.nren.C}$: Cooling non-renewable primary energy factor [-].
- $f_{P.nren.H}$: Heating non-renewable primary energy factor [-].
- α_C: Cooling share factor [-].
- $E_{i.C}$: Energy input of carrier "i" in cooling technology applications [kWh].
- $E_{i.H}$: Energy input of carrier "i" in heating technology applications [kWh].
- $E_{i.HC}$: Energy input of carrier "i" in equipment used for both cooling and heating applications (shared) [kWh].
- $Q_{j.C}$: External heat input used exclusively for cooling applications [kWh].
- $Q_{j.H}$: External heat input used exclusively for heating applications [kWh].
- $Q_{j.HC}$: External heat input used for cooling and heating applications (shared) [kWh].
- $E_{imp.C}$: Auxiliary electrical energy imported from the grid used exclusively for cooling applications [kWh]. It does not include the electrical energy from the self-consumption of PV-generated electricity.
- $E_{imp.H}$: Auxiliary electrical energy imported from the grid used exclusively for heating applications [kWh]. It does not include the electrical energy from the self-consumption of PV-generated electricity.
- $E_{imp.HC}$: Auxiliary electrical energy imported from the grid used for both cooling and heating applications (shared)[kWh]. It does not include the electrical energy from the self-consumption of PV-generated electricity.
- E_{exp}: Net exported electricity [kWh].
- $Q_{H.del}$: Delivered heat [kWh].

- $Q_{C.del}$: Cooling delivered [kWh].
- $Q_{HC.del}$: Heat consumed for cooling production at the consumer side [kWh].
- $f_{nr.el}$: Non-renewable primary energy factor of electricity mix [-].

As in the calculation of RER, non-renewable and renewable energy factors are taken from Table 4.4, from ISO 52000-1 [90].

Capital Expenditures (CAPEX) The capital expenditures (CAPEX) encompass the expenses associated with procuring and installing all necessary assets for initiating a facility, as well as enhancing existing assets. This encompasses direct construction costs, project engineering, project development, project financing costs, and contingencies. The CAPEX for the district heating or cooling system is measured in terms of cost per capacity [€/kW]. If the system is capable of both heating and cooling, it is recommended to split this indicator into separate values. One for providing heating service, and another for providing cooling service. For this project, CAPEX will be split using the same consideration used for the environmental KPIs. For those technologies applied in both heating and cooling, the cooling share will be used to distribute these costs between the corresponding services. A new variable, β_C, will be defined to account for the distribution of these costs accounting for cooling share (Equation 4.8). This value will be considered the "CAPEX cooling share factor".

$$\beta_C = \frac{C_{d.C} + \alpha_C C_{d.HC}}{C_{d.C} + C_{d.H} + C_{d.HC}} \tag{4.8}$$

Using this value, the definition of the different CAPEX are as follows.

$$CAPEX_C = \frac{C_{d.C} + \beta_C(C_{d.HC} + C_{p.e} + C_{p.d} + C_{p.f} + C_{p.c})}{P_C} \tag{4.9}$$

$$CAPEX_H = \frac{C_{d.H} + (1 - \beta_C)(C_{d.HC} + C_{p.e} + C_{p.d} + C_{p.f} + C_{p.c})}{P_H} \tag{4.10}$$

Where,

- β_C: CAPEX cooling share factor [-].
- $C_{d.C}$: Direct construction costs for the equipment used exclusively for cooling [€].
- $C_{d.H}$: Direct construction costs for the equipment used exclusively for heating [€].
- $C_{d.HC}$: Direct construction costs for the equipment used for heating and cooling [€].
- $CAPEX_C$: Total normalized CAPEX for the equipment providing cooling service [€/kW].
- $C_{p.e}$: Project engineering costs [€].
- $C_{p.d}$: Project development costs [€].
- $C_{p.f}$: Project finance costs [€].

- $C_{p.c}$: Project contingency costs [€].
- $CAPEX_H$: Total normalized CAPEX for the equipment providing heating service [€/kW].
- P_C: System cooling capacity [kW].
- P_H: System heating capacity [kW].

Operational Expenditures (OPEX) The operational expenditures (OPEX) encompass the continuous expenses associated with running the district heating and cooling network. These costs include energy consumption, licensing fees, maintenance and repair charges, labor wages, utilities, as well as replacement costs. The OPEX is divided into two types, fixed and variable. Fixed costs are associated with the scale of the facility and are quantified in terms of cost per thermal capacity. Labor, maintenance, performance monitoring, indirect operation, and maintenance costs are included in this type (Equations 4.12,4.11). Variable costs are associated with the production of heating and cooling in the plant and are expressed as the cost per unit of thermal energy delivered [€/kWh]. These costs include fuel, electricity, and consumables such as chemicals, along with their waste disposal. In the case of a system that includes both heating and cooling, the calculation of this indicator will be separated into two parts, one for providing heating services, and another for providing cooling services. This will be done in the same manner as it has been for the total capital expenditure.

$$OPEX_{F.C} = \frac{\sum_i O_{F.C.i} + \beta_C(\sum_i O_{F.HC.i})}{P_C} \tag{4.11}$$

$$OPEX_{F.H} = \frac{\sum_i O_{F.H.i} + (1-\beta_C)(\sum_i O_{F.HC.i})}{P_H} \tag{4.12}$$

Where,

- $OPEX_{F.C}$: Total normalized fix operational costs for cooling [€/kW].
- $OPEX_{F.H}$: Total normalized fix operational costs for heating [€/kW].
- $O_{F.C.i}$: Fix operational costs for cooling service only [€].
- $O_{F.H.i}$: Fix operational costs for heating service only [€].
- $O_{F.HC.i}$: Fix operational costs shared between heating and cooling service [€].
- β_C: CAPEX cooling share factor [-].
- P_C: System cooling capacity [kW].
- P_H: System heating capacity [kW].

While for variable costs OPEX calculations are as follows:

$$OPEX_{V.C} = \frac{\sum_i O_{V.C.i} + \alpha_C(\sum_i O_{V.HC.i} - \sum_i E_{exp.i} p_{exp.i})}{Q_{C.del}} \tag{4.13}$$

$$OPEX_{V.H} = \frac{\sum_i O_{V.H.i} + (1-\alpha_C)(\sum_i O_{V.HC.i} - \sum_i E_{exp.i} p_{exp.i})}{Q_{H.del}} \tag{4.14}$$

Where,

- $OPEX_{V.C}$: Total normalized variable operational costs for cooling [€/kWh].
- $OPEX_{V.H}$: Total normalized variable operational costs for heating [€/kWh].
- $O_{V.C.i}$: Variable operational costs for cooling service only [€].
- $O_{V.H.i}$: Variable operational costs for heating service only [€].
- $O_{V.HC.i}$: Variable operational costs shared between heating and cooling service [€].
- $E_{exp.i}$: Exported energy carrier "i" [kWh].
- $p_{exp.i}$: Price of energy exported by energy carrier "i" [€/kWh].
- α_C: Cooling share factor [-].
- $Priceofenergyexportedbyenergycarrier"i"$: Cooling delivered [kWh].
- $Q_{H.del}$: Heat delivered [kWh].
- $Q_{C.del}$: Cooling delivered [kWh].

Please note that for equations 4.13 and 4.14 variables are in terms of energy delivered (kWh), which depend on the system operation, while equations 4.11 and 4.12 depend on installed capacities (kW).

Levelized Cost of Energy (LCoE) The Levelized cost of energy (LCOE) evaluates the average net present value of energy expenditures during a system's lifespan. It is an important instrument for comparing various power generation technology options, particularly in situations where significant initial investments are required but operating costs decrease over time. This situation frequently occurs in systems that rely heavily on renewable sources. The levelized cost of energy (LCOE) methodology involves the discounting of future expenditures and earnings to their current value in a designated base year, thereby enabling the determination of unit costs for generating energy. These unit costs represent the ratio between discounted lifetime expenses and projected net present value (NPV) of total energy output. In effect, they correspond to an average price that consumers would need to pay in order to cover all associated costs while yielding a rate-of-return equivalent to that defined by the chosen discount rate. CAPEX calculations are done through the software, the value from the total system cooling capacity is also taken from the simulation results for this calculation.

The rest of the economic values are added in postprocessing by the script, fixing these values by the user.

$$LCOE = \frac{CAPEX \cdot CRF + OPEX_f + OPEX_v}{Q} \tag{4.15}$$

$$CRF = \frac{i(1+i)^n}{[(1+i)^n] - 1} \tag{4.16}$$

Where,

- $LCoE$: Levelized cost of energy [€/MWh].
- $CAPEX$: Capital expenditure for the equipment [€/MWh].
- $OPEX_f$: Fix operational costs for energy [€/year].
- $OPEX_v$: Variable operational costs [€/year].
- CRF: Capital recovery factor
- i: Interest rate.
- n: Project lifetime and number of annuities received.
- Q: Energy supplied per year [MWh/year].

Carbon Dioxide Emissions Coefficient (k_{CO_2}) The concept of equivalent emission coefficient pertains to the quantification of non-renewable fuel-derived greenhouse gas emissions within a district heating and cooling system. It is important to note that carbon emissions generated by biofuels are not considered, while accounting for the ones related to extraction, transformation, and transportation processes. The calculation is as follows:

$$k_{CO_2} = \frac{\sum_i E_i \cdot k_i}{Q} \tag{4.17}$$

Where,

- k_{CO_2}: CO_2 emission coefficient [kg/ MWh].
- E_i: Energy supplied by energy carrier i per year [MWh/year].
- k_i: Emissions coefficient of energy carrier i [kg CO_2/ MWh].
- Q: Energy supplied per year [MWh/year].

For CO_2 emissions table 4.4 has been taken as seen in the reference [87], from ISO 52000-1 [90, Table B.16.].

	Energy carrier	***Delivered from distant***	f_{Pnren}	f_{Pren}	$f_{P}tot$	k_{CO_2e} *(g/kW)*
1		Solid	1,1	0	1,1	360
2	Fossil fuels	Liquid	1,1	0	1,1	290
3		Gaseous	1,1	0	1,1	220
4		Solid	0,2	1	1,2	40
5	Bio fuels	Liquid	0,5	1	1.5	70
6		Gaseous	0,4	1	1.4	100
7	Electricity [c]		2.3	0.2	2.5	420
	Delivered from nearby					
8	District heating [a]		1,3	0	1,3	260
9	District cooling		1,3	0	1,3	260
	Delivered from on-site					
10	Solar	PV electricity	0	1	1	0
11		Thermal	1	1	0	0
12	Wind		1	1	0	0
13	Environment	Geo-, aero-, hydrothermal	0	1	1	0
	Exported					
14	Electricity[b,c]	To the grid	2,3	0,2	2,5	420
15	To non EPB uses	To non EPB uses	2,3	0,2	2,5	420

a Default value based on a natural gas boiler. Specific values are calculated according to M3–8.5.
b It is possible to differentiate between different sources of electricity like wind or solar.
c These values are established in line with the default coefficient provided in Annex IV of Directive 2012/27/EU. This default coefficient is currently being reviewed and a later amendment of the above factors could be needed.

Table 4.4: Weighting factors (based on gross or net calorific value) from [90, Table B.16.]

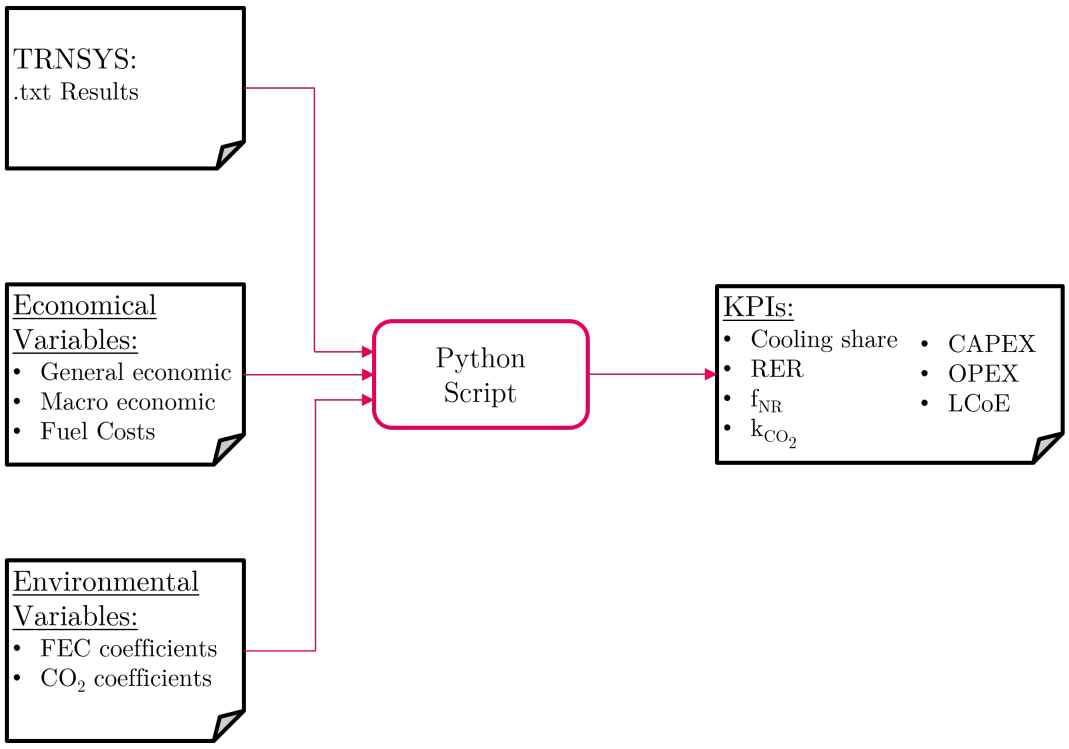

Figure 4.10: KPI calculation in MSM.

KPIs Calculation

A results script was developed to gather the information produced by TRNSYS automatically into Python data frames. Having a fixed set of results for each macro has led to the possibility of developing matrices to be filled by reading the text files produced by the simulation. Different decks have different calculations for KPIs associated. Cooling share, for example, depends on the technology selection in the network, and how heating and cooling generation interact. This gathered information was then used to perform the calculations described in Section 4.1.3. A graphical representation of this procedure is shown in Figure 4.10.

In this script, Final Energy Consumption empty matrices are developed and filled by the result files developed by each macro. The files to be read are determined by an identity matrix, which determines which technologies are involved in the different decks. So, when a deck is selected, only those text files are sought in the results path. The script works along with an Excel template, which supplies all the economical and environmental variables, which can be changed by the user. Economical variables are divided into three types. First, "General Economic" variables, are the electricity price, the expected lifetime of the network, the discount rate, the heating energy purchase and sell price, and the Cooling energy sell price. Second, the "Macro economic" variables, which are the unit CAPEX for the different technologies and the $OPEX_f$ assumed by the user. Thirdly, but not less important, "Fuel costs", which have a great impact on the plant's economic KPIs. Environmental variables are also loaded into the script, and two types are identified, "FEC coefficients" and "CO_2 coefficients". Both these values are in line with what was shown in Table 4.4, although it allows user changes. Besides reading TRNSYS results, the script must also be capable of

reading input parameters of the different simulations, in order to calculate, for example, prices of the different equipment involved, for which the size of each equipment is necessary. To do so, the script is able to isolate the input parameters from the deck file and generate a dictionary with the different values. Depending on the Macro presence in the identity matrix, the values needed for calculation are extracted from the deck parameters and identified in their corresponding macro. For example, for solar field cost calculation, square meters of the field are taken as the basis for the calculation.

The calculation of KPIs developed for the script has been migrated to the tool, making the web interface, corresponding to the use of the Excel file for the result script, by providing the user input needed.